Keele
UNIVERSITY

This work is protected by copyright and other intellectual property rights and duplication or sale of all or part is not permitted, except that material may be duplicated by you for research, private study, criticism/review or educational purposes. Electronic or print copies are for your own personal, non-commercial use and shall not be passed to any other individual. No quotation may be published without proper acknowledgement. For any other use, or to quote extensively from the work, permission must be obtained from the copyright holder/s.

Application of musculoskeletal modelling to evaluate movement and muscle activity patterns in shoulder instability

Martin Augustin Seyres

This thesis is submitted in partial fulfilment of the requirements for the degree of:

Doctor of Philosophy

March 2025

Keele University

This electronic version of the thesis has been edited solely to ensure compliance with copyright legislation and excluded material is referenced in the text. The full, final, examined and awarded version of the thesis is held by the University Library.

Abstract

Shoulder instability is a complex impairment that presents as the shoulder sliding out of its support. It challenges current clinical practice in its definition, assessment, classification and long-term outcome. An improved understanding of its mechanisms, as well as the identification of specific biomarkers may inform treatment allocation which motivated this body of work.

Data was analysed from an established cohort study to examine patterns of shoulder instability. A kinematic and electromyography analysis was performed on fifteen young subjects with shoulder instability and fifteen healthy age equivalent controls. Shoulder instability participants were found to have characteristic patterns of compensation, both in the way they move and in the way their muscles contract, which adds valuable information to the current literature.

A novel study design is presented to examine a subgroup of pathological individuals that presented with normal kinematics and muscle contraction patterns, and were virtually indistinguishable from the healthy control group using a standard motion analysis approach. Using musculoskeletal modelling techniques, static optimisation and statistical analyses, a new approach was demonstrated that provided indication of non-obvious compensatory patterns that inherently characterise this impairment.

One of the main challenges that this pathology can present is the assessment of small compensatory patterns that are linked to this condition and are likely to create long term complications and ultimately prevent full recovery. By assessing the neuromuscular behaviour based on the individual kinematics, strong indication can be provided of an impaired muscle control behaviour. This important information provides an insight that is currently lacking or not observable in the assessment of patients that could otherwise appear healthy based on the current evaluation methods. Therefore, it could prove to be an important objective marker in their rehabilitation.

Finally, the results of this study advocate for the streamlining of the use of modelling techniques in clinical settings, to assess both joint angles and muscle control in this population. This thesis provides a groundwork for longer term goals in upper limb biomechanics in general, and patient-specific modelling approaches.

Acknowledgements

First of all, I would like to thank my supervisors, Dr Caroline Stewart, Professor Ed Chadwick and Dr Fraser Philp for their invaluable advice and assistance at every stage of my research project. They have sacrificed large amounts of their time into guiding me and helping me develop throughout this PhD and without their support and encouragement, this project would not have been possible.

Finally, I would like to thank my family, friends and coworkers for all the support they gave me on this arduous but exhilarating journey.

Table of Contents

1. Introduction

The shoulder is a highly mobile complex involved in the motion of the upper limb. It is made of several bones and joints, the glenohumeral, sternoclavicular and acromioclavicular joint. The efficient functioning of the shoulder girdle relies on the interplay and perfect coordination of several layers of muscles that are acting on its parts. The muscle contractions are the results of neuromuscular interactions that ultimately allow the function of the shoulder. Beyond the morphological and mechanical aspects, it is the muscular contractions that control the function.

The complex nature of the shoulder girdle, as well as the diversity of the motions allowed and the elaborate functioning of the underlying muscle interactions, make the shoulder susceptible to a broad range of pathologies. Therefore, numerous classification systems attempt to make distinctions between the most common pathologies, such as rotator cuff tear or tendinopathy, adhesive capsulitis, glenohumeral instability, and acromioclavicular joint abnormalities (McClure, 2015).

Among the shoulder pathologies, and due to the unstable nature of the shoulder joint, shoulder instability (SI) is a complex impairment which manifests as an excessive and undesirable translation of the humeral head within the glenoid fossa. It results in a partial subluxation or a complete dislocation of the glenohumeral joint, the most commonly dislocated joint in the body (Stokes, 2023). It is a relatively common pathology affecting around 1.7% of the general population (Hettrich et al. 2019) that can impair general function and have short- and long-term consequences such as pain or decreased movement abilities, increase the risks of shoulder arthritis and several possible changes to the joint (Philp et al. 2022). It has many causes, and the pathophysiological mechanisms of

shoulder instability are also numerous and diverse. They include traumatic or atraumatic injury mechanisms, different instability directions, frequencies and severities of subluxation or dislocation. Different classification systems are used in the attempt to diagnose, label and orientate treatments of Shoulder Instability in order to try to recover the function and the range of motion.

Shoulder Instability presents challenges to current clinical practice. Individuals with Shoulder Instability often experience delayed diagnosis (Lawton et al., 2002), and have a generally variable clinical outcome, especially in paediatric populations. Further episodes of instability occur in 40-100% of children depending on the studies (Leroux et al. 2015; Deitch et al. 2003; Kudora et al. 2001).

A poor understanding of the causes and presentations of Shoulder instability led, over the years, to numerous classification systems, and therefore to different treatment pathways. They are built on underlying assumptions about the motor control and muscle structure and function (Shumway et al. 2012; Philp et al. 2022) that don't always appear to represent the reality of the patients. More specifically, the way the muscles contract is interchangeably seen as a cause or consequence of the instability which changes drastically the clinical approaches to addressing the condition with some primarily focusing on restoring a "normal" pattern in muscle behaviour.

In summary, the complexity of the shoulder, the general assumptions about the basic components of the motion, as well as the general lack of understanding of this specific pathology (illustrated by the many different classification systems), are likely related to the poor clinical results that these patients exhibit. The evidence currently available on shoulder instability is therefore limited and has led to a body of work that provides no

consensus on the clinical outcome. Consequently, several aspects of research could be explored in order to benefit the general outcome of these patients. First, a better understanding of the initial clinical problem is required. Taking into consideration the unique motor control of this population during their assessment could be a groundwork that allows a patient-centered and patient-specific approach to care, and ensuing clinical considerations could then rely on less biomechanical assumptions. Further work could be done on the modelling aspect specific to shoulder instability in order to better characterise those patients and objectify the way they move and control their muscles. Additionally, motor control can be investigated with personalised biomechanical models of the glenohumeral joint. The models can use each unique kinematic pattern to predict muscle activation based on a cost function, and the relationship between predicted and measured muscle activity can be used to explore motor control as a novel way to investigate shoulder instability.

This method differs from the standard approach that compares directly the experimental muscle activity of a pathological group to that of a control group (Spanhove 2021, 2022). While the standard approach is commonly used in lower limb analysis for example, the upper limb provides greater kinematic variability (Goetti et al. 2020, Ludewig et al. 2009) and therefore the normal muscle activities of upper limb tasks contain a larger variety of patterns. Consequently, a given set of experimental muscle activity could match normal activations which would be associated with slightly different (but still within the norm) kinematics. In other words, the more ways there are to perform a motion or task in a normal fashion, the less relevant a direct comparison of muscle activities might be. This could be a limitation in cases of shoulder instability which is characterised by small compensatory patterns in both kinematics and muscle activities. This limitation might be

removed by using predicted activations. In this case, the norm would be defined by a variation around the prediction that takes into account (is based on) the specific kinematics of the participant.

Further detailed biomechanical data would include joint forces and would cover a range of ages and clinical presentations. Finally, longitudinal studies based on this objective biomechanical data could allow a more accurate assessment, comparison and prediction of the long-term clinical outcome than what is currently available in the literature mainly due to the diversity in protocols and parameters used. This current research is located at the beginning of this pipeline. Its purpose of this research is to produce a body of work that investigates this pathology from a biomechanical perspective in order to increase our understanding and investigate new ways to assess muscle function.

Roadmap

This thesis starts with a review of basic anatomy that provides the fundamental knowledge required for the understanding of the rest of the work (chapter 2).

The Literature Review (chapter 3), which is a summary of the current knowledge relevant to this topic, covers the functional anatomy and biomechanics, provides a review of shoulder instability and existing classification systems, and shows the available technologies, modelling techniques and recent advances in research that can complement and improve the current understanding. It is followed by the aims and objectives of the thesis (chapter 4).

The Methods chapter (5) then describes the experimental methods performed in this study, therefore which data was collected and how, as well as the modelling methods and utilisation of the data.

The main findings are presented in three self-contained chapters: chapter 6, 7 and 8. They cover, respectively, kinematical and electromyography analysis (6), static optimisation to predict muscle control based on the kinematics alone in the control (7) and shoulder instability (8) groups, as well as the demonstration of an approach to discriminate a subgroup of participants of the shoulder instability group that exhibited normal kinematics and muscle activity patterns (8).

Finally, in the last part of chapter 8, **Static Optimisation and a statistical analysis are used on the subgroup of participants of the SI group that exhibited normal kinematics and muscle activity patterns ("subset")**.

The final chapters cover the general discussion (9), conclusions and limitations (10) of this research.

2. Basic anatomy and definition

The shoulder complex is formed of bones, capsules, ligaments and muscles and connects the upper limb to the trunk via the scapula. The main role of the shoulder is to contribute to the orientation of the hand in space. The following anatomical reminders provide an overview of the basic components of the shoulder girdle area that are of importance to understand and study shoulder instability. The modification of any of those components will impact the way muscles work, and this will be covered in the next section in the literature review, in the functional anatomy and biomechanics section.

2.1 Osteology

2.1.1 The humerus

The humerus is the bone of the upper arm that articulates with the scapula from the **head of the humerus** that forms one third of a sphere of 5-6cm of diameter (Hurov 2009) and is covered roughly by 26 to 37 cm^2 of articular cartilage. Below the head, the humerus narrows down into the anatomical neck. It is oriented superiorly, forming the neck/shaft angle of 130°, and posteriorly, forming an angle of retroversion of 35-40°. The greater (lateral and lesser (anterior) tubercles extend from the humerus just below the anatomical neck. In between them is the bicipital groove, locating and guiding the tendon of the long head of the biceps brachii muscle. Inferior to the tubercles, the humerus narrows down once again in a region known as the surgical neck.

2.1.2 The scapula

The scapula (Fig. 2.1) is a flat and triangular bone with lateral, superior and inferior corners. Its anterior or ventral surface is smooth covered by muscles and allows the sliding of the scapula on the thorax. Its posterior surface is transversally subdivided into two parts by the spine of the scapula that differentiates two portions: the supraspinous fossa above and the infraspinous fossa below.

On the lateral angle of the scapula and following the neck of the scapula - a thickening of the bone - is the **glenoid fossa or cavity** that articulates with the head of the humerus. The glenoid fossa sits laterally on a thick bony ridge, the lateral pillar of the scapula.

The glenoid fossa is a pyriform articular surface of 6 to 9 cm^2 (Hurov 2009). On its superior margin, on the supraglenoid tubercle, originates the tendon of the long head of the biceps brachii muscle. On its inferior margin, the long head of the triceps brachii rises from the infraglenoid tubercle.

`

Fig 2.1) Glenohumeral osteology (Gosling et al. 2016). Anterior view (left) and Posterior view (right). Acromion (A), Coracoid process (C), Glenoid fossa (G), Greater tubercule (GT), Head of the humerus (H), Infraspinous fossa (ISF), Lateral pillar (LP), Lesser tubercule (LS), Spine of the scapula (Sp), Surgical neck (SN), Supraspinous fossa (SSF).

Laterally, in continuation with the superior portion of the spine is the **acromion**, a bony process that extends over the posterosuperior region of the glenoid fossa. On the anterosuperior region of the glenoid fossa is the **coracoid process**.

2.1.3 The clavicle

The clavicle is a long-shaped bone and is the osseous link between the thorax (from the sternal region) and the scapula. It keeps them at constant distance throughout motion (Dufour, 2017).

2.2 Arthrology

2.2.1 Gleno-humeral joint

When the arm is hanging beside the body in the anatomical position, the articular surfaces of the head of the humerus and of the glenoid cavity are in contact on a surface of 4 to 5

cm^2. This surface varies throughout motion from a minimum of 2.59 cm^2 to a maximum of 5.07 cm^2 of contact (Soslowsky et al. 1992). These results of variable contact surface, as well as the shallow aspect of the glenoid fossa, show the importance of the surrounding structures to prevent excessive translations during range of motion and more specifically the necessity of complex muscle interactions.

The articular surfaces are enclosed in the articular capsule that has an outer fibrous layer and an inner synovial layer. The joint line is crossed superiorly by the tendon of the long head of the biceps that originates from the supraglenoid tubercle and goes in the bicipital groove. While this tendon is within the intracapsular space it remains extrasynovial.

Surrounding the capsule is a **ligamentous system** whose purpose is to keep the articular surfaces in contact. Enclosing the capsule and the ligaments are the **rotator cuff muscles** that originate on the scapula and attach to the humerus as seen on Fig. 2.2.

Fig. 2.2) Muscles around the shoulder joint (Gosling et al. 2016). On the left: Anterior view of the rotator cuff (subscapularis (SSc), supraspinatus (SSp)), and on the right: Posterior view of the rotator cuff (supraspinatus (SSp), infraspinatus (ISp), teres minor (TM), long head of the triceps brachii (LHT)).

2.2.2 Scapulothoracic joint

The scapulothoracic joint is not a true anatomical joint, and is the sliding plane between the anterior aspect of the scapula (covered by the subscapularis muscle) and the thorax (covered by the serratus anterior).

2.2.3 Acromioclavicular joint

The attachment of the lateral end of the clavicle on the scapula is the acromioclavicular (AC) joint that allows slight gliding movement.

2.2.4 Sterno-costo-clavicular joint

The attachment of the clavicle on the thorax is the sterno-costo-clavicular (SCC) joint as it articulates between the manubrium, clavicle and costal cartilage of the first rib. It is often referred to as sterno-clavicular joint.

3. Literature review

3.1 Functional Anatomy and biomechanics

This first section of the literature review explains the functioning of the different anatomical components introduced in the previous section. It shows different ways to describe motions, illustrates the high degree of interdependence of all the components to stabilise the joints and produce motion, and presents the complexity of the muscular system in that anatomical region.

3.1.1 Functional and anatomical movements

The description of the motion of a joint is commonly based on the **standard terminology provided by the American Orthopaedic Society, the SFTR system** (sagittal, frontal, transverse) as seen in Fig. 3.1. Anatomical motions are described in those pre-defined orthogonal planes and are intuitive. The term physiological motion is sometimes used when described specifically in the planes of the joint (Maitland, 2013).

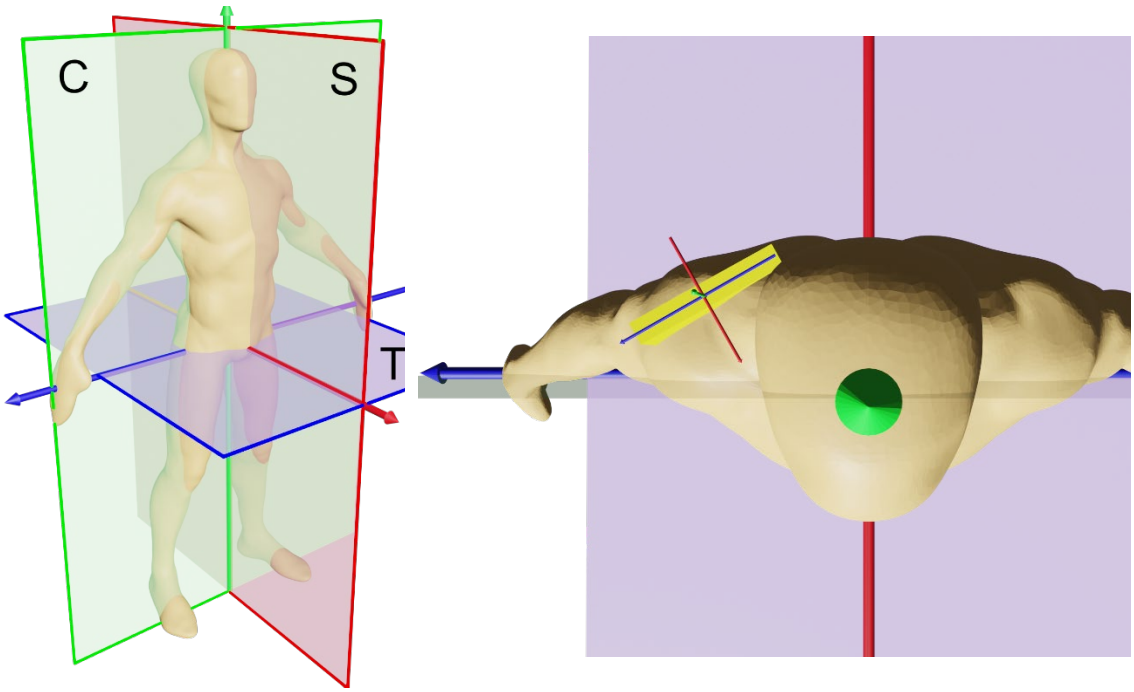

Fig. 3.1) Left: Anatomical planes and axes. Coronal plane (C), Sagittal plane (S) and Transverse plane (T), defining the the Sagittal or Anterior (red), Transversal or Lateral (blue) and Longitudinal or Superior (green) axes. Right: Local reference plane of the scapula (in yellow), illustrate the modification of orientation of the axes when describing the physiological motions.

When describing the shoulder, the SFTR system can be ambiguous if the humerus is not strictly in those planes (i.e. during activities of daily living or combined motions, the arm can be in a position that is not easy to describe with those intuitive planes of reference, neither strictly in front nor strictly on the side of the body) and alternative systems of description have been proposed for clinical practice, such as the globe system. In the globe system the initial plane in which the elevation of the humerus is performed is specifically defined (Pearl et al., 1992).

The globe system, defined in the anatomical planes, is a simplification of the standard set by the International Society of Biomechanics (ISB) (Rab, 2008). ISB recommends describing each segment in a local coordinate system relative to the one of the proximal segments, and more specifically describe the motion of the GH joint relative to the scapula as a

sequence decomposition that is often misunderstood by clinicians. **In this section, the SFTR convention will be used to describe anatomical movements.**

3.1.2 Several joints working together

The joints of the shoulder girdle are inter-dependent. From the sternum on the thorax, the sternoclavicular joint articulates with the clavicle, which then articulates with the scapula via the acromioclavicular joint, which finally articulates with the humerus via the glenohumeral joint.

The glenohumeral joint is a six degree of freedom ball-and-socket joint (Goetti et al. 2020). The very small translations (around 2mm) that occur in the glenoid fossa are often omitted and the glenohumeral joint is generally described as a three degree of freedom joint which allows the motions of flexion and extension, internal and external rotation, abduction and adduction represented in Fig. 3.2.

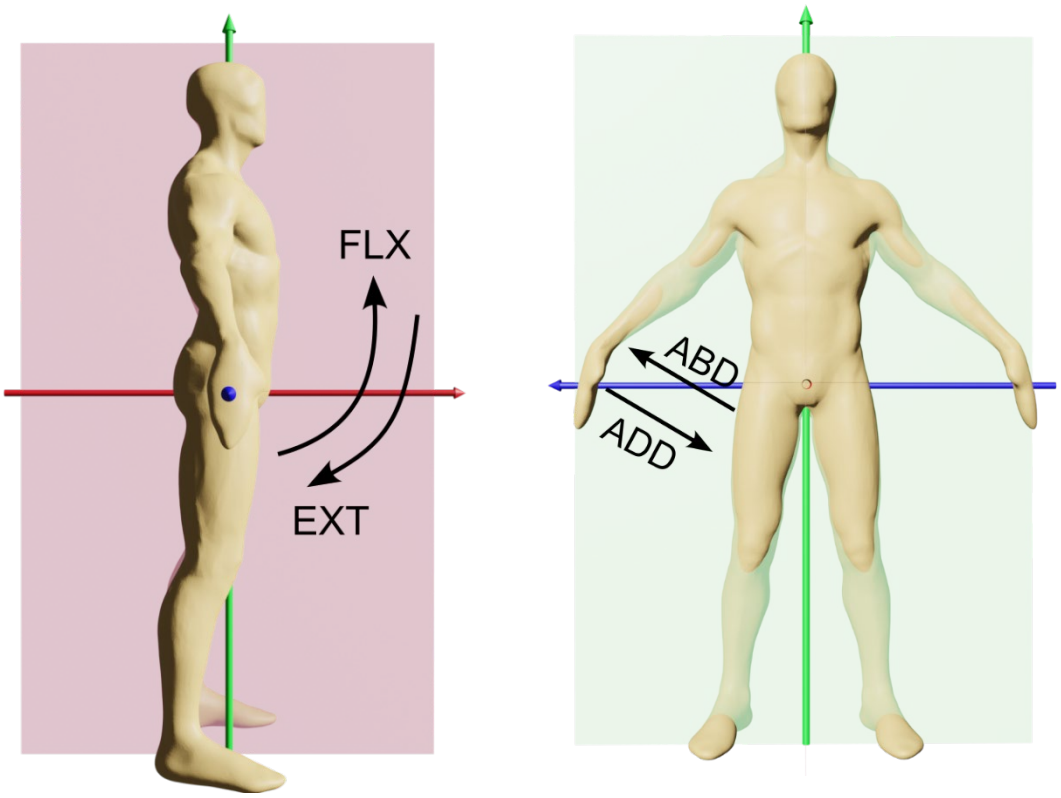

Fig. 3.2) Left: SFTR representation of the motions flexion ("FLX") and extension ("EXT", or "return of flexion") of the glenohumeral joint, in the sagittal plane. Right: SFTR representation of the motions abduction ("ABD") and adduction ("ADD") of the glenohumeral joint, in the frontal plane.

The following Table 3.1 describes the roles of the principal anatomical actors of the glenohumeral joint during anatomical motions.

Table 3.1) Anatomical actors in the glenohumeral motion, listing the acting and limiting elements per motion

Motion	**Plane**	**Axis**	**Main muscles acting**	**Main muscles preventing**	**Capsulo-ligamentous limits**
Abduction	Coronal	Sagittal	Deltoid Supraspinatus	Pectoralis major Pectoralis minor Latissimus dorsi Teres major Teres minor Infraspinatus Subscapularis	Anterior capsule Glenohumeral ligaments[1]
Adduction	Coronal	Sagittal	Pectoralis major Pectoralis minor Latissimus dorsi Teres major Teres minor Infraspinatus Sub-scapularis	Deltoid	Coracohumeral ligaments[2]
Flexion	Sagittal	Transversal	Anterior deltoid	Posterior deltoid Pectoralis minor Long head of the triceps brachii	Posterior glenohumeral ligament
Extension	Sagittal	Transversal	Posterior deltoid Pectoralis minor Long head of the triceps brachii	Anterior deltoid	Anterior glenohumeral ligament
Medial rotation	Transversal	Vertical	Latissimus dorsi Teres major Sub-scapularis	Teres minor Infraspinatus	Posterior glenohumeral ligament
Lateral rotation	Transversal	Vertical	Teres minor Infraspinatus	Latissimus dorsi Teres major Sub-scapularis	Anterior capsule Glenohumeral ligaments

[1], [2] Lugo et al (2008)

Most movements of the glenohumeral joint are accompanied by a motion of the scapula as seen in Fig. 3.3 below, and the orientation and position of the scapula is modified to allow an optimal range of motion of the humerus. Therefore, any limitation in scapular motion will have a negative impact on the GH range of motion.

Fig. 3.3) Physiological motions of the scapula (Ludewig et al. 2009). Motions of the scapula are defined as internal-external rotation (A) as seen in the superior view of a right shoulder, with the ghosted image representing increased internal rotation; upward-downward rotation (B) as seen in the posterior view of a right shoulder, with the ghosted image representing increased upward rotation; anterior-posterior tilting (C) as seen in the lateral view of a right shoulder, with the ghosted image representing posterior tilting; the glenohumeral plane of elevation (D) as seen in the superior view of a right shoulder, with

the ghosted images representing anterior and posterior positions relative to the plane of the scapula; and elevation angle (E) as seen in the posterior view of a right shoulder.

The motion of the scapula is restricted by its attachment to the clavicle via the acromioclavicular joint and is therefore restricted by the mobility of the clavicle on the sternum and the first rib (subclavius muscle). It also relies on the action of the different muscles arising from the thorax. The motion of the clavicle is mainly the consequence of the motion of the scapula.

The sternoclavicular joint is a diarthrosis linking the clavicle and the manubrium sterni. As the manubrial notch partially receives the cartilage of the first rib (Le Loet and Vittecoq, 2002), we can refer to the sternoclavicular joint as sterno-costo-clavicular (SCC) joint. It is a universal joint with three degrees of freedom and allows anterior and posterior rotation, elevation and depression, protraction and retraction, as seen in Fig. 3.4.

Fig. 3.4) Physiological motions of the clavicle (Ludewig et al. 2009). Motions of the clavicle are defined as protraction-retraction (A) as seen in the superior view of a right shoulder, with the ghosted image representing increased protraction; elevation-depression (B) as seen in the anterior view of a right shoulder, with the ghosted image representing increased elevation; and anterior-posterior rotation (C) as seen in the lateral view of a right shoulder, with the ghosted image representing posterior rotation.

The following Table 3.2 describes the roles of the different anatomical actors of the sterno-costo-clavicular joint during the physiological motions.

Table 3.2) Anatomical actors in the motion of the clavicle, listing the acting and limiting elements per motion

Motion of the clavicle (SCC)[1]	**Motion of the scapula[2]**	**Main muscles acting**	**Main muscles preventing**	**Capsulo-ligamentous limits**
Anterior/posterior rotation	Anterior/posterior tilting	Pectoralis major (clavicular portion) Anterior deltoid Pectoralis minor	Trapezius (superior fibres) Trapezius (inferior fibres) Pectoralis minor	Sterno-clavicular ligaments
Elevation/depression	Upward/downward rotation	Trapezius (superior fibres) Latissimus dorsi	Pectoralis major Pectoralis minor Subclavius muscle	Costo-clavicular ligaments Acromio-clavicular ligaments
Protraction/retraction	Internal/external rotation	Trapezius (middle fibres) Rhomboids Serratus anterior		

[1] *Ludewig et al. (2009)*

[2] *Karduna et al. (2000), Ludewig et al. (2009)*

The shoulder is a complex that includes several joints with different capacities and configurations. Each joint plays a part in the global, final movement of the upper limb.

3.1.3 Shoulder stability

Glenohumeral stability is the ability to maintain the humeral head centered within the glenoid fossa. There are two categories of stabilisers in this joint: capsules, ligaments, fascias and the labrum are passive (or “static”) stabilisers and act mainly at the end of the range of motion (Lugo, 2008), while muscles are defined as dynamic stabilisers and act throughout the range of motion (Veeger and van der Helm 2007). The muscles have a decisive role in the motion of the GH joint, and have to adapt their tension in order to compensate the instability within the three planes of space. A more in-depth description of the role of the muscles is in the next two sub-sections.

3.1.4 The muscles of the rotator cuff

The four muscles of the rotator cuff (Supraspinatus, Infraspinatus, Teres minor and Subscapularis) are deep muscles that originate from the scapula and connect to the head of the humerus, and that play a major role in GH stability, and also in the rotation of the humerus. They form a cuff around the GH joint as they cover the anterior, superior and posterior part of the capsule. Their fibres are oriented transversally and the scapula moves on the thorax accordingly to the humerus in order to maintain the most effective action of those muscles on the humerus. With the arm in neutral position hanging beside the body, the four muscles of the rotator cuff are the main actors of the axial rotation of the humerus. The supraspinatus, infraspinatus and teres minor are lateral rotators of the humerus while the subscapularis is a medial rotator. The rotator cuff muscles are particularly suitable for providing compressive forces to the joint without introducing large moments due to their small moment arms, compared to the prime movers such as deltoids.

3.1.5 Several layers of muscles working together

The shoulder is made up of several muscles acting on the glenohumeral joint that are arranged in two layers.

The deep muscle layer, comprised of the rotator cuff muscles, depending on the level of contraction can either change its rigidity and therefore compensate the instability of the shoulder, or allow the motion of the humerus in relation to the scapula. It has to act in a precise sequel/sequence of timings of contractions to allow a good balance of rigidity and mobility throughout the movement (Longo et al. 2011).

The superficial muscle layer is mainly responsible for the flexion and abduction – or general elevation - of the shoulder. It is made up of the deltoid that has three distinct sets of fibres (the anterior deltoid is responsible for shoulder flexion, and the lateral and posterior deltoid is responsible for abduction. The posterior deltoid also participates in lateral rotation). The timings within the deltoid are complex as it is possible to differentiate up to 19 muscle segments organised in seven groups (Brown et al. 2007).

Each muscle layer has a precise timing to respect in order to achieve their respective function throughout a motion, and those two layers have to interact together in a seamless way. **The scapula** is controlled by muscles arising from the trunk on its anterior aspect (pectoralis minor), lateral aspect (serratus anterior), and posterior aspect (trapezius, rhomboids, levator scapulae). Therefore, the scapula needs to be stabilised and oriented to allow precise motion of the humerus. The synchronized kinematic interaction between the humerus and the scapula was first described by Codman in 1934.

The muscles around the glenohumeral joint as well as the muscles stabilising and orienting the scapula have to work in harmony and at a precise timing, which **defines cocontraction,**

co-activation or co-ordination patterns. These patterns are dictated by the biomechanics of the anatomy and bone structure, and **the fine tuning of this pattern and timing is individual to every subject. It is also variable and can be modified by external factors (such as goal constraint) or by internal factors** (such as morphology, force, flexibility, past medical history, training, tiredness, etc.), and therefore the exact patterns of muscle contraction in GH stability remain poorly understood (Belli et al. 2023).

The norm of muscle patterns (MP) in the upper limb is based on variable normal kinematics (compared to the lower limb for example). Therefore, a considerably large variation in muscle patterns and associated muscle activity profiles is commonly accepted as normal, in order to represent the diversity of healthy kinematics. As a consequence, single reference surface electromyography could be of limited value in distinguishing pathological muscle activity patterns, or at least in assessing them.

In other words, each unique kinematic pattern in the normal solution space can be the result of a range of normal muscle forces and therefore the accepted normal shoulder muscle activities are even broader than the normal kinematics. The norms of function, kinematics and MP are independent, as normal function could exist with abnormal kinematics (and therefore abnormal MP), and normal function and kinematics could exist with an abnormal MP.

While the standard approach, described above, of describing muscle pattern with one large norm might be relevant in the lower limb for most applications due to the limited angle variations, it only allows to highlight very extreme impairments in the upper limb (i.e. patterns that would fall outside of the solution space of all the normal kinematics).

Therefore, assuming normal motion - so if the function is normal and the kinematics fall within the norm - there is a potential for false-negative (EMG would appear normal) in the muscle patterning that would provide no useful clinical information on the inner workings or potential muscle control impairments. Similarly, if assuming abnormal kinematics, the EMG data becomes of little relevance as it should also appear out of the norm. **For these reasons, narrowing down the muscle pattern accepted solution space to each specific kinematics** by solving a load-sharing problem (which is covered in section 3.4) could allow for a better estimation of muscle pattern impairments.

3.1.6 Conclusion of functional anatomy

The shoulder is a complex layout of joints, passive and active elements. Its biomechanics, kinematics and optimal efficient functioning depend on static and dynamic stabilising structures. It also relies on the synchronisation, the timings and the balance of activation and cocontraction amongst different muscles, muscle groups and muscle layers that contribute to both the mobility and the stability of the shoulder girdle and more specifically of the glenohumeral joint.

The general tendency of cocontraction patterns and timings are dictated by the structure and biomechanics of the shoulder as well as the activities undertaken. The patterns are variable in time and adapt to internal and external factors. Failure or disturbance of one or more of these mechanisms will break the overall harmony, potentially impacting stability and motion. In a snowball effect, instabilities can lead to perturbations in the proprioception and neuromuscular control, and to a misuse of the different anatomical components with overloading for example. Ultimately, this can lead to wear and tear, pathologies, pain, reduced range of motion or function, and can therefore impair the shoulder (Vinti 2012, Morrison et al. 2000, Bateman et al. 2018). Shoulder pathologies, with a focus on shoulder instabilities which are associated with major biomechanical changes, are the focus of the next section.

3.2 Shoulder pathologies and Shoulder Instability

The shoulder girdle is more complicated than it first appears. The two previous sections, anatomy and functional anatomy, showed the complexity of interaction of the many elements of the shoulder girdle, as well as the need for stabilisation of the highly mobile GH joint.

Due to its mobility and its use, many elements and mechanisms can go wrong in the shoulder. With so many elements relying on each other, the classification of shoulder pathologies is not an easy task and several models of general classification for shoulder pathologies have been developed.

The next two sections (3.2.1-2) review common shoulder pathologies, classification and clinical management as well as the standard ways of assessing the shoulder. Sections 3.2.3-4 focus on Shoulder Instability and present its specific challenges.

3.2.1 Common shoulder pathologies and their clinical management

The variety of actors on which the shoulder girdle relies for an efficient functioning throughout large ranges of motion, as well as the elaborate functioning of all its active parts to ensure both stability and mobility, make disorders and impairments of the shoulder a common musculoskeletal problem. Classification systems and diagnostic algorithms have been developed to inform diagnostic and clinical decision making.

Pathoanatomical diagnoses are based on a likelihood that specific tests or examinations can be linked to a specific condition, and look into identifying an anatomical cause, such as labral or muscle tears, adhesive capsulitis, glenohumeral instability or arthritis (Palmer et al. 2000, Uhthoff et al. 1990). This approach suggests that each pathology will receive a standardised care, which can be problematic when patients exhibit varying degrees of

possibly overlapping impairments that might require a more personalised rehabilitation approach.

Rehabilitation models do not focus on a specific anatomical cause nor look for it, and base the treatment decisions on physical assessment findings throughout the rehabilitation (Huges et al. 2008, Lewis et al. 2008, Klintberg et al. 2015, Ludewig et al. 2022). It is for example examining the impact that posture and surrounding joints, as well as strength and flexibility, have on the symptoms.

The STAR-Shoulder (Staged Approach for Rehabilitation Classification of Shoulder Pain) attempts to incorporate both of the above models to inform clinical decision making, using the pathoanatomic model for the initial diagnosis and informing treatment decisions through rehabilitation approaches (McClure, 2015).

Amongst the most common shoulder pathologies, such as rotator cuff tear or tendinopathy, adhesive capsulitis and acromioclavicular joint abnormalities, shoulder instabilities are ones of the most complex to classify and rehabilitate.

3.2.2 Standard shoulder assessment

Several outcome measures are used to assess the patient during the course of rehabilitation (Wilcox et al. 2005). Numerous shoulder tests, assessments and protocols are used in clinical practice. Some of the most common are listed below in table 3.3 with a summary of the information they gather.

Table 3.3) Summary of the most common shoulder tests used in clinical practice

Name of the test	Main Information gathered
Constant-Murley Shoulder Score (CMS)	Pain, activities of daily living, strength, range of motion
Upper extremity functional index	Difficulty of performing 20 functional tasks
Disabilities of the arm, shoulder and hand (DASH)	Difficulty of performing 30 functional tasks
Quick-DASH	Same as above, with 11 questions on functional tasks
Shoulder pain and disability index (SPADI)	Rates shoulder pain and disability on 13 items
Penn Shoulder Score (PSS)	Difficulty of performing 20 functional tasks
Simple shoulder test	Difficulty of performing 12 functional tasks

The Constant-Murley Score (CMS) is considered as the gold standard for shoulder assessment. CMS is promoted by the European Society of Shoulder and Elbow surgery (ESSE) in addition to being available and used in many different languages (Rocourt et al. 2008, Katolik et al. 2005). Unlike the others, CMS gathers subjective and objective information and takes into account ROM, strength and basic functional tasks. The other protocols are mainly subjective based on questions regarding pain and ADL, thus require an additional assessment of ROM and strength to be performed by the clinician.

The tools that are used to conduct the examination are generally based on “tradition or what was learned during initial professional training” (Cleland et al. 2011) and on the time and accuracy required by the examination (Clarkson and Hazel, 2013). Normal equipment includes goniometers, tape measures, inclinometers, and more rarely plumb lines. Visual examination is also used when time matters (for a rapid assessment) or when there is no need or possibility for accuracy (Magee 2006, page 26).

Based on the definition of the International Classification of Functioning, Disability and Health (Ustun et al., 2010), the functional scales described above allow the assessment of **disability** (task accomplishment and function such as reaching, etc.) and can measure the **recovery** (the change in the ability to perform a task or function). They do not allow the assessment of the inner workings of the shoulder girdle, i.e. the **impairments** (muscle patterns, coordination, etc.) which indicate the presence of compensatory strategies. A compensatory strategy is, for example, bending the trunk or over-using certain muscles or muscle groups while performing a task and is an indication of the performance of the task and of the quality of the recovery (the reappearance of “healthy” motor patterns). Compensatory movements, such as modified cocontraction patterns, can help in recovering function in the short term but can also lead to long-term complications (Levin et al. 2008). Some shoulder assessment scales or assessments do take impairments into account, but are not based on objective measurement tools and are therefore lacking reliable high-quality data.

Conclusion of standard shoulder assessment

The traditional tools allow for the assessment of range of motion and subjective muscle strength, and do not allow for the assessment of muscle activity. None of the standard tests reviewed in this section takes them into account. As a consequence, the cocontraction patterns are not generally studied in standard clinical setting nor taken into account during the rehabilitation of the patients. In this way, standard assessments focus on the evaluation of disability (function) and not on the objective evaluation of impairments (strategies used during function).

3.2.3 Shoulder instability

In a very simple way, Shoulder Instability is the opposite of shoulder stability, to an extent that is detrimental enough to be pathological. Anatomically, what happens (the mechanism, or the “how”) is that the head of the humerus is sliding out of the glenoid. Therefore, Shoulder Instability is a pathology that disrupts the mechanisms presented in the functional anatomy section that normally keep the glenohumeral joint stabilised during motion.

As the humeral head is unable to be maintained properly in the glenoid fossa, shoulder instability ranges from a slight ‘catching’ feeling to a full dislocation. This can be due to a disruption in the integrity of bony, ligamentous or muscle structures around the glenohumeral joint, to a disruption in muscle control, or to anatomical variations like a shallow glenoid for example. Shoulder instabilities can be directional as they occur on different aspects of the glenohumeral joint: anterior, posterior, or multiple directions. Anterior dislocations have the highest prevalence and can occur in 1.7% of the general population (Hettrich et al. 2019).

There is very limited research and robust scientific data evaluating shoulder instability in the general population and more specifically in young people. Current literature on its overall incidence, prevalence, mechanisms and long-term outcomes either focuses on case studies, specific surgeries or does not isolate this age group, therefore current knowledge is extrapolated from related but not directly comparable studies. However, dislocations in patients appear extremely rare under 10 (Leroux 2015, Zacchilli 2010) and in the 10-14 year-old range (Longo 2020, 2021). Subjects around the age of 20 are at most significant risk of dislocating their shoulder (Longo 2020). The incidence in the 10-19 year-old range is 39.17 per 100.000 people per year, compared to 47.76 in the 20-29 year-old range

(Zacchilli 2010), although the reported incidence and age vary depending on the studies (Kroner et al. 1989, Simonet et al. 1984). Males are often reported as being twice as likely to develop shoulder instability in all age groups including under 16, and are more likely to have a traumatic onset (Lawton 2002, Longo 2020). Approximately 10% of people who presented to emergency departments in America and Denmark with a shoulder dislocation could not identify a traumatic onset, which is likely to be an underestimate as people with atraumatic shoulder instability can experience multiple episodes before presenting to a healthcare professional (Lawton et al. 2002, Leroux et al. 2015, Hung et al. 2020).

There are two types of instabilities. Traumatic instabilities result from a dislocation with a loss of joint integrity (Shields et al. 2018). It is estimated that over 90% of the shoulder dislocations result from traumatic cases (Hayes et al. 2002), and they are often associated with rotator cuff tears (Gomberawalla and Sekiya, 2014), glenohumeral ligament lesions and loosening of the joint capsule. Atraumatic instabilities can appear slowly over time with repetitive microtraumas often due to overhead motions as found in sports. They can also be caused by symptomatic congenital laxities (presenting with pain or abnormal function (Bateman et al. 2018)), bony anomalies, or control issues. Control issues are either due to underlying neurological pathologies (Makki et al. 2014), or due to a poor synchronisation or weakness of the muscles (Ansanello et al. 2018) as discussed in 3.1.5.

Defining two main types (traumatic and atraumatic) of shoulder instability is however oversimplifying and can be misleading. The causes as well as the clinical presentation (the symptoms) are diverse, multiple and complex and have led to many different definitions (Kuhn 2009) that attempt to answer the fundamental questions such as “to what extent does the humerus dislocate?”, “how frequently?”, “does it need to be accompanied by an impairment?” or “to what extent is it part of the normal constantly changing neuromuscular system?”. The multitude of definitions lead to a plethora of classification

systems that have been subsequently developed (Lewis et al. 2004), sometimes with a great amount of discordance that can lead to different diagnoses depending on the system used (McFarland et al. 2003). Two main categories of classification systems are described below.

The simple classification systems

Sometimes, the cause of instability is clear and identified, and the "how" (mechanism) also answers the "why" (cause): it is the case in some congenital deformities like a shallow glenoid, or more often in traumatic cases where a specific anatomical structure has been damaged. For example, tears in the labrum of the glenoid can be seen on an MRI, and could explain both the mechanism of dislocation and the cause (no or less cartilaginous support at a specific place).

In those straightforward cases, simple models such as TUBS (Traumatic Unilateral dislocation with a Bankart lesion requiring Surgery) and AMBRI (Atraumatic, Multidirectional, Bilateral, Rehabilitation, Inferior capsular shift) (Thomas et al. 1989) are relevant, and have a similar approach to the pathoanatomic models of the previous section on general shoulder pathologies. Simple models generally recommend surgical intervention to remove an anatomical cause, which should logically remove the symptoms by restoring – to the best extent possible – function to prior level. In these uncomplicated and well identified cases, the rationale is simple, backed-up by numerous studies showing good clinical outcome as seen in the next section, and the clinical management follows well defined protocols. However, reality is not always that simple, and while these approaches are intuitive to use in a clinical setting, they also fail to capture the complex

presentations and the key role of muscle patterning (Lewis et al. 2004). For this, reason, different systems were developed.

The complex classification systems

Sometimes, none of the possible anatomical causes – even when all combined – could fully explain or truly justify the symptoms. For example, very minor damage in the glenoid labrum and a small degree of laxity in ligaments could fail to explain frequent dislocations or the associated impairment. At other times, such as in some atraumatic cases, no anatomical cause can be found while dislocations still persist. In both those cases, when there is no clear anatomical cause, more information has to be taken into account such as the way the muscles that control the shoulder girdle and stabilise the GH joint work (muscle patterning). For these reasons, more complex classification systems such as the Stanmore Classification or Bayley Triangle, or FEDS (Kuhn, 2009), have been developed, that take into account the four most common features that are aetiology, direction, severity and frequency.

There is no perfect classification system as it is always a trade-off between usability and accuracy, is highly dependent on the definition used for shoulder instability, and this pathology is generally complex. This has led to much confusion in the literature. Standardising the definition in shoulder instability could allow comparing treatments (Kuhn, 2009) and ultimately help determining standardised classification systems in the future.

Many studies have been published on shoulder instability, assessing reflexes, force, muscle activity patterns and kinematics of different categories of shoulder instability and during different movements. The electromyography recordings often involve intramuscular

electrodes to access the deep muscles (Barden, 2005, McMahon, 1996, Morris, 2004, Pizzari, 2008), and the motions often cover standard physiological motions of flexion and extension, abduction and adduction of the arm, or standardised motions on equipment such as arm cycling (Hyndza, 2006).

The result of the studies regarding the muscle activity patterns are often contradictory or assess different parameters.

Hundza (2006) reported, in 21 participants, an increased activity of the deltoid, upper trapezius, infraspinatus and serratus anterior only in physiological motions and not in functional tasks such as reaching, while the supraspinatus was found having less activity in the shoulder instability group in a study by McMahon (1996), and was found having similar activity that the control group by Morris (2004).

Barden (2005) in a study on 7 multi-direction shoulder instability patients found difference in timings of activation of several muscles but no in the overall amplitude. One specific muscle, the pectoralis major, was found active throughout the motions of shoulder flexion and extension in SI patients while it had distinct activity patterns in the control subjects. Jaggi (2012) found, in 131 patients and on average, an increased in the pectoralis major, latissimus dorsi, deltoid anterior and infraspinatus, while Pizzari (2008) found no difference in these muscles and reported a lower activity of the trapezius in the shoulder instability group.

Overall, a review of 12 articles by Struyf (2014) found no consensus in muscle patterns of shoulder instability due to the contradiction of some results. This could be closely related to the range of possible clinical presentations described in the previous section covering the numerous classification systems.

From a kinematical point of view, apart from an increased translation of the head of the humerus in the direction of the instability, there is also no consensus in the literature. Spanhove (2021), in a review of 12 articles, found moderate evidence that shoulder instability patients have less upward rotation and more internal rotation of the scapula during arm elevation in the scapular plane, which is directly contradicted by Ernstbrunner in 2022 who reported, in 20 patients, an increase in upward scapula rotation.

The current knowledge on shoulder instability is also focused on adult populations with limited information available in young people. The differences in clinical presentations or response to treatment between adults and young people are still unclear (Lawton 2022). One of the largest studies available from Lawton (2002) focuses on the 13-16 age range and found that strength and range of motion was likely to be normal while the main complaint was instability and pain, which is similar to the reports in older age groups (Maruyama 1995). The diversity of subluxations (such as complete dislocations or multidirectional instability) also appears similar to adults, therefore most characteristics and parameters that do not depend on modelling or rely on electromyography assessments closely parallel those in adults.

Clinical assessment and outcome measures

In standard clinical settings, the assessment of shoulder instability can differ from the standard shoulder assessments seen in 3.2.3. In addition to imaging techniques, the clinical assessment of shoulder instabilities - and therefore the different forms of clinical presentations - can include:

- Observations of muscle wasting, dynamic scapula winging, or of limited active range of motion in overhead positions due to pain or apprehension.

- Hypermobility assessment with the Beighton score, or the observation of excessive shoulder range of motion in external rotation (>90°) or abduction (>180°) (Bateman et al. 2018). The Beighton score quantifies the laxity and hypermobility of different joints of the upper limb, taking into account active and passive motions.

- Laxity tests (sulcus sign, load and shift test, shoulder drawer test) that are rather subjective due to some patients not being able to relax their muscles and due to the lack of objective outcome measure in the “feeling of excessive movement”.

- Instability provocation tests such as the apprehension test (or Crank test), the relocation test, and the posterior jerk test.

- Subjective isometric muscle power compared to the contralateral side, with resisted ranges of motion, and special tests for the external rotators such as the “full can” and “empty can” tests.

- Evaluation of the muscle-patterning through manual palpation of muscle tone, which is difficult to assess without the means of EMG. Jaggi et al. (2012) found that manual assessment was only able to find 11% of 122 muscle patterning cases identified with EMG.

There are validated outcome measures for shoulder instability, such as the Oxford Instability Shoulder Score (OISS), the Rowe score, the Melbourne Instability Shoulder Score (MISS) and the Western Ontario Shoulder Instability Index which has the most supporting evidence (Rouleau et al. 2010). As outcome measure, these tools are used to monitor the efficacy of a given treatment throughout the rehabilitation, however they only provide subjective reports from the patients.

Management and treatment

The existing guidelines are different for traumatic or atraumatic mechanisms (Brownson et al. 2015, Noorani et al. 2019). During the management of traumatic instability, early mobilization is indicated for all age ranges and demographics. For young and active male athletes, surgical referral is indicated within 6 weeks given the risk of recurrent instability. For atraumatic instability, initial conservative management through physiotherapy is recommended, with a positive outcome in 50% to 80% of cases (Burkhead and Rockwood 1992, Burkhart and De Beer 2000). A systematic review of physiotherapy treatment programmes for atraumatic shoulder instability identified a single control trial comparing two exercise programmes, with the Watson programme resulting in better outcomes at 12 and 24 weeks (Warby et al. 2018, Griffin et al. 2022). However, this program has not been widely adopted in practice, possibly due to its complexity (Griffin et al. 2022, Philp et al. 2022).

A challenge that clinicians face when dealing with shoulder instability is the difficulty of getting and providing objective, quantified feedback on muscle control and muscle activity in general, which is always a key component of shoulder instability. Clinicians rely on subjective visual inspection or manual palpation to assess muscle patterns and activities which can lead to incorrect or partially incorrect identification of the specific muscle activities in 91% of the cases (Jaggi et al. 2012). From the patient's perspective, while function is a conscious phenomenon, the specific kinematics and their underlying muscle activity is not.

In adults, the cocontraction patterns and timings of activation are constantly adapting to internal factors (such as tiredness, injuries, physiological changes, etc.) (Belli et al. 2023)

and to external factors (physical activity, function, etc.), as covered in part 3.1.6 “Conclusion of functional anatomy”. Young adults are possibly required to adapt even more, as they undergo strong physiological changes inducing a constant adaptation of their central nervous system to follow the normal maturation.

In pathological situations or after traumatic events, however, several factors such as pain or fear might have longer lasting effects on muscle patterns than the anatomical damage would dictate alone. The patient could instinctively keep avoiding a certain situation or motion which in turn could impede a re-patterning, entering a vicious circle. If the changes impact function, a clinician can guide the motion to induce re-training. If or when the motion appears normal, muscle activity can be guided as well, away from detectable wrong patterns so as to allow the central nervous system to adapt. The Alexander technique (Preece et al. 2016) is one example of a) the importance of the clinician in providing guidance and b) the importance of the patient to have access to feedback, in order to become aware of harmful habits of muscle use and unlearn those unwanted patterns. Increasing proprioceptive awareness - the general sense of positioning, movement and force or tension (Ager et al. 2020) - can guide the patient into improving their coordination and preventing harmful habits of muscle use and shoulder therefore be considered in clinical practice. This is however constrained by the limited ability of clinicians to assess muscle patterns, and by the limited ability of the patients to perceive their own proprioception in general. This is an area that can benefit from technology such as electromyography, together with the use of biomechanical models. Valuable information can be gained from models that can provide quantitative data on the way patients are moving or on the way patients are controlling their muscles to inform clinical decision making and guide rehabilitation while empowering the patients. Existing research

making use of the models to provide biofeedback is often centered on evaluating its impact on stroke rehabilitation. In general, the literature shows benefits such as Lirio-Romero et al. (2020) who demonstrated a significant increased upper extremity motor function using biofeedback of joint angles and levels of muscle activation. That information could also be useful for shoulder instability patients in making them more aware of the motions there are making.

3.2.4 Outcomes of shoulder instability

There is extensive literature on the outcome of shoulder instability surgeries and conservative management. **Most studies show an overall positive outcome** for different surgical interventions of traumatic instabilities (Guala et al. 2018, Brilakis et al. 2018, Coughlin et al. 2018, Levine 2018, Lazarides et al. 2019) with variable satisfaction, and limitations in function being more frequent after some surgeries than others (Dumont et al. 2011), and also show generally positive outcome for conservative management of atraumatic instabilities (Watson et al. 2018, Hayes et al. 2002).

However, the numbers reported vary greatly between the studies. This can be due to the fact that inclusion criteria and assessment tools are not consistent across the studies (Robinson et al. 2006, Warby et al. 2013), that it is difficult to follow-up certain categories of patients, or that depending on the study the clinical tests used for the clinical outcome measure are based on different tests (Jaeger et al. 2004, Robinson et al. 2006), some of which are described in section 3.2.2. This variety is also found in clinical settings. A survey on nearly 200 surgeons from different countries reveals that there is a high variety and no consensus in the use of diagnostic tools (Weel et al. 2016).

The questionnaires used can ask the patient about functional activities, return of shoulder function and ROM, stability and Visual Analog Scale (VAS) for pain (Jaeger et al. 2004), or ask about any additional dislocations, symptoms or treatment (Robinson et al. 2006). It is also mentioned that the patient-reported outcome measures are sometimes not used on appropriate group-ages, and that there is a need for a more standardised outcome measure across the studies (Kocher, 2018).

Overall, reviews either ask for more high-quality studies (Barlow et al. 2018, Warby et al. 2013) or mention the poor quality, inconsistencies (Harris et al. 2013, Coughlin et al. 2018, Warby et al. 2013) or risk of bias of the studies (Warby et al. 2013), which limited their abilities to make definite statements on the outcome of shoulder instabilities (Coughlin et al. 2018, Barlow et al. 2018, Lazarides et al. 2019, Warby et al. 2013). This makes the estimation of pain, deficit of function, ROM or strength, difficult in shoulder instability patients.

Muscle patterning is not part of the standard clinical outcome. As seen in 3.1, in clinical settings muscle patterning is "grossly underestimated" (Lewis and Bayley, 2004) and sometimes not taken into account (Weel et al. 2016), or only using manual palpation which is not reliable at identifying poor patterns (Jaggi et al. 2012). Lewis and Bayley (2004) emphasise the importance of a normal scapulothoracic rhythm, based on a smooth and coordinated muscle coupling activity, in maintaining dynamic constraint to the glenohumeral joint. They state that electromyography should be used during the clinical assessment and report observing, in their own patients, over-activity of the rotator cuff muscles in patients with generalised laxity. However, as seen in 3.2.3, there is no consensus on the clinical presentation of muscle patterning of shoulder instability.

Unstable shoulders often present with abnormal muscle patterning. Studies find that 93% (on 131 recurrent instability shoulders) (Jaggi, 2012) to 100% (on 11 multidirectional instability shoulders) (Barden, 2005) of the patients had abnormal patterns prior to surgery. This is often associated with a deficit in proprioception (Barden 2005). More detail has been given in 3.2.3 on how the abnormal muscle patterning was analysed in the different studies.

Addressing abnormal patterning can increase the likeliness of a good outcome. When there is no clear anatomical cause for the instability, such as some atraumatic presentations, the involuntary recruitment of abnormal couples can be the cause of the dislocations (Lewis et al. 2004). Addressing this is mostly done with specialised physiotherapy treatments based on biofeedback, proprioceptive treatment and glenohumeral and scapulothoracic pattern correction (Burkhart et al. 2003), which is further developed in part 3.2.2. Otherwise, abnormal force couples applied on the joints, due to abnormal muscle forces, will interfere with a successful outcome. This is not always possible however, but these options should be explored first, and further clinical decision should be made accordingly.

Conclusion of Outcomes of shoulder stability

The same way the definition and standardisation of classification systems of shoulder instability proved difficult in the previous section, estimating its clinical outcome is problematic. Reviews recommend better quality studies that are more consistent in their design. In general, muscle patterning should be assessed in clinical practice using specialised equipment such as electromyography, and it is believed to be a key element in some atraumatic cases, and in rehabilitation for all shoulder instability types.

3.2.5 Conclusion of shoulder instability

Shoulder instability has a high variety of causes and can have complex clinical presentations. Consequently, it has many definitions, and no clear consensus or standardisation for its definition, classification or management. This is especially true in young populations where the evidence available is based on small size studies with design limitations that present highly variable results (Leroux, 2015) – partly due to their

dependency on parents for accessing health service. It is therefore likely that young adults are diagnosed and treated based on generalisation from the data available in adult populations, while their neuromuscular system might behave differently as it is constantly developing alongside possible changes to their body structure, body function and personal factors that can contribute to the impairment of their instability (Seyres and Philp, 2024). Given the limited data available in young population compared to adults, the known differences in motor control as well as the extrapolation and assumptions made from adult studies make, more research focusing on this age group is needed.

Shoulder instability is intimately linked to the overall biomechanics of the shoulder and can be the consequence of a disrupted pattern of contraction of the muscles of the shoulder, or be the cause of a disrupted pattern. Muscles are the actors of the motion, and regardless of if they manage to compensate for the anatomical variations (traumatic, atraumatic or congenital) they are a key element of the whole system. This new biomechanics changes the normal pattern and timing of cocontraction of the muscles of the shoulder girdle (Walker et al. 2015) and forces the individuals to learn a new way to use the different elements of their shoulder by finding new, individual cocontraction patterns and timings to perform functional tasks and regain range of motion. As seen in 3.2.3, difficulties in finding optimal and efficient patterns, regardless of the overall function, can negatively impact the recovery in addition to leading to further impairments. Muscular activities and kinematics therefore provide important clinical information to study the impact of shoulder instabilities, and it could increase the success rate of conservative (Jaggi et al. 2012) and surgical management.

Muscle patterning diagnosis is however not part of standard clinical shoulder protocols. The tools used in standard clinical practice do not allow to assess precisely the muscular activities during a motion and therefore do not allow to monitor the changes in the new pattern developed by the patient. Such equipment exists and is used in research and specialized settings. The next section will review the tools that can gather useful biomechanical information in this situation and that are not used in standard clinical practice. Some of the preventing factors of their use in standard practice will also be analysed.

3.3 Research and specialised equipment, clinical benefits and barriers to its use

3.3.1 Motion capture

There are many ways to assess kinematic measurements such as ranges of motion, and this section reviews the main methods used in biomechanics. In clinical applications, it is the role of the clinician to decide what tools they want to use, based on how much reliability is acceptable in one specific context (Cleland et al. 2011).

Goniometers are mechanical devices that allow measuring a joint angle in a single plane of motion. This requires placing the goniometer manually around the joint of interest throughout the range of motion, and therefore stabilising the joint, palpating the appropriate bony landmarks and reading the measures. While these techniques are quick and portable which makes them popular in clinical practice, they are limited to accessible single joints and motions, and each step of the manual process can increase the error in measurement. Electro-goniometers are a digital alternative that increase accuracy (Christensen, 1999) but suffer from the same limitations introduced by the manual handling.

Inertial Measurement Units (IMU) report the angular rate and orientation of a body using a combination of gyroscopes, accelerometers and magnetometers. They are increasingly used in biomechanics to track joint angles (Gu et al. 2023), and provide an affordable and portable solution to many clinical applications. Their accuracy is impacted by challenges in the calibration and filtering (most notably in drift over time (Digo et al. 2022)), and they are currently overall inferiorto marker-based motion capture systems.

Markerless 3D cameras capture can be based on a single or on multiple cameras. They both present advantages over the marker-based approach that is reviewed in the next

paragraph, as they allow quicker examinations, eliminate the need for manual palpation, and provide increased portability in the case of single cameras. It is however recognised there is a trade-off between usability and accuracy (Scott et al., 2022), which can vary greatly depending on the joint and motion assessed, the morphology, and more generally depending on the training data on which the markerless approach relies. The accuracy has been found comparable to that of a goniometer in shoulder abduction (Johnson et al. 2015), although many parameters can vary. Overall, the accuracy is still inferior to that of marker-based approaches for most clinical applications (Scott et al. 2022), and limitations such as a reduced field of view (occlusion) in some motions and poor performance determining axial rotations make this technology impractical in some cases.

Camera-based 3D motion capture systems are the state-of-the-art in clinical motion capture. They yield the best accuracy compared to the alternatives reviewed above, and allow the simultaneous assessment of several joints in different places. Spherical markers with infrared reflective material are typically taped on bony landmarks and detected by the cameras that emit infrared light. A calibration procedure is required that uses Direct Linear Transformation to establish the relationship between the 2D coordinates of the image of each camera and the 3D location in space. During calibration, a wand that has markers placed at a known distance from each other is typically used. The wand (rigid body with markers) is then moved in space in front of the fixed cameras. This provides information on where the cameras are with respect to each other (position and orientation). Additional use of markers typically placed on a rigid body (“L-shaped”) on the floor provide the direction of the cameras with respect to the environment (ground and world axes). Once this is established (the calibration is done), the 3D position of each

marker can be calculated inside the calibrated space so long as the cameras are not moved.

This approach allows for the most versatile and flexible joint angle determination. Using markers mounted on rigid clusters and strapped on a segment reduces visual occlusions, and allows local coordinate systems to be determined in a standardised way which is covered in more detail in part 3.4.2 that covers inverse kinematics.

3.3.2 Muscle activity

Electromyography (EMG) is a technical means of assessing the electrical activity produced by the contraction of a muscle. As a muscle contracts, muscle fibres – or more precisely each motor unit, comprised of one motor neuron and several muscle cells - form a myoelectric signal that can be detected by the electrodes of the EMG and used to assess muscle activity.

The most common use of EMG is surface EMG, with electrodes placed on the surface of the skin. High density EMG uses arrays of electrodes for a higher spatial resolution and to gain information on the different muscle fibres and on the conduction velocity.

To investigate deep muscles, the electrodes can be placed inside of the belly muscle with a needle (“fine wire electrodes”) as seen in Fig. 3.5 below.

Fig. 3.5) Fine-wire EMG placed by a needle (Konrad, 2005)

EMG signals are commonly band-pass filtered between 10-400Hz. Then, in order to calculate an activation level from the signal, a full-wave rectification can be performed (i.e., obtaining the absolute value of the signal) followed by a low-pass filter with a cut-off frequency of 6Hz using a second order Butterworth filter (Winter, 2009) that provides the linear envelope. This last step is the equivalent of a moving root mean square (RMS) with a moving window that is also commonly used.

3.3.3 Barriers of use of technology in standard practice

There are several preventing factors to the use of specialised equipment in standard clinical setting. Amongst them, the cost is likely to be too high for standard practice (Lehman, 2004) and the skills involved might involve too much training time. This could also have a repercussion on the time needed to use the equipment- as the more complex the equipment, the more time it will take for the clinician to perform the assessment. In the original publication of what is today the gold-standard of the shoulder assessment ("CMS" as seen in 3.2.2), Constant (1987) explicitly described that the main objective of the shoulder tests is to be "easy to perform" and have to require "a minimal amount of time for evaluation" estimated between 5 to 7 minutes to be completed. Finally, acceptability for the patient is an additional aspect to take into account.

3.3.4 Conclusion of research equipment

Several technologies from specialised settings can be used to gather the data necessary to assess the outcome of shoulder instability patients. Using technologies such as EMG and three-dimensional cameras to study the shoulder before and after surgery or throughout rehabilitation provides several advantages compared to a standard assessment. More specifically, it allows, via the use of biomechanical models described in the next section (4.4), the assessment and the studying of contraction patterns and of range of motion. Both technologies bring objective, accurate and reliable information during the assessment as well as comparative data during the follow-ups.

3.4 Musculoskeletal modelling

Musculoskeletal (MSK) models allow the studying of the complex dynamics that underlie human movement. Research in MSK modelling has expanded in the past 30 years (Hicks et al. 2015) and allows applications in a large range of clinical scenarios, such as calculating internal forces, joint angles and loads. A typical MSK model is a set of mathematical equations describing a physical (human) system, in the form of rigid multibody skeletal structure in which bodies (bones) move relative to each other in the presence of internal (such as muscle forces) and external forces (such as gravity or added weights). Simulations are the result, or outputs, of a model that allows the studying of specific aspects or components.

This section reviews the main components and models relevant to this thesis.

3.4.1 Introduction to musculoskeletal models

A model is composed of rigid bodies, moving in relation to each other, a graphical illustration of which is presented below in Fig. 3.6. Each body is defined in a local coordinate system defining a joint permitting motion representative of the physiology, and international standards have been set for the formulation of internal coordinate systems of multibody dynamic models (Wu et al, 2005). While many anatomical components can be integrated such as menisci, ligaments or fasciae, and many axes of motion can be defined in specific ways based on three-dimensional scans for example, a typical MSK model is based on reasonable approximation of the underlying physiological components and system in the form of basic mechanical joints and muscles, with added constraints.

Fig 3.6) Graphical illustration of a rigid-body musculoskeletal system (Bourgain et al. 2018) from two different angles. The scapula is highlighted in two different positions.

Models are commonly validated based on experimental data based on dissections and imaging procedures, and these parameters are then often scaled which is covered at the end of this section.

3.4.2 Muscle models

In musculoskeletal models, the actuators controlling the degrees of freedom of the model are typically muscles based on the Hill-type muscle model (such as the Millard (Millard, 2013) or Thelen (Thelen, 2003) models) that consist of a contractile element with two spring elements, one in series that represents the tendon and one in parallel that defines the passive force of the connective tissues. It defines the force-generation behaviour of the muscle based on a force-length-velocity relationship.

The general geometry of a muscle-tendon unit can include detailed via points, insertion points and wrapping objects, in order to ensure realistic muscle lines of action in all configurations of the model. Each muscle is also defined by individual internal parameters, such as maximum isometric force based on the physiological cross section area, pennation angle, optimal fiber length, and tendon parameters such as slack length. Some studies ignore the series-elastic element which is reported to have little impact in muscles with short or stiff tendons (Anderson, 2001).

3.4.3 Inverse Kinematics

A musculoskeletal model, as multibody physical system, allows the calculation and definition of acceleration, positions and velocities of its rigid bodies over time. A common approach for this is to use three-dimensional motion capture equipment that provides the coordinates of markers taped on bony landmarks, in order to calculate joint angles.

Each body or bone in the model is defined in the local coordinate frame of a joint, itself defined in the coordinate system of a bone following a parent-child hierarchy. Therefore, the internal coordinate system is unique to each body and international guidelines for standardisation have been set by the International Society of Biomechanics (Wu, 2005), as well as the order of rotations that defines the position of one body relative to another. Within each body's coordinate system, the positions of the relevant virtual markers can be calculated.

Inverse Kinematics is a global optimisation process that minimises the total errors between modelled and experimentally recorded marker positions as shown in Eq. 3a below. Markers are defined in the model at the same bony landmarks than have been obtained from the motion capture system, calibration or virtualisation steps, and this processed is described in more detail in Fig 3.7. For each time step, the sum of weighted squared errors of the markers positions is minimised, resulting in the determination of joint angles (the generalised coordinate trajectories) through the discrete time series. The weight, or importance given to a marker, is typically lowered when artefacts are likely to take place. A balance should also exist between the sum of the weights of every segment that is modelled. This trade-off is an intrinsic problem that has no straightforward solution (Mantovani and Lamontagne, 2016) apart from ensuring that the artefacts have been

minimised with prior steps such as digitization, and manually changing the weights according to the marker errors reported during the analysis.

$$J = min_q \left[\sum_{i \in markers} w_i \, ||x_i^{exp} - x_i(q)||^2 + \sum_{j \in unprescribed\ coords} \omega_j \left(q_j^{exp} - q_j \right)^2 \right]$$

Eq. 1) cost-function

*with: **q** the generalised coordinates being solved for,*
$\boldsymbol{x_i}^{exp}$ the experimental marker coordinates in world,
$\boldsymbol{x_i}(q)$ the position of the virtual marker in the model coordinates,
$\boldsymbol{w_i}$ and $\boldsymbol{w_j}$ the weight of the marker and the weight of the coordinates

In upper limb models, different published approaches allow calculating the origin of the glenohumeral joint and defining the position of the scapula, which are both necessary to perform the inverse kinematics.

The glenohumeral joint's origin is commonly defined by regression equations from both other angles and bony landmark positions or either or them (Magermans 2005), functional methods using instantaneous helical axes (IHA) (Stokdijk, 2000) or the alternative SCoRE method (Ehrig 2006, Monnet 2007, Nikooyan 2011), or an offset (Williams 2005, Rab 2002) which is the most conventional approach.

Several ways exist to determine the position of the scapula during dynamic motions. Regression methods define a standard scapulohumeral rhythm (Nicholson 2017, Rapp 2017, Matsumura 2019, Xu 2014, Stokdijk 2000) based on the scapulothoracic and humerothoracic angles as well as the position of the acromion. Participant-based regression equations can alternatively be defined when dynamic imaging is available, such as MRI or 3D-xray scans.

The use of an acromion marker cluster (AMC) is common and illustrated below in Fig 3.7.

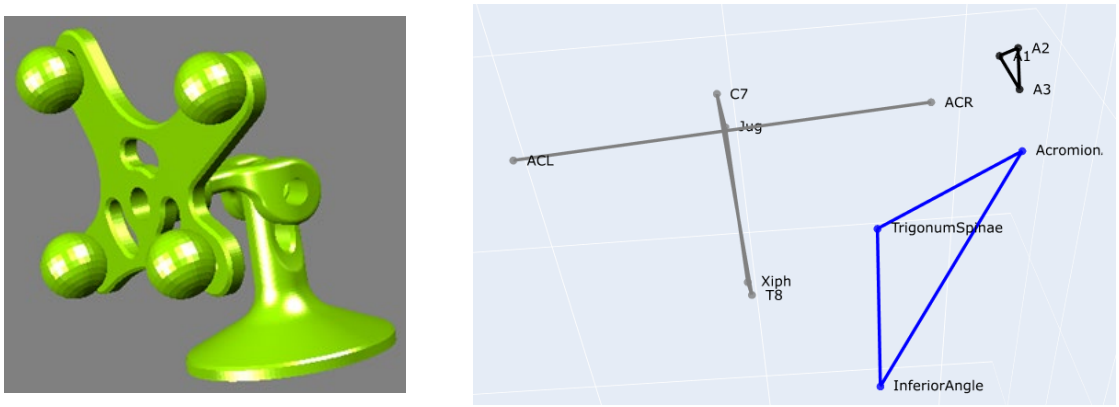

Fig. 3.7) illustration of an AMC cluster used for the scapula digitization. The AMC is used as a standard marker cluster during the calibration procedure using a wand. The scapula's bony landmarks' local positions are calculated within the reference frame of the AMC. The AMC is then used to virtualise the position of the scapula over time. Left is the 3d printed AMC, right is the graphical representation of a frame where the coordinates of the scapula bony landmarks are reconstructed from the AMC position.

In a calibration phase, a wand is used to point to three anatomical landmarks of the scapula (Acromial Angle, Trignum Spinae and Inferior Angle) whose local coordinates are calculated with regards to the coordinate system defined by the AMC. This allows the reconstruction of these anatomical points during dynamic motions, and subsequently the reconstruction of the angles of the scapula in the kinematic chain of the model. A single calibration can be used, which is the most applicable and quickest use of the AMC cluster, although its main limitation is that it is prone to errors above 120° of shoulder elevation (Lempereur et al., 2014) as it assumes a constant positional relationship between the AMC and the scapula. Dual calibrations are also documented, that use two semi-static calibrations. It is however representative of a single plane of humeral movement (defined by the two calibrations), and multiple calibration methods refine the relationship between the AMC and the scapula in different planes of motion that are more representative of activities of daily living but require more calibration phases in different elevation planes and elevation angles.

3.4.4 Static Optimisation, Dynamic simulations and Computer Muscle Control

With arbitrary controls provided such as forces or muscle excitations, the model is driven through a **forward dynamic** simulation to predict the motion resulting from the application of forces.

Alternatively, in an **inverse dynamic** simulation, a prescribed motion is used to predict the forces that caused that motion. The forces are the generalised forces (e.g. net forces and torques acting along the coordinate axes) that caused the particular motion at each joint.

Static optimisation is an extension of inverse dynamics and is also based on the known motion of the model which can be the result of the inverse kinematics process (i.e. joint angles over time). During a static optimisation analysis, the net joint moments are further resolved into individual muscle forces. Because there are more muscles than there are degrees of freedom, no unique solution exists to the set of excitations producing the joint moments leading to the desired kinematics – in other words several combinations of muscle activities could lead to the specific kinematics. This is represented by an indeterminate problem, or a degree of freedom problem sometimes referred to as the "muscle redundancy" problem (Mulla, 2023). In order to decide on a unique solution, a load-sharing approach uses a standard cost function. It estimates healthy muscle control and assumes an effort minimisation approach by minimising the squared activations during the optimisation as shown in Equation 2 below as described in Wu (2016). The Static Optimisation approach assumes independent control of the musculotendon units and considers the muscles to be the only contributors to joint torques, not taking ligaments or other passive structures into account.

$$J = \sum_{m=1}^{n} (a_m)^p$$

Eq. 2)

*with: **J** the cost function to be minimised, **n** the number of muscles in the model, $\boldsymbol{a_m}$ the activation level of the muscle, **p** is the power, commonly squared*

This most straight-forward way of solving the muscle redundancy problem simplifies the multibody dynamics approach by ignoring activation dynamics (that describes the function from muscle excitation to activation) and therefore allowing a robust optimisation on linear constraints, as the muscle activation becomes the only variable. The definition of the muscles varies, as it can consider or not the force-length-velocity relation (Equation 3c). It always assumes a fixed length tendon.

$$\sum_{m=1}^{n} [a_m f(F_m^0, l_m, v_m)] r_{m,j} = \tau_j$$

Eq. 3)

*with **n** the number of muscles in the model, $\boldsymbol{a_m}$ the activation level of the muscle, $\boldsymbol{F^0_m}$ its maximum isometric force, $\boldsymbol{l_m}$ its length, $\boldsymbol{v_m}$ its shortening velocity, $\boldsymbol{r_{m,j}}$ is the moment arm around the j^{th} joint, $\boldsymbol{\tau_j}$ is the generalised force acting on the j^{th} joint*

Reserve actuators, specific to the Opensim framework, are added to each coordinate to achieve dynamic consistency. In other words, they are pure torques or forces applied at a joint level that compensate forces when muscles are not able to generate sufficient accelerations, and account for small discrepancies between the model and the measured motions and forces. They are highly penalised in the optimisation, and are sometimes referred to as simply “residuals” or “hand of god forces” (Hicks, 2015).

Computed Muscle Control is a specialised combination of forward dynamics and static optimisation (Thelen et al. 2003) that also computes a set of muscle excitations and forces that drive a model to follow prescribed kinematics. The main difference is that CMC allows the inclusion of muscle synamics (activation and contraction dynamics). For this, it uses forward dynamic simulations on small time-steps, to match the kinematics as closely as possible, thus making the simulation more flexible. However, no benefits to the use of CMC compared to Static Optimisation are reported (Anderson 2001, Lin 2012, Roelker 2020).

3.4.5 Statistical Parametric Mapping

Statistical Parametric Mapping (SPM) is the application of the Random Field Theory (RFT) that assesses the features of statistical testing over a continuous function, emerged in brain mapping studies in the mid 1990's (Friston et al., 1995) and has only recently been applied to biomechanics.

Biomechanical data such as kinematics and EMG inherently have a degree of spatio-temporal smoothness, in the way that each value (or time-step) is correlated to the one before and the one after, due to physiological or mechanical constraints (Robinson et al. 2015). Therefore, no random variation is expected in the waveform. SPM, using Random Field Theory, allows us to understand the level of dependency between the values of our waveforms. In other words, if a statistical test such as a t-test is performed on each value of waveforms, then Random Field Theory can be applied to estimate if the changes in the results between time-steps are due by chance, while taking the full waveform into account (Vanmechelen 2023, Wattananon 2023, Papi 2020). In the context of biomechanical data, the input of an SPM analysis is for example a time-series of joint angles or EMG data, and the result is also a time-series (of t-values) which provides important information of the times at which areas of significance occur. Therefore, the use of SPM provides benefits compared to data reduction (to a single value) approaches, such as Root Mean Square Error (Pataky, 2016).

3.4.6 Upper-limb models

Many different upper-limb models have been created for specific purposes, and each model is a combination of components, some of which are reviewed earlier such as bones, joints and muscles. They are usually developed with a specific application in mind, and validated accordingly. Therefore, there are differences in the number of components as well as their type and final use of the models.

For example, some models focus on specific anatomical regions, such as the Upper Extremity Dynamic Model (Saul et al. 2014) that describes a more detailed hand but a less detailed shoulder compared to the Delft model (Nikooyan et al. 2011).

Some models have more actuators representing a single large muscle than others, such as the Delft model that has a total of over 130 actuators compared to Wu's (Wu et al. 2016) or the Scapulothoracic Shoulder model (Seth. et al. 2015) that have a total of 26 and 33 actuators respectively.

The scapulothoracic joint is also represented in different ways, and can be constrained with a built-in rhythm such as in the model described by Saul, have enforced constraints of scapular motion based on a thoracic ellipsoid such as the model described by Seth et al., or free to move (unconstrained) such as in Wu's model.

Finally, there are differences in the abilities of each model as they have been developed for a specific application or applications. For example, Wu's model was specifically published with Hill-type muscles which insertions were defined from cadaveric studies. The joint moments and muscles parameters of the models were tested against maximal

voluntary isometric, isokinetic contractions and surface EMG recorded in vivo, in healthy males.

3.4 Overall conclusion of the literature review

The biomechanics of the shoulder is complex and relies on the synchronisation, timing, and balance of activation of several muscles and muscle layers.

Shoulder instability has a high variety of causes and presentations, and ultimately changes or disturbs the harmony of the muscle patterns of the shoulder girdle. Patients suffering from this condition might exhibit different control strategies from healthy subjects due to the additional need to stabilise further the glenohumeral joint, and specialised technologies such as electromyography are required to provide information on these muscle activity patterns.

The lack of consensus or standardisation of Shoulder Instability makes its understanding challenging, and its long-term outcome difficult to assess. More specifically, there is very limited characterisation of its impact on young people.

The use of rigid-body musculoskeletal models can provide objective information on the kinematic chain, and additional understanding of the inner workings and behaviour of the neuromuscular system on a case-by-case basis, which could help gain clinically valuable information on this pathology.

4. Aims and objectives

Firstly, this study will help fill a gap in the current knowledge regarding the complex interaction of the kinematics and muscles activities of the shoulder girdle. Knowledge will be gained and added to the existing literature on the normal contraction patterns and kinematics, as well as in a specific children and young people population which has undergone little research.

Secondly, we will aim to explore a new way of assessing movements in the shoulder-girdle area by exploring to what extent musculoskeletal modelling techniques can predict normal muscle patterns, as well as their ability to discriminate between experimentally collected muscle patterns among a healthy and pathological group.

Overall aim:

The overall aim of this research is to demonstrate a novel method for quantifying muscle function and co-contraction in shoulder instability patients, as the ground work to improve clinical assessment and outcome prediction.

Hypothesis:

Some shoulder instability patients may be kinematically indistinguishable (i.e. they fall within the norm) from a healthy control group, but can be differentiated on the basis of their muscle control.

Objectives:

Following the literature review, three objectives have been defined and will be covered in three distinct chapters:

A) Characterise movement and muscle activity pattern differences between young people with shoulder instability and an age-matched control group, based on three-dimensional motion capture and surface electromyography data.

B) Use musculoskeletal modelling techniques and the kinematic data alone to predict muscle activations in the healthy group. This will define a baseline of a) which muscles are most reliably predicted using our techniques and b) reference value for each muscle.

C) Assess the differences in muscle activation prediction abilities between the control and shoulder instability groups. This third chapter will develop a new approach for identifying pathological muscle activation patterns based on prescribed kinematics.

5. Methods

This chapter first describes the methods of experimental data collection in section 5.1, then introduces the modelling methods used to characterise the data in section 5.2.

5.1 Experimental data collection

The raw experimental data of this thesis has been provided by the Orthotic Research & Locomotor Assessment Unit (ORLAU) based at RJAH Orthopaedic Hospital NHS Foundation Trust in Oswestry, that gained a favourable ethical opinion to collect data on young people with and without shoulder instability from West Midlands - South Birmingham Research Ethics Committee REF:20/WM/0021.

The study was advertised across regional clinical centers over a period of 24-months and two groups were recruited, a ground of young people with shoulder instability (SI) and an age- and sex-matched control group (CG). Following informed consent, each participant attended a single measurement session. The recruitment rate was 81%, with seven out of thirty-seven participants approached unable to participate.

The inclusion criteria for the shoulder instability group were to have subjective reports of instability with additional symptomatic instability in at least one direction in the clinical assessment, and specific exclusion criteria were to have been surgically managed and not have had instability episodes since. The control group is comprised of healthy subjects with no current or previous instability. An exclusion criterion for both groups was to have co-existing pathologies or deficits.

Data were collected in 30 young adults aged between 8 and 18, 15 for the shoulder instability group and 15 for the age matched control group. The most common form of

instability reported in the shoulder instability group was subluxation, experienced by 13/15 participants. Only one participant reported a dislocation, and one participant was unsure. Three participants presented with a first-time episode of instability, and twelve with recurrent episodes of instability. Ten participants had an atraumatic etiology, four a traumatic one, and one reported an ambiguous overlapping. The direction of instability was diverse, seven reported for anterior instability, two for posterior, two for inferior and two for multidirectional. At data collection, the time since the last episode of instability ranged from four hours to thirty-two weeks (mean time 7 weeks, standard deviation 9 weeks), with two participants unable to recall. The number of self-reported dislocations ranged from one two over ninety.

The control group had an averages age of 13.3 (standard deviation 3.1), height of 160.6cm (16.8) and weight of 52.4kg (15.1), with 8 males and 7 females. The shoulder instability group had an average age of 13.9 (2.9), height of 163.0cm (15.7), weight of 56.6kg (17.5), with 6 males and 9 females.

The data collected (dataset) comprised 3D motion capture and electromyographic data in a series of movements of the upper limb. The movements recorded are shown in table 5.1 below and form the basis of many activities of daily living. Each movement was demonstrated before being performed, with instructions regarding the start and finish positions. The motion of only one arm was recorded, the affected arm for the instability group, and the dominant arm for the control group. For the weighted motions, a self-selected weight of 0.5kg, 1kg or 1.5kg was used and kept across all movements. The control group selected those weights 1, 3 and 11 times respectively, while the shoulder instability group selected those weights 1, 5 and 9 times respectively. Each non loaded

motion was repeated over 2 sets of 6 repetitions. Each loaded motion was repeated over 2 sets of 3 repetitions.

Table 5.1 Description of the movements and tasks
Flexion (with and without weight)
Starting position: Participant in standing. Anatomical position i.e. Lateral aspect of the hypothenar eminence resting on the lateral aspect of their thigh (in keeping with the midline of the body in the coronal plane). Movement task: Participants will be instructed to lift their arm out to their side as high as they possibly can and then return it to the starting position.
Abduction (with and without weight)
Starting position: Participant in standing. Anatomical position i.e. Lateral aspect of the hypothenar eminence resting on the lateral aspect of their thigh (in keeping with the midline of the body in the coronal plane). Movement task: Participants will be instructed to lift their arm out to their side as high as they possibly can and then return it to the starting position.
Lateral rotation at ~45° abduction
Starting position: Participant in standing. Elbow flexed to 90^{o} with hand in thumbs up position. Movement task: Participants will be instructed to lift their arm out to their side up to ≈45^{o} ^{o} at the shoulder. Maintaining the arm in this position, participants will then be asked to laterally rotate their shoulder as far as is comfortable for the required or maximally tolerable number of repetitions. Following this, participants will be instructed to then return it to the starting position.
Hand behind head
Starting position: Participant in standing. Palmar surface resting on the lateral aspect of their thigh (in keeping with the midline of the body in the coronal plane). Movement task: Participants will be instructed to place their hand on the top of their head and then return it to the starting position.

The 3D motion capture data was captured at 100Hz using a Vicon system (12 V5-Vantage motion analysis camera). It provides 3D coordinates of reflective markers in space over

time, and is the information on which the modelling section (5.2) is based in order to scale a model and calculate joint angles.

The axes of the laboratory (or “world” axes) were defined with markers placed on the floor, and the volume of the laboratory was calibrated using an active wand from Vicon as shown in Fig. 5.1.

Fig. 5.1) Active wand used for volume calibration of the three-dimensional motion capture system

The first step in 3D motion capture data collection is the placing of clusters of reflective markers on body segments, strapped so that to ensure that they are rigidly mounted, with a minimum of 3 non-collinear markers per cluster in order to define a coordinate frame, and with a space of two to three markers in between them. They are typically arranged in a non-symmetrical fashion that allows them to be uniquely identified. The description of the marker cluster placement is adapted from Jaspers et al (2011s) and is described in the table below.

Clusters were placed on the sternum, acromion (single calibration), humerus, forearm and hand as previewed in Table 5.2 below, with the full description available in the Appendix Table 5.2.

Table 5.2, placement illustration of a marker cluster during the experimental data collection.

Placement illustration	Description of cluster placement
	Sternal marker cluster, positioned using double sided tape on the anterior aspect of the thorax, approximately one finger width below the sternal notch. Placement was below the sterno-clavicular joint and in keeping with the midline of the body. The antero-superior border of the thorax is defined by the insicura jugularis (IJ) point and the antero-inferior border is defined Processes Xiphoideus (PX) point. For participants with breast tissue, a more superior placement of the sternal cluster may have been required, not exceeding the antero-superior border of the thorax. In this case, adequate visibility of the marker cluster was ensured prior to identification of virtual markers. The inferior edge of the cluster was marked.

Each participant was then seated with their hands resting on their thighs while the assessor then pointed at bony landmarks listed in Table 5.3 (with the full illustration in Appendix Table 5.3) with a wand on which markers are mounted. This allows further digitisation of the anatomical bony landmarks, and definition of joints and bone coordinate frames described in the modelling section.

Table 5.3, anatomical and virtual markers		
No.	Name	Abbreviation
1	C7 Spinous Process	C7
2	T8 Spinous Process	T8
3	Insicura Jungularis - (Jugular notch)	IJ
4	Processus Xiphoideus - (Xiphisternum)	PX
5	Art. Sternoclavicularis – (Sternoclavicular joint)	SC
6	Art. Acromioclavicularis - Acromioclavicular joint	AC
7	Processus Coracoideus - Coracoid process	PC
8	Trigonum Scapulae – medial border spine of scapula	TS
9	Angulus Inferior (AI) - inferior angle of the scapula	AI
10	Angulus Acromialis - Latero-inferior edge of scapula spine	AA
11	Glenohumeral rotation center	GH
12	Lateral epicondyle	LE
13	Medial epicondyle	ME
14	Centre of the elbow (digitized during data processing)	centelbow
15	Radial Styloid	RS
16	Ulnar Styloid	US
17	Styloid process of 3rd Metacarpal	MC3
18	Distal head of 2nd Metacarpophalangeal joint	MCP2
19	Distal head of 3rd Metacarpophalangeal joint	MCP3
20	Distal head of 5th Metacarpophalangeal joint	MCP5

The electromyography data was collected in synchronization with the 3D markers using a surface EMG from a Delsys Trigno system sampling at 2000Hz with a built-in 20-450Hz band-pass filter. After skin preparation with alcohol and shaving if required, surface

electrodes were placed on the middle trapezius, infraspinatus, triceps, latissimus-dorsi, deltoid (posterior and anterior), pectoralis-major, biceps, wrist flexors and extensors muscles according to SENIAM guidelines (Merletti et al. 2000) and Criswell et al. (2011). Quality checks of the placement of the electrodes were performed by examining the baseline noise as well as the activity on a biofeedback, in a series of generic isometric contractions depending on the targeted muscle (shoulder push, pull, shrug, lateral rotation, hand grip, wrist flexion and extension).

5.2 Data analysis using biomechanical models

This section describes how, for each participant, the data provided by the motion capture system and the EMG was processed, used to create a scaled model, then run inverse kinematics and static optimisation. The model and tools were chosen after multiple trials and data processing of pilots.

The choice of a model is always a trade-off between its complexity and its simplicity, in order to answer specific research questions. While increased complexity could represent more of the features of the biological system, it comes with increased computational cost and more potential sources of errors, and it is generally recommended to "focus on a minimalistic model that represents only the required components" (Hicks, 2015). For this reason, the Wu (2016) model was chosen, as other alternatives described in the literature review provided either excessive numbers of actuators for this study (such as the Delft model described in Nikooyan et al. 2011), or constraints in the scapular definition and motion (such as the the Scapulothoracic Shoulder model described by Seth. et al. 2015). Wu's model is a 10-degree-of-freedom (DOF) model of the upper limb actuated by 26 muscle-tendon units. It focuses on the shoulder girdle area, with 3 DOF ball and socket joints for the glenohumeral and acromioclavicular joints, while the sternoclavicular joint and elbow are modelled as 2-DOF universal joints (Wu, 2016). The muscle insertions were originally defined from Garner and Pandy (2001), then optimised to match muscle parameters of cadaveric studies of Ackland et al. (2008. 2012) and Kuechle et al. (1997). Preliminary tests showed the importance of having a model allowing for pathological degrees of freedom, especially at the scapula level, where the range of motion of the

models was sometimes exceeded. The constraints in scapular motion were specifically important, as they impacted preliminary tests

The preprocessing of the raw data consisted of several steps. The first step was gap filling of the 3D coordinates of each marker, performed using rigid body, pattern and spline filling pipelines available within Vicon Nexus 2.12.1. The labelling of the markers and motion times was also performed in the Vicon Motive software. Then, custom Python scripts performed the cutting of each motion into set and repetition, re-labelling as appropriate, and export in appropriate formats.

The second step was to determine the 3D position of each anatomical marker indicated with a wand during the subject calibration procedure, in the coordinate system of the body it belongs to. For example, every time the wand pointed to an anatomical marker such as the lateral epicondyle at the elbow level, the humeral cluster markers were used to define a local coordinate system and describe the location of the anatomical marker within, in other words transforming global coordinates into local coordinates. In this way, with all local coordinates of the anatomical markers known, the dynamic motion files (movements) were processed at each time step in reverse, identifying the cluster markers, and transforming the local anatomical marker coordinates into global ones.

The geometrical scaling of the model scaled the bones and muscle parameters (fiber length and tendon slack length) of the generic model to represent each participant, according to the best practice frameworks (Hicks et al., 2015).

Virtual markers were added to the model in order to match those used on the participant. One static position was taken from the subject calibration procedure, and the location of

the markers on the participant and on the model was compared to define scale factors as per the table 5.4 below.

Table 5.4 Scaling of rigid bodies. A scaling ratio for each bone was estimated from the static calibration trials, following marker pairs

Bone	X axis	Y axis	Z axis
Thorax	IJ-C7	PX-IJ	AC-IJ
Clavicle	-	-	SC-AC
Scapula	AC-AA	TS-AI	TS-AA
Humerus	ME-LE	AC-centelbow*	ME-LE
Ulna	ME-centelbow	ME-US	ME-centelbow
Radius	LE-centelbow	LE-RS	LE-centelbow

* With the GH being defined with the standard scaling method within the model, the scaling ratio for the longitudinal axis of the humerus was estimated in a sitting position between the elbow center and AC which is a reliably palpable landmark and allows a simple single pipeline to process and compare the two datasets with RMS errors within the standardly accepted values.

Inverse kinematics (IK) was performed in the OpenSim 4.4 framework. Virtual markers were added to each motion file prior to running the analysis, and kinematic data were smoothed in Python using a Savitzky-Golay filter with a window size of 99 and a polynomial order of two, which were selected as they perform well during high-frequency acceleration-time signals when compared to alternative methods, and based on this dataset performed the best for removal of noise whilst preserving the underlying signal

(Sahrom et al. 2021). The quality of the IK was checked by ensuring the maximum error was less than 2cm as advised in the Opensim guidelines.

Static Optimisation (as described in 3.4.4) was then performed on Inverse Dynamics results for each repetition of each motion file, taking the force-length-velocity relation into account, and with reserve actuators added on each axis. Reserve actuators were checked so that they would not exceed 5% of the net joint moment as recommended by Hicks (2015). For motions that were performed with added weight, the mass of the hand of the model was increased accordingly. With no difference between the two tools found in the literature review, and following a first analysis of the dataset, SO was preferred to CMC due to the extensive time of analysis as well as the increased number of errors and need for subject-specific and motion-specific modifications when compared to the SO analysis.

Surface EMG data were band-pass filtered between 20-450 Hz in hardware, then rectified and low-pass filtered at 6Hz as described in the literature review (3.3.2). EMG was normalised to the maximum encountered activation across any of the movement activities. As a quality control check, used to ensure sufficient electrode placement, contact and adequate signal recording (including avoidance of unwanted noise), participants were instructed to carry out a single resisted movement against the assessor at a consistent submaximal intensity. Movements included shoulder elevation, shoulder lateral rotation, combined shoulder extension and adduction, shoulder push, elbow flexion, elbow extension, wrist flexion and wrist extension. No maximum voluntary contraction (MVC) testing was carried out to minimise risk of further instability during data collection as this is known to be highly variable, particularly in pathological populations (Spanhove et al., 2022). Normalising the muscles to the maximum encountered activation

within each motion would lead to unreasonably high values for muscles with little overall activation such as the Latissimus Dorsi, which could lead to problems when comparing to the predicted values from the model during Static Optimisation. For these reasons, it was chosen to normalise each EMG of each participant to its maximum value encountered across all motions and strength tests.

The statistical analysis, to calculate the significant differences between the model's ability to predict muscle activations in the two groups (Control Group (CG) and Shoulder Instability group (SI)), required additional processing steps as the RMS data was not normally distributed. Even after logarithmic transformation (Baker et. al 2008, Speciali et. al 2014) most distributions failed the Kolmogorov-Smirnov and Shapiro-Wilk tests for normality. The (non-parametric) permutation test approach was therefore chosen, as it makes no assumption on the distribution of the data used.

A permutation test is comprised of three steps: determine and calculate the initial test-statistic, approximate the test-statistic distribution, and calculate the p-value.

In this case, the permutation test allows to find if there are any statistical differences between the two groups (CG and SI) in the ability of the model to predict muscle activations (i.e. in the difference between the prediction and the experimental EMG). For each motion and muscle, the **null hypothesis** made is that being part of the SI group does not change (increase or decrease) the accuracy with which we can predict the muscle activations (represented by the RMSE or correlation values of the difference between the prediction and the experimental EMG). The **alternative hypothesis** is that being part of the SI group does change (increase or decrease) the accuracy.

An example of the difference between the predicted and experimental activations is represented graphically in Fig. 5.2 below, for one muscle in one motion of one participant.

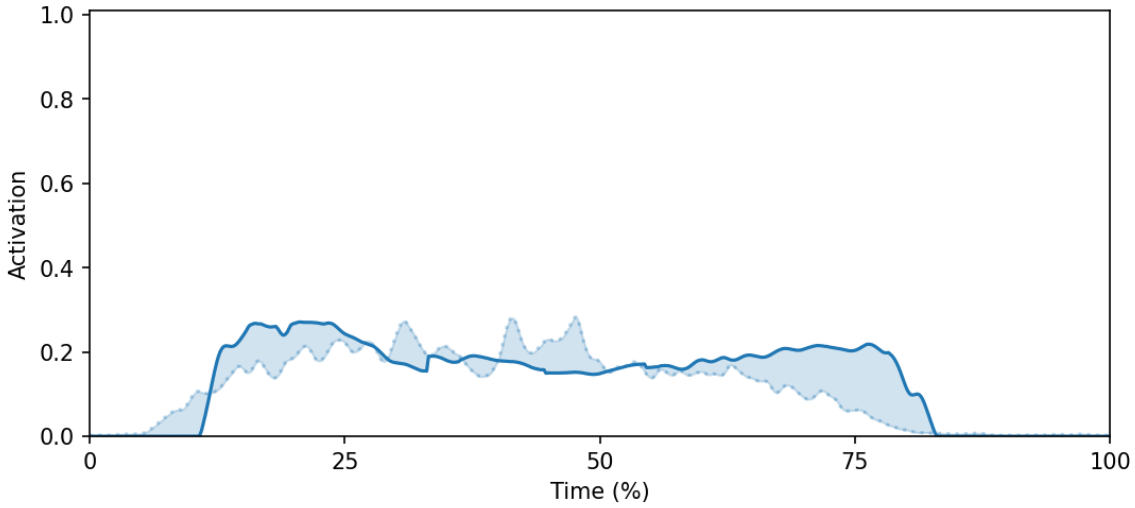

Fig. 5.2) Example based on one repetition of one motion of one participant: the blue solid line is the predicted activation from the static optimisation, the blue dotted line is the experimental EMG, the shaded area is the difference.

For a given motion and muscle, the repetitions of all participants are sorted in one of the two groups (CG and SI), as seen in Fig. 5.3 below. Each repetition has its associated RMSE or correlation measure value that represents the accuracy of the prediction of the muscle activity. **The initial test-statistic is the difference in mean value between the two groups.**

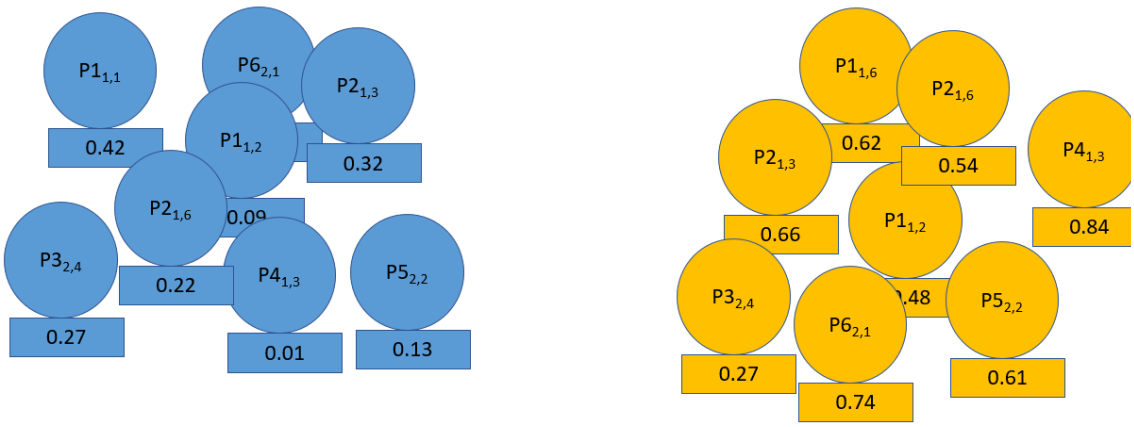

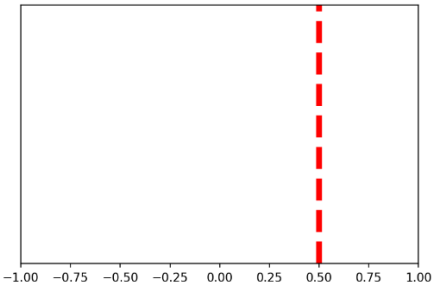

Fig. 5.3) For a given muscle and motion, the repetitions of the CG (blue) and SI (orange) groups are shown at the top. Inside the circle is the participant number as well as the set and repetition numbers, and each associated rectangle displays the value representing how well the muscle activity was predicted for this given muscle and repetition. The initial test-statistic is shown as the dotted red line at the bottom and is the difference in mean values between the two groups.

The permutation, or randomisation, shuffles the data between the two groups. After one permutation, the test-statistic is recalculated, and this is shown in Fig. 5.4 below.

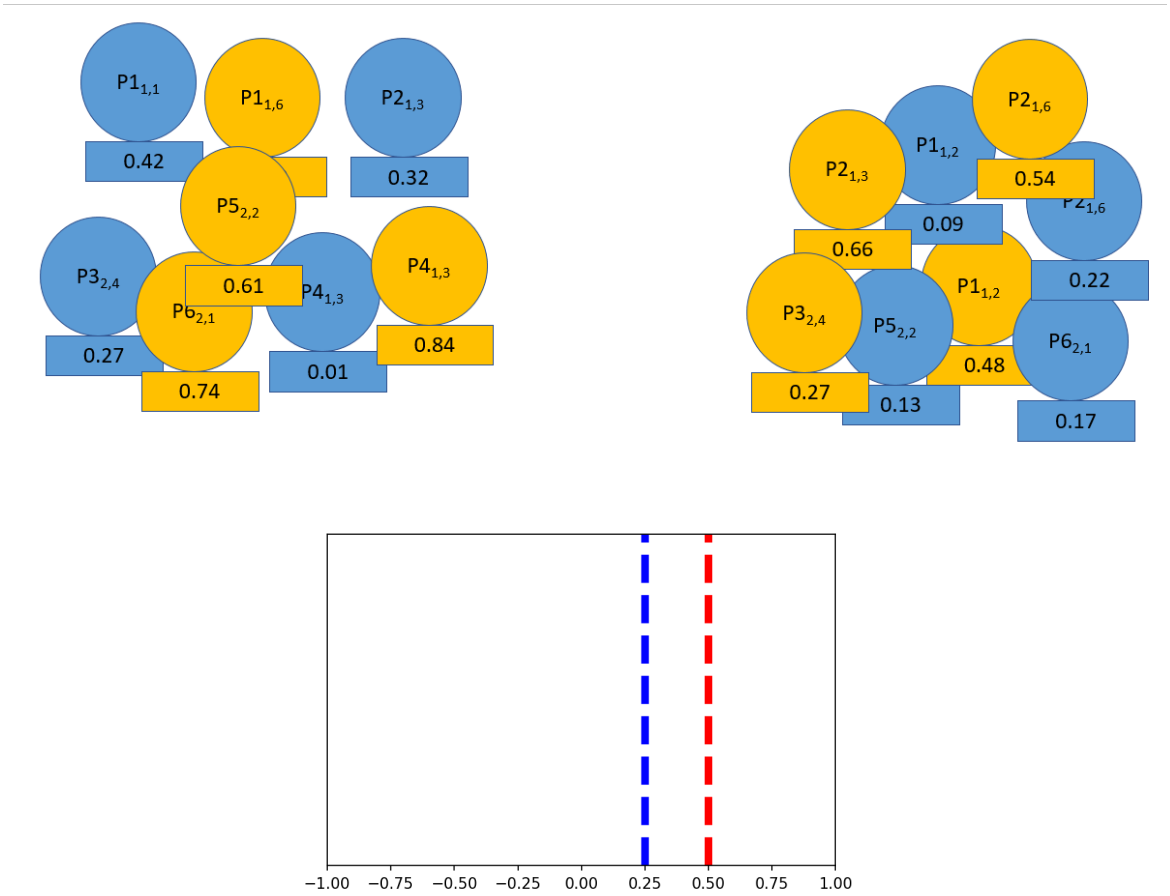

Fig. 5.4) Every permutation shuffles the data points between the groups (top), and a record of the test-statistic (blue bar at the bottom) is kept alongside the original test-statistic (dotted red line).

Through the iterations, an **approximate distribution of test statistics** under our null hypothesis is obtained (Fig. 5.5). From this distribution, the probabilities associated with the different mean-difference values can be calculated, in other words the probability that the SI group is predicted the same way than the SI group. **The p-value** is the probability under the assumption of no effect or no difference (null hypothesis), of obtaining a result equal to or more extreme than what was actually observed. In this case, it is the probability of obtaining the difference in prediction accuracy (RMSE or correlation value) between the two groups (initial test-statistic), assuming that SI does not impact it. The p-value is the number of t-statistics (resulting from the permutations) that are as or more extreme than our initial t-statistic, divided by the total number of t-statistics that were calculated to approximate the distribution.

The Null hypothesis used is that SI does not increase or reduce the RMSE of the Static Optimisation. If it is truly the case, then obtaining the initial difference (our first t-statistic) would occur with a probability of p*100%. In other words, if the p-value is above 0.05, the result is said statistically not significant and we cannot reject the null hypothesis that SI did not change the accuracy of the prediction of the Static Optimisation. If the p-value is below or equal to 0.05, we reject our Null hypothesis and accept our alternative: SI changes the accuracy of prediction of the Static Optimisation (and is therefore different from what would be expected to happen by chance, in the Control Group). Unlike in the other analyses (sections 8.2a,b) where the average values were considered, the permutation test is based on the individual values of each repetition.

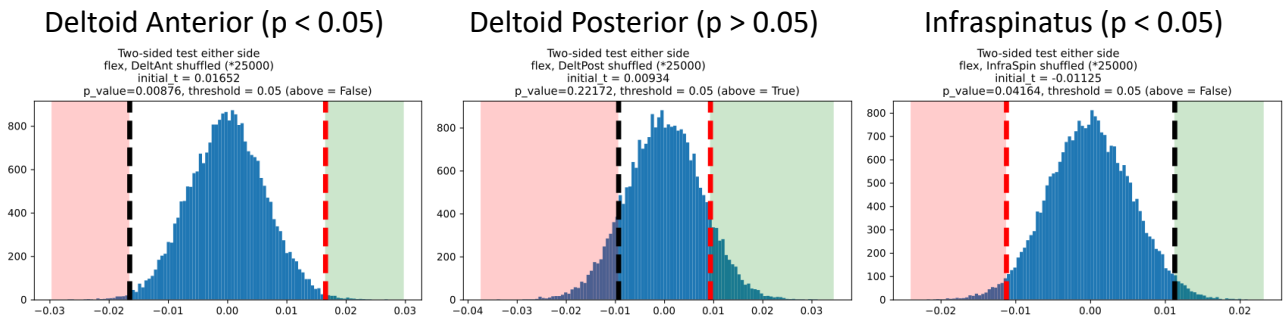

Fig. 5.5) Each plot illustrates the testing of the null hypothesis that belonging to the SI group does not impact the way the model predicts muscle activations for a given motion. Each plot presents the distribution of the test-statistic and permutation tests for one muscle in one motion, based on the two groups CG and SI. Plots show the initial t-statistic (dotted red line), its opposite (dotted black line), the general distribution (blue lines) as well as the number of permutation tests for which the test-statistic is more extreme than the initial test-statistic (shaded areas) which is then translated into a p-value (graphically the area under the curve in the shaded area). The p-value is used to accept or reject the null hypothesis.

Chapter 6:
Movement and muscle activity pattern differences between young people with shoulder instability and an age-matched control group

Seyres, Martin, Neil Postans, Robert Freeman, Anand Pandyan, Edward K. Chadwick, and Fraser Philp. 'Children and Adolescents with All Forms of Shoulder Instability Demonstrate Differences in Their Movement and Muscle Activity Patterns When Compared to Age- and Sex-Matched Controls'. Journal of Shoulder and Elbow Surgery, March 2024, S1058274624001617. https://doi.org/10.1016/j.jse.2024.01.043.

This chapter is based on an article which was proof-read and edited for publication. All data analysis was done by the author of this thesis and the editorial work was done in collaboration with the whole team.

6.1. Introduction

The sixth chapter of this PhD covers objective (A) which is to characterise Shoulder Instability (SI) in young people and identify any observable differences compared with typically developing children in kinematics and EMG patterns. The following chapters will be investigating alternative ways to compare the two groups, in order to further discriminate individuals who may be hard to differentiate on the basis of kinematics and EMG alone.

This chapter uses data collected on young people aged between eight and eighteen recruited in two groups of shoulder instability (SI) and age and sex matched controls (CG). All forms of SI were included and young-people with co-existing neurological pathologies or deficits were excluded. The participants attended a single session and performed four unweighted and three weighted tasks in which their movements and muscle activity was measured using 3d-movement analysis and surface electromyography (EMG) as described in the Methods chapter section 5.2.

The collected data is first separated in motions and repetitions. Individualised biomechanical models are created and scaled for each participant, and inverse kinematics is used to compare joint angles. The EMG data is also processed and used to compare muscle activities between groups.

The results are presented in the form of average joint angles, maximum amplitude per angle, and normalised muscle activations. Statistical analyses are then used to provide information on the times of the motions at which joint angles and muscle activities were significatively different between the two groups across motions.

6.2. Results

6.2a. Kinematics

First, individual reports are prepared for each subject. Kinematics results for a single participant from the control group are presented in Fig 6.1 as an example of the intermediary step of inverse kinematics across all repetitions of all sets. It shows the deviation from normal in each specific joint over time. The repetitions are then averaged per participant in each group.

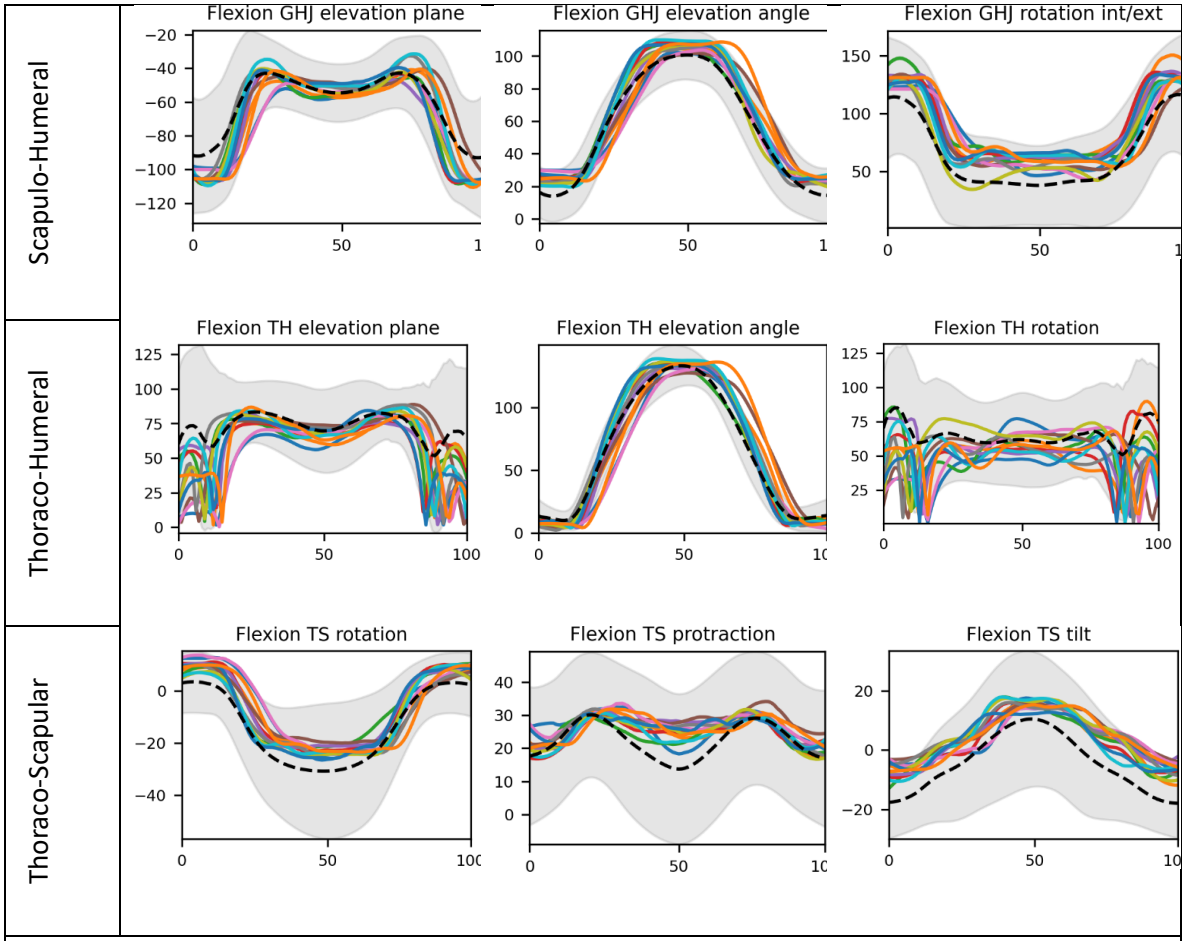

Fig. 6.1) Joint angles for all joints and all movements of one (healthy) participant in one motion (Flexion). Each solid trace is a repetition, dotted black lines are the normal average, shaded areas indicate the two standard-deviation of the norm. The rows Thoraco-Scapular and Thoraco-Humeral angles describe the orientation of the scapula with regards to the thorax, and humerus with regards to the thorax, respectively. They are not real anatomical joints and are used to provide an intuitive orientation of the shoulder and arm.

Once the joint angles have been processed over time and across all motions, in all participants of the Control Group (CG), the 95% confidence interval of the Range of Motion (RoM – maximum angle reached by a joint) is calculated and presented in the Table 6.1 below. It provides an indication of where the mean value lies for each joint across motions, and allows identifying the variability associated with this group following the protocol used. The majority of movements have a 95% confidence interval (CI) that does not exceed 10°, which shows an overall good repeatability across angles and motions as within the commonly admitted minimal clinically important difference (MCDI). The largest CI are found in the weighted abduction for the planes of thoracohumeral elevation and rotation.

Table 6.1) Mean range of motion (RoM) [95% CI] in the CG, values for all joints and movements (degrees)*. Highlighted cells indicate 95% CI ranges ≥ 10 degrees, commonly assumed as a magnitude likely apparent with clinical observation. TH = thoracohumeral, ST = scapulothoracic, GHJ = glenohumeral joint, ACJ = acromioclavicular joint, SCJ = sternoclavicular joint.*

Motion	Flexion	Flexion with weight	Abduction	Abduction with weight	Abduction at 45° with axial rotation	Abduction to 45° with axial rotation and weight	Hand to back of head
TH plane	93.8 [90.3, 97.3]	96.5 [91.1, 101.8]	97.9 [93.0, 102.8]	93.8 [86.4, 101.2]	23.4 [21.7, 25.1]	24.7 [21.9, 27.4]	92.3 [87.1, 97.5]
TH angle	129.6 [128.1, 131.1]	134.2 [132.3, 136.1]	131.6 [130.5, 132.7]	133.0 [131.4, 134.6]	16.7 [15.4, 18.0]	18.9 [16.8, 21.0]	113.3 [111.4, 115.3]
TH rotation	99.1 [95.4, 102.7]	103.1 [97.7, 108.5]	99.3 [94.4, 104.1]	97.9 [91.2, 104.6]	97.3 [95.3, 99.3]	95.6 [92.2, 99.0]	106.1 [102.4, 109.9]
ST protraction	24.1 [23.1, 25.1]	26.7 [25.4, 27.9]	16.9 [15.8, 18.1]	17.5 [16.2, 18.8]	10.7 [9.9, 11.5]	14.6 [13.4, 15.9]	16.5 [15.3, 17.7]
ST rotation	39.5 [38.2, 40.7]	43.4 [41.4, 45.5]	42.0 [40.4, 43.6]	46.2 [43.9, 48.5]	11.8 [10.9, 12.7]	14.8 [13.2, 16.3]	37.4 [36.3, 38.6]
ST tilt	32.8 [31.1, 34.5]	36.8 [34.1, 39.4]	23.2 [21.7, 24.6]	20.3 [18.2, 22.4]	8.4 [7.8, 9.0]	12.6 [11.4, 13.8]	24.5 [23.1, 25.9]
GHJ plane	73.7 [70.6, 76.7]	79.6 [73.7, 85.5]	58.0 [55.4, 60.6]	53.5 [49.7, 57.2]	14.2 [13.0, 15.4]	18.8 [15.1, 22.4]	54.0 [49.6, 58.4]
GHJ angle	91.4 [89.9, 93.0]	93.5 [91.4, 95.6]	98.0 [96.6, 99.5]	96.0 [94.2, 97.9]	15.3 [14.4, 16.1]	15.7 [14.3, 17.1]	81.0 [79.3, 82.7]

GHJ rotation	100.1 [97.2, 103.1]	102.4 [97.5, 107.2]	70.3 [66.8, 73.9]	66.6 [62.0, 71.1]	85.9 [83.6, 88.2]	86.6 [82.9, 90.3]	98.0 [94.7, 101.3]
ACJ protraction	33.9 [32.3, 35.5]	36.6 [34.0, 39.2]	34.6 [33.3, 36.0]	33.5 [31.3, 35.8]	8.8 [8.2, 9.5]	14.0 [12.6, 15.3]	33.9 [31.7, 36.1]
ACJ rotation	16.7 [15.9, 17.4]	17.5 [16.5, 18.6]	15.2 [14.5, 16.0]	14.0 [13.0, 15.0]	8.6 [8.1, 9.0]	9.1 [8.4, 9.8]	14.0 [12.9, 15.1]
ACJ tilt	31.6 [30.5, 32.8]	33.1 [31.5, 34.7]	28.6 [27.1, 30.1]	30.8 [28.7, 32.8]	7.4 [6.8, 7.9]	8.7 [7.8, 9.5]	25.6 [24.6, 26.6]
SCJ protraction	24.1 [23.2, 25.1]	26.4 [25.2, 27.6]	25.0 [24.1, 26.0]	26.9 [25.5, 28.4]	6.4 [5.8, 6.9]	9.5 [8.6, 10.5]	22.1 [21.1, 23.2]
SCJ elevation	10.7 [10.3, 11.1]	13.1 [12.4, 13.7]	12.4 [11.8, 12.9]	14.5 [13.8, 15.3]	5.8 [5.4, 6.3]	7.6 [6.9, 8.3]	10.6 [10.2, 11.0]

The comparison of the Range of Motion (ROM), of the SI to the CG group, is shown in Fig. 6.2 for the motion Flexion and weighted Flexion as a visual illustration of the differences in amplitude between the different angles in both groups. The complete table is available in Appendix Fig. 6.2 and the detailed table is on the next page.

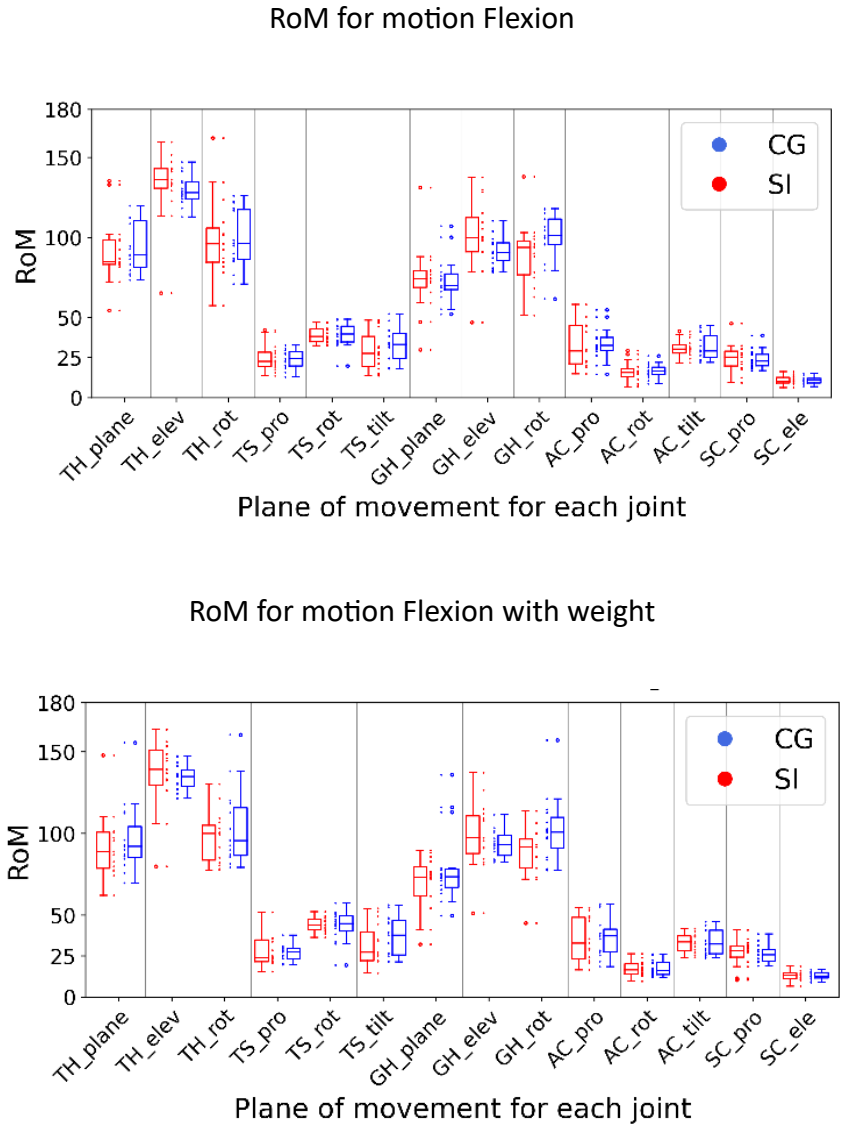

Fig. 6.2) RoM per group: Shoulder Instability group (SI) vs Control Group (CG).

The boxes extend from the first to third quartile, with a line at the median. The whiskers extend to 1.5 times the inter-quartile range. Flier points are above the whiskers. Headings: TH = thoracohumeral, TS = thoracoscapular, GH = glenohumeral, AC = acromioclavicular, SC = sternoclavicular, elev = elevation, rot = rotation, pro = protraction.

The detailed comparison of the mean RoM value in both groups is presented below in Tables 6.2 (unweighted motions) and 6.3 (weighted motions). The most frequently occurring differences of more than 10 degrees with the control group being higher are observed in the Glenohumeral rotation plane for the motion of flexion and abduction (both weighted and unweighted).

***Table 6.2) Mean range of motion (RoM) per group in degrees and their standard deviation**: Shoulder Instability group (SI) vs Control Group (CG) in **unweighted motions**. The cells that are highlighted represent a difference of 10 degrees or more between the two groups, commonly assumed as a magnitude likely apparent with clinical observation and larger than the error of measurement thresholds used in clinical movement analysis.*

Motion	Flexion		Abduction		Axial rotation		Hand to head	
	SI	CG	SI	CG	SI	CG	SI	CG
TH plane	91.7 (14.2)	93.8 (14.7)	106.6 (14.6)	97.9 (15.6)	22.6 (6.8)	23.4 (6.1)	97.4 (13.0)	92.3 (18.7)
TH elevation	133.0 (4.1)	129.6 (4.5)	136.9 (4.0)	131.6 (3.8)	16.3 (4.6)	16.7 (4.2)	116.0 (4.5)	113.3 (4.7)
TH rotation	99.8 (14.0)	99.1 (14.8)	106.7 (13.7)	99.3 (16.0)	94.1 (7.4)	97.3 (8.3)	104.9 (13.2)	106.1 (15.1)
TS protraction	24.8 (4.1)	24.1 (3.6)	17.7 (3.2)	16.9 (3.6)	10.8 (3.2)	10.7 (3.0)	16.5 (3.2)	16.5 (4.0)
TS rotation	39.1 (3.2)	39.5 (3.4)	39.7 (3.2)	42.0 (2.8)	12.1 (3.3)	11.8 (3.4)	33.9 (3.0)	37.4 (2.7)
TS tilt	29.3 (4.1)	32.8 (4.6)	21.7 (3.1)	23.2 (4.1)	11.0 (2.7)	8.4 (2.6)	23.4 (2.9)	24.5 (3.5)
GHJ plane	73.9 (10.9)	73.7 (11.5)	57.5 (8.8)	58.0 (11.2)	14.9 (5.1)	14.2 (5.5)	55.6 (9.5)	54.0 (17.6)
GHJ elevation	100.7 (4.5)	91.4 (5.6)	105.4 (3.2)	98.0 (4.3)	14.3 (3.7)	15.3 (4.1)	86.4 (4.5)	81.0 (6.5)
GHJ rotation	88.9 (12.0)	100.1 (11.5)	59.6 (10.3)	70.3 (12.5)	93.7 (9.8)	85.9 (9.0)	93.3 (10.6)	98.0 (11.4)
ACJ protraction	32.4 (4.1)	33.9 (3.9)	32.0 (3.0)	34.6 (3.3)	10.2 (2.5)	8.8 (2.7)	29.8 (3.2)	33.9 (4.8)
ACJ rotation	16.2 (1.9)	16.7 (2.4)	16.8 (2.7)	15.2 (2.5)	9.0 (2.2)	8.6 (2.1)	14.3 (2.1)	14.0 (3.1)
ACJ tilt	31.0 (2.5)	31.6 (2.3)	28.3 (2.5)	28.6 (2.2)	7.4 (2.2)	7.4 (2.3)	24.3 (2.1)	25.6 (2.3)

TH plane	24.9 (2.7)	24.1 (2.9)	25.3 (3.2)	25.0 (3.3)	6.6 (1.8)	6.4 (1.9)	19.9 (2.9)	22.1 (3.1)
TH angle	11.0 (1.9)	10.7 (1.8)	11.8 (2.0)	12.4 (2.0)	5.2 (1.5)	5.8 (1.4)	10.1 (1.6)	10.6 (1.7)

Table 6.3) Mean range of motion (RoM) per group in degrees and their standard deviation*: Shoulder Instability group (SI) vs Control Group (CG) in* ***weighted motions****. The cells that are highlighted represent a difference of 10 degrees or more between the two groups, commonly assumed as a minimal clinically important difference (MCID) using MOCAP systems.*

Motion	**Flexion weight**		**Abduction weight**		**Axial rotation weight**	
	SI	CG	SI	CG	SI	CG
TH plane	92.2 (11.6)	96.5 (12.2)	104.4 (14.2)	93.8 (14.3)	22.7 (6.1)	24.5 (6.1)
TH elevation	136.4 (3.6)	134.2 (4.1)	138.2 (3.7)	133.0 (3.7)	20.6 (5.6)	18.8 (5.2)
TH rotation	97.8 (11.8)	103.1 (11.2)	101.6 (15.8)	97.9 (14.0)	94.8 (6.0)	95.6 (8.6)
TS protraction	27.8 (3.1)	26.7 (3.2)	19.8 (3.6)	17.5 (3.0)	14.0 (2.7)	14.7 (3.2)
TS rotation	44.5 (2.6)	43.4 (3.2)	43.5 (2.6)	46.2 (2.5)	15.6 (2.8)	14.8 (3.0)
TS tilt	32.4 (4.0)	36.8 (4.0)	19.4 (3.2)	20.3 (3.4)	14.5 (2.8)	12.6 (2.7)
GHJ plane	69.5 (7.9)	79.6 (11.5)	53.6 (6.6)	53.5 (8.3)	13.6 (4.8)	18.7 (4.7)
GHJ elevation	99.4 (3.7)	93.5 (5.0)	104.3 (3.4)	96.0 (4.2)	16.5 (3.9)	15.7 (4.8)
GHJ rotation	87.2 (8.5)	102.4 (11.2)	56.7 (8.9)	66.6 (11.0)	91.9 (8.4)	86.5 (9.4)
ACJ protraction	35.6 (3.7)	36.6 (3.9)	32.0 (2.7)	33.5 (3.2)	14.3 (3.1)	13.9 (3.1)
ACJ rotation	17.3 (1.9)	17.5 (2.2)	17.0 (2.5)	14.0 (2.1)	10.8 (2.4)	9.1 (2.3)
ACJ tilt	33.2 (1.8)	33.1 (2.3)	28.6 (2.0)	30.8 (1.8)	9.3 (1.9)	8.7 (2.0)
TH plane	26.9 (2.4)	26.4 (2.2)	26.6 (2.5)	26.9 (2.0)	9.8 (2.0)	9.6 (2.2)
TH angle	13.1 (1.8)	13.1 (1.8)	14.3 (1.5)	14.5 (1.5)	6.9 (1.2)	7.6 (1.3)

The statistical differences, using Statistical Parametric Mapping (SPM) described in the literature review chapter 3.4.5, are presented below in Fig 6.3. The main interest of SPM in this application is to highlight the differences between the SI and CG groups throughout the time series of each motion and angle.

The angles the most sensitive to Shoulder Instability pathology are the sternoclavicular protraction/retraction and elevation/depression planes that have consistent differences across the entire movement cycle, in all movements. The SI group adopts a more protracted and elevated sternoclavicular joint, and this is accompanied in most movements by less internal rotation and upward tilt at the acromioclavicular joint.

Overall, most angles and motions exhibit a degree of statistical difference at some point throughout the movement, apart from the glenohumeral elevation plane in flexion (weighted and unweighted) and axial rotation with weight, and the acromioclavicular protraction/retraction in axial rotation (weighted and unweighted).

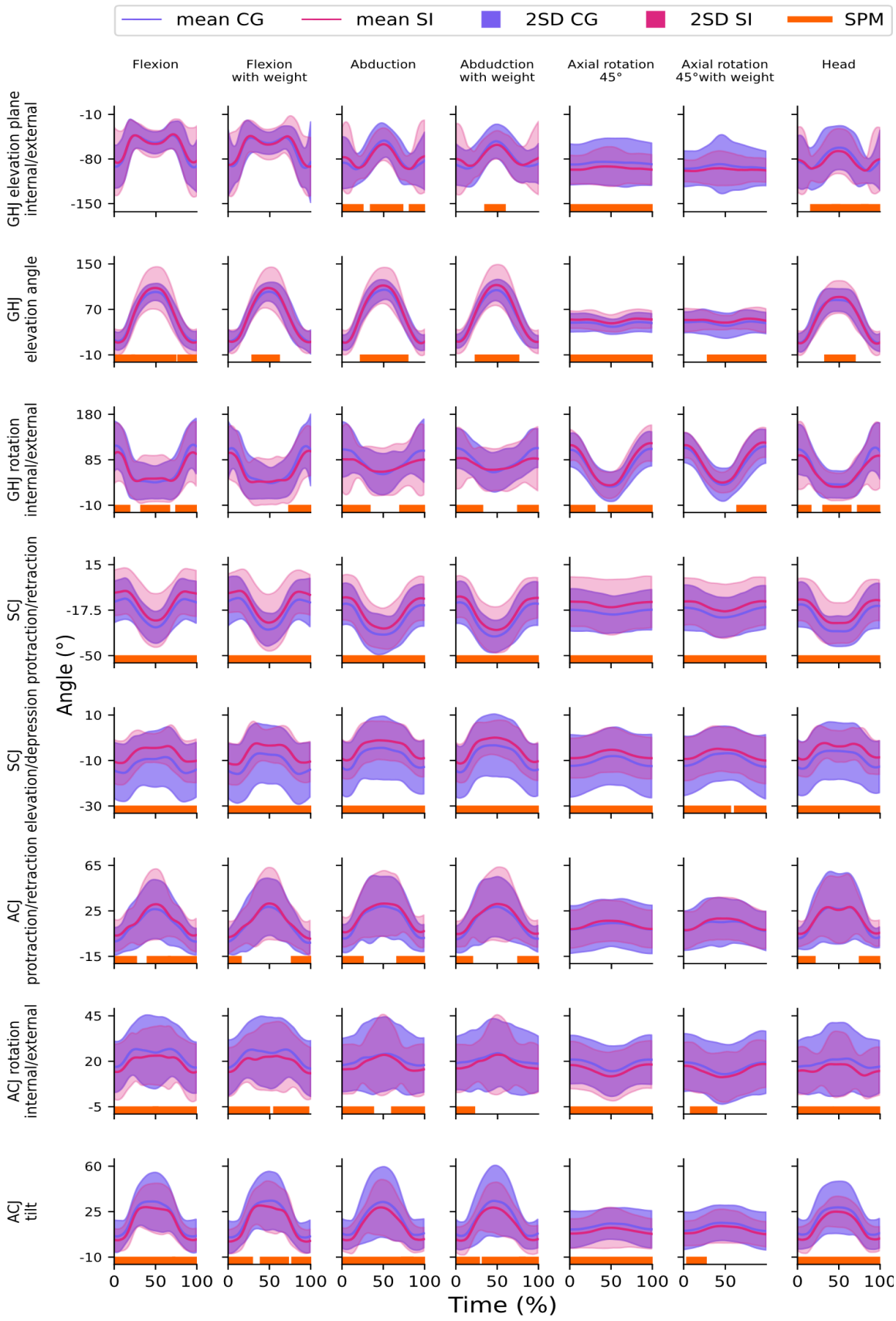
mean CG
mean SI
2SD CG
2SD SI
SPM
Flexion
Flexion with weight
Abduction
Abdudction with weight
Axial rotation 45°
Axial rotation 45°with weight
Head
GHJ elevation plane internal/external
GHJ elevation angle
GHJ rotation internal/external
SCJ protraction/retraction
SCJ elevation/depression
ACJ protraction/retraction
ACJ rotation internal/external
ACJ tilt
Angle (°)
Time (%)

Fig. 6.3) Comparison of joint kinematics per group (SI vs CG) showing angles for all joints and all movements, following inverse kinematics. Lines show mean group angles, shaded areas indicate the two standard deviations, and the orange bars on the horizontal axis highlight regions of statistically significant difference between groups using statistical parametric mapping (SPM).

The thoracohumeral and thoracoscapular angles are also reported separately in Fig 6.4. They are non-articulating joints, or relative orientations between segments not directly linked via a single anatomical joint (and therefore not part of the model's kinematic chain). They are shown to reflect the clinician's observation in practice with the positions of the arm and scapula with respect to the thorax. The thoraco-humeral angles show no difference in flexion and weighted flexion, and little difference in abduction and weighted abduction, despite differences in joint angles within the shoulder girdle.

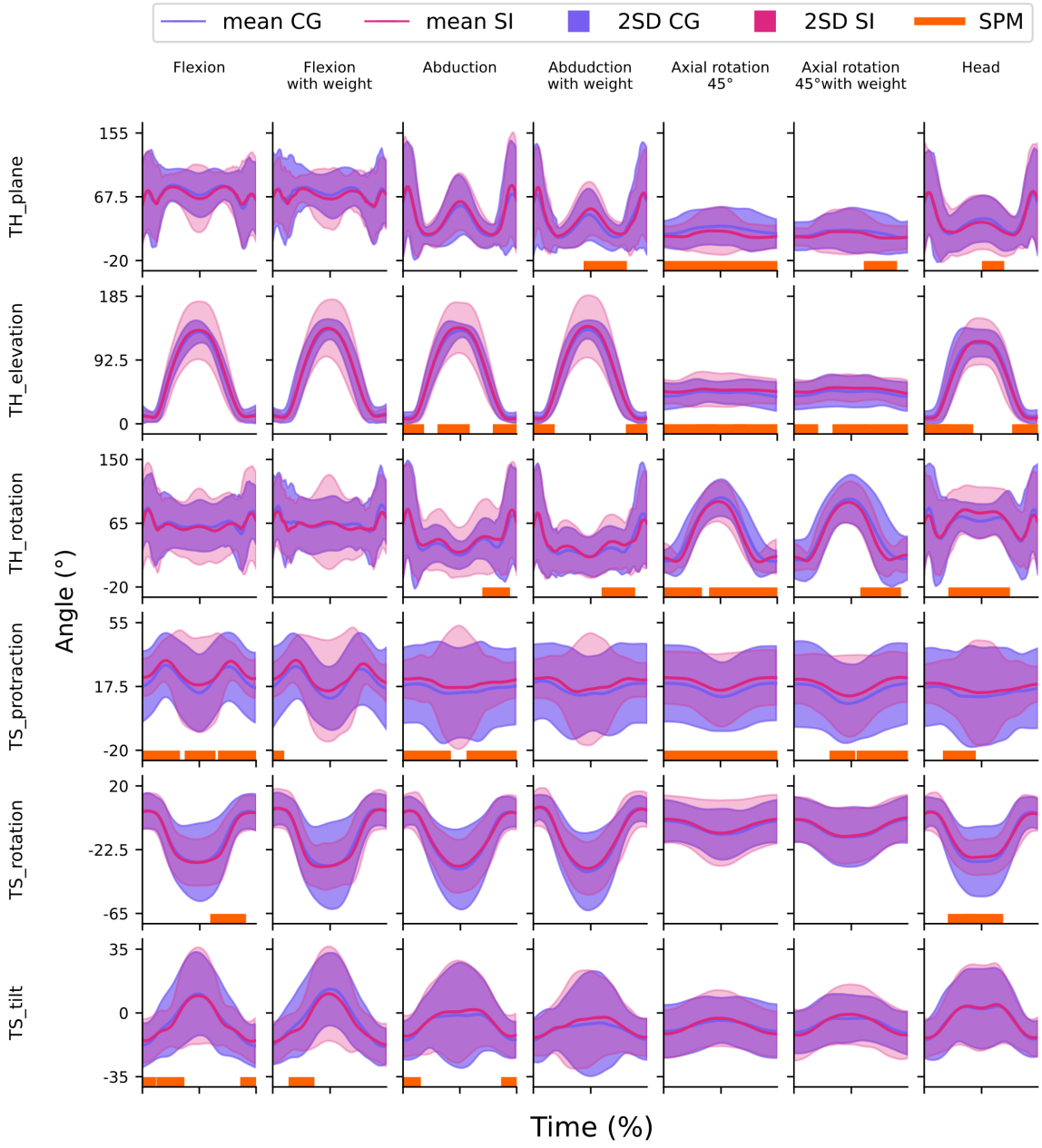

Fig. 6.4) Kinematics per group (SI vs CG) showing thoracohumeral and thoracoscapular angles for all movements. Lines show mean group angles, shaded areas indicate the two standard deviations, and the orange bars on the horizontal axis highlight regions of statistically significant difference between group using statistical parametric mapping (SPM).

6.2b. Muscle activity

The EMG data was normalised to the maximum encountered activation across any of the movement activities, weighted and unweighted tasks. The number of times this maximum value was encountered in each task is shown in Table 6.4 which is used as a manual sanity check in the scaling or normalisation procedure.

Table 6.4) Overview of in which movement each muscle (EMG) found its reference normalisation value in all participants of CG and SI group.

Motion	Trap. middle	Deltoid Ant.	Deltoid Post.	Lat. Dorsi	Pect. Major	Infraspin.	Triceps	Biceps
Flexion	1	2	1	0	1	0	1	1
Abduction	3	6	0	0	0	0	1	0
Axial	0	0	0	0	0	0	0	0
Hand to	0	0	1	0	0	1	0	6
Flexion with	3	6	1	0	11	3	2	5
Abduction	19	15	12	4	3	3	6	1
Axial	1	0	0	1	0	4	0	0
Grip	0	0	0	3	1	0	3	0
Shoulder	0	0	0	2	0	14	0	0
Shoulder	0	0	11	16	1	0	2	0
Shoulder	0	1	0	0	11	0	2	0
Shoulder	3	0	0	0	1	0	0	0
Elbow	0	0	4	4	0	1	12	0
Elbow	0	0	0	0	1	0	1	15
Wrist	0	0	0	0	0	4	0	0
Wrist flexion	0	0	0	0	0	0	0	2

Partial results for a single participant (Fig. 6.5) are shown as an illustration of the intermediary step of EMG processing to obtain normalised RMS values for each muscle activity and motion. The repetitions are then averaged per participant in each group.

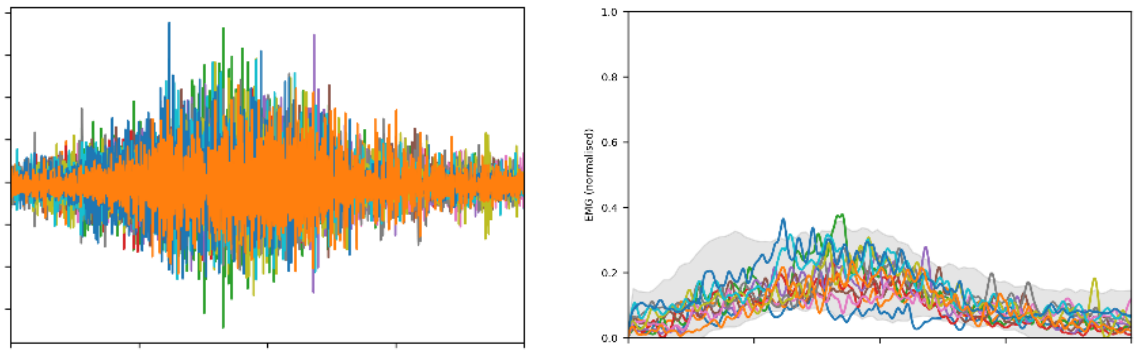

Fig. 6.5) Single muscle EMG for one participant (waveform), raw (left) and normalised rms (right), showing all repetitions of the motion Flexion.

The EMG and statistical differences on EMG (Fig. 6.6) show no differences in the Pectoralis major muscle in any of the movements, while the Latissimus dorsi shows differences across all tasks through nearly the whole time series with decreased normalised activity in the Shoulder Instability group.

In general, unweighted tasks tend to have more statistical differences in muscle activity overall compared to weighted versions.

In general, when compared to the CG group, the SI group has:

- increased normalised activity of their middle trapezius (mainly start and end of motion), posterior deltoid (mainly in the middle of the motion) and biceps muscles,

- decreased activity of their latissimus dorsi (consistently), triceps and anterior deltoid (mainly in the middle of the motion).

It appears that, in the Shoulder Instability group, muscles which control scapular movement on the posterior compartment of the body (middle trapezius, posterior deltoid) have a higher normalised activity than in the Control Group whilst muscles that primarily control humeral movement (latissimus dorsi and triceps) have a lower normalised activity. However, the inverse is true for muscles on the anterior portion of the body with increased biceps and decreased anterior deltoid activity.

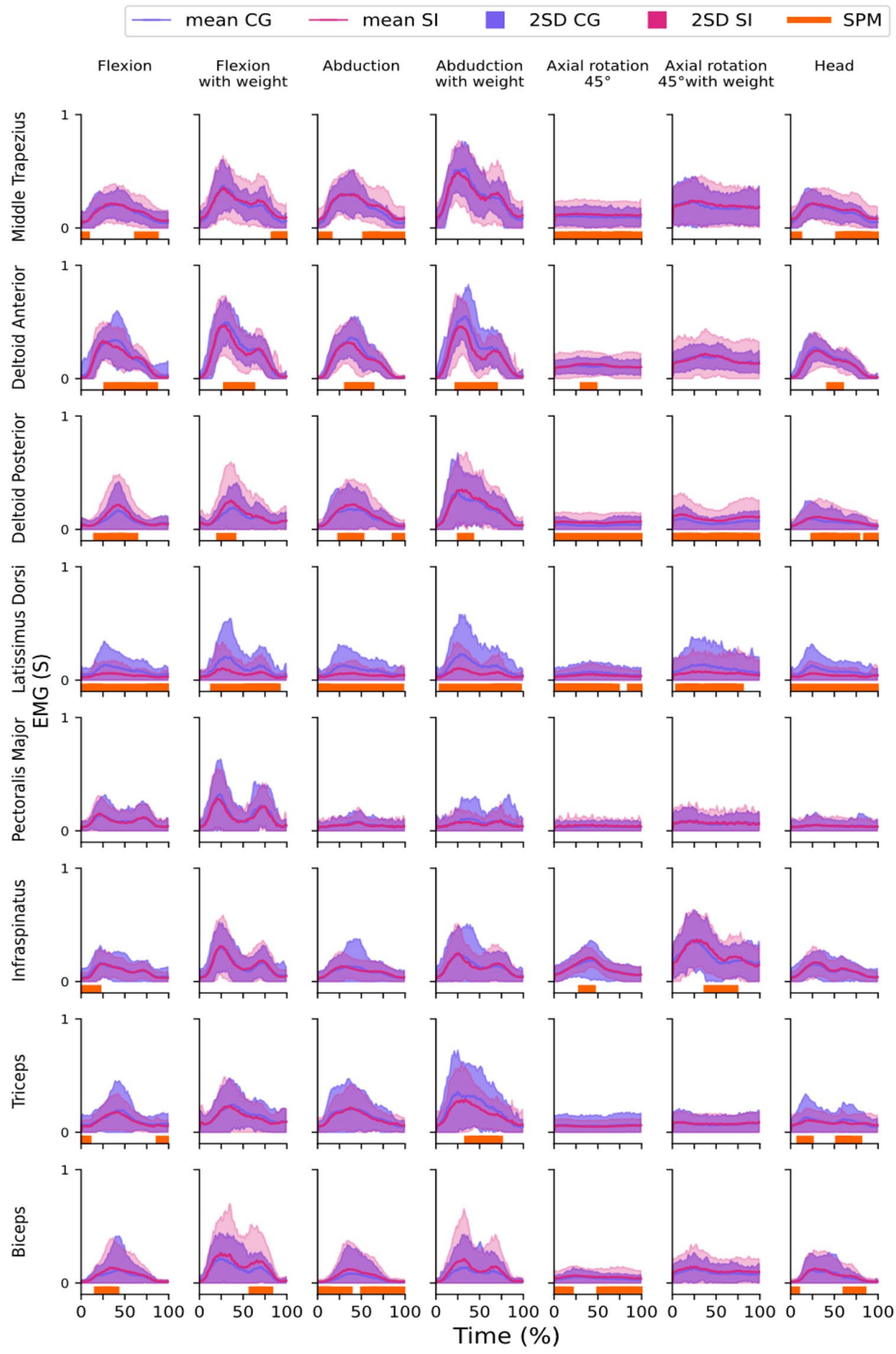
mean CG
mean SI
2SD CG
2SD SI
SPM
Flexion
Flexion with weight
Abduction
Abdudction with weight
Axial rotation 45°
Axial rotation 45°with weight
Head
Middle Trapezius
Deltoid Anterior
Deltoid Posterior
Latissimus Dorsi
Pectoralis Major
Infraspinatus
Triceps
Biceps
EMG (S)
Time (%)

Fig. 6.6) EMG per group (SI vs CG) for all muscles and all movements. Lines show mean group activity, shaded areas indicate the two standard deviations, and the orange bars on the horizontal axis highlight regions of statistically significant difference between group using statistical parametric mapping (SPM).

Within the Shoulder Instability group is identified a subgroup of participants that are virtually indistinguishable from the norm for a given motion. In other words, where the average across all repetitions of all joint angles of the model falls within two standard deviations of the norm throughout the whole timeseries. The information is presented in table 6.5 below, and 11/15 participants had at least one such motion identified. The two motions that were identified across most participants were axial rotation and weighted axial rotation (8 and 10/15 respectively), while abduction and weighted abduction were only identified in one specific participant. For comparison purposes, the same table for the individuals of the Control Group is in Appendix Table 6.5.

Table 6.5) Identifying the participants from the SI group that have motion across all angles of the model indistinguishable from normal kinematics, at each time step.

Participants from SI group	Flexion	Abduction	Axial rotation 45	Hand Head	Flexion with weight	Abduction with weight	Axial rotation 45 with weight
0WL1RZ767E							TRUE
7SJS0JZX3A	TRUE	TRUE	TRUE	TRUE		TRUE	TRUE
7X0AGZUZFG							
26MIB6XDC6			TRUE		TRUE		TRUE
905G3EUHWJ			TRUE				TRUE
B6SNJ3SBIW							
CL966HXS0C			TRUE				
FEH3JSLARJ							TRUE
HACIMVVX5A			TRUE				TRUE
PJ3URGRTWJ							
S6IRQQNB3G							
TKTEK8R7A0			TRUE				TRUE
WWO521323K			TRUE				TRUE
WX3800CYC3	TRUE				TRUE		TRUE
YRG37Y39YS			TRUE				TRUE

Within those motions, the muscle activities that are within two standard deviations of the norm are also assessed and presented Table 6.6. Each participant has, in every motion identified as normal, at least one muscle whose activity was within the norm. Those

normal muscles across normal motions of the participants of the subgroup will be referred to as “subset”.

Across all participants, two motions (axial rotation unweighted and weighted) showed the highest number of muscles with normal activity (2 to 3 instead of 1 to 2 for the other tasks).

The muscles are consistently Pectoralis Major, Latissimus Dorsi and Deltoid Posterior for unweighted axial rotation, and Pectoralis Major and Latissimus Dorsi for weighted axial rotation.

Table 6.6) Within the kinematics that were identified as normal in the subgroup, this table describes the muscles for which the EMG was within two standard deviations of the norm*. Shaded cells are normal motions, and contain the name of the muscles with normal activity if any.*

Participants from SI group	Flexion	Abduction	Axial rotation	Hand Head	Weight Flexion	Weight Abduction	Weight Axial
0WL1RZ767E							['LatDorsi; ', 'PecMajor; ']
7SJS0JZX3A	['LatDorsi;]	['InfraSpin; ', 'PecMajor; ']	['DeltPost; ', 'LatDorsi; ', 'PecMajor; ']	['LatDorsi; ', 'PecMajor; ']		['LatDorsi; ', 'PecMajor; ']	['LatDorsi; ', 'PecMajor; ']
7X0AGZUZFG							
26MIB6XDC6			['DeltPost; ', 'LatDorsi; ', 'PecMajor; ']		['LatDorsi; ']		['LatDorsi; ', 'PecMajor; ']
905G3EUHWJ			['DeltPost; ', 'LatDorsi; ', 'PecMajor; ']				['LatDorsi; ', 'PecMajor; ']
B6SNJ3SBIW							
CL966HXS0C			['DeltPost; ', 'LatDorsi; ', 'PecMajor; ']				
FEH3JSLARJ							['LatDorsi; ', 'PecMajor; ']
HACIMVVX5A			['DeltPost; ', 'LatDorsi; ', 'PecMajor; ']				['LatDorsi; ', 'PecMajor; ']
PJ3URGRTWJ							
S6IRQQNB3G							
TKTEK8R7A0			['DeltPost; ', 'LatDorsi; ', 'PecMajor; ']				['LatDorsi; ', 'PecMajor; ']
WWO521323K			['DeltPost; ', 'LatDorsi; ', 'PecMajor; ']				['LatDorsi; ', 'PecMajor; ']
WX3800CYC3	['LatDorsi; ']				['LatDorsi; ']		['LatDorsi; ', 'PecMajor; ']
YRG37Y39YS			['DeltPost; ', 'LatDorsi; ', 'PecMajor; ']				['LatDorsi; ', 'PecMajor; ']

6.3. Discussion

The objective of this chapter was to characterise Shoulder Instability (SI) in young people and identify any observable differences compared with typically developing children in kinematics and EMG patterns. Fundamental research evaluating mechanisms for shoulder instability in young people is very limited and this cohort is one of the youngest evaluated (Bateman 2019, Jaspers 2011). This chapter provides evidence that **differences in ranges of motion, kinematics and muscle activity exist** between the Control and Shoulder Instability groups. Additionally, a hypothesis was made that "some shoulder instability patients may be kinematically indistinguishable from a healthy control group", which was found proven true as subgroup of participants from the SI group exhibit normal kinematics and muscle activity. Subgroup will refer to the list of participants (from SI) that had at least one normal muscle and motion, and Subset will refer to the list of normal muscle motions from all participants of the Subgroup.

In the kinematics results, while the overall thoracohumeral angles, and therefore arm positions are similar between groups, the SI group demonstrates different movement strategies across the joints of the shoulder girdle to achieve arm positioning, mainly at the sternoclavicular and acromioclavicular joints. This led the SI group to adopt a more protracted and elevated sternoclavicular joint during the motions, which was often accompanied by less internal rotation and upwards tilt at the acromioclavicular joint.

Surprisingly, the SI group exhibits higher range of motion in arm elevation (both glenohumeral and scapulohumeral) than the CG. While the SI group is likely to present with increased laxity, a protective behaviour limiting the overall RoM could have been expected, as is found in Robinson et al. (2006) in a study on 252 participants. The fact that

the tasks were constrained with the indication of raising the arm up towards the ceiling during data collection might however not be representative of the full potential range of motion of both groups. Additionally, the mixed population of traumatic and atraumatic participants with different directions of instability could have influenced these results and make comparisons to other studies difficult.

Differences in EMG patterns do exist, and in general weighted tasks tended to have fewer differences in muscle activity compared to unweighted versions. This result was expected, as higher degrees of contraction would be present in all participants when increasing weights, and therefore reducing the difference between the two groups.

When comparison to other studies is possible, the muscles posterior deltoid, infraspinatus and triceps muscles are found to have higher normalised muscle activities in the SI group, and decreased activity for the muscle deltoid anterior, in accordance with Illyes (2007, 2009) and Spanhove (2021, 2022). The biceps however in our research shows higher activity in SI than in CG, contrary to other published studies (Illyes 2007, 2009, Spanhove 2021). This difference might be due to the fact that whilst movements between studies were broadly similar, they might not have been kinematically identical, and contradictory results between studies regarding the triceps have been found (Spanhove, 2020).

EMG SPM results showed that the **Latissimus Dorsi was consistently different** across all tasks. It is the only muscle creating a direct link between the humerus and the spine and pelvic area, and has therefore some degree of activity in all motions of the upper limb. This can explain the fact that it reflects any difference in muscle activity of the shoulder girdle. Considering the kinematic differences, it is therefore expected to have differences in all motions. **The pectoralis major muscle showed no statistical difference** between the

two groups. It is not expected to provide significant activities when not performing a task against resistance and acting concentrically. It accompanies the motions during the elevation, and as the arm is lowering down with gravity the agonists of the elevation provide most of the work eccentrically. Other deeper muscles, such as the subscapularis, might show more activity and differences.

We have also identified a **subgroup of SI participants** that have motions virtually indistinguishable from the norm. The motion that was identified the most often was axial rotation at 45° abduction (weighted and unweighted). Within those, some muscles had activities consistently within the norm, namely Pectoralis Major, Latissimus Dorsi and Deltoid Posterior. In this limited motion, these muscles are constrained to their specific role of internal and external rotator. This can explain that they only show differences in their activations in motions with larger amplitudes, where they will also have a stabilising role throughout the full range of motion. The high constraints on the way to perform the motion of axial rotation offers limited possibility of kinematic variation, and the results show that it is therefore more likely to find normal angles and activities.

This subgroup of shoulder instability participants with normal kinematics and muscle activities (referred to as “subset”) will be used in objective C. This objective will test the ability of a musculoskeletal model to discriminate these participants from the control group based on predicted muscle activations derived from the kinematics alone.

Chapter 7:
How well does the model predict muscle activities from kinematics in the control group?

7.1. Introduction

Chapter 6 (objective A) defined kinematic and EMG differences between a normal and a shoulder instability group. The second objective (B) of this PhD is to use musculoskeletal modelling techniques to predict muscle activations in the healthy group, based on the kinematic data alone. This is used to define a baseline of a) which muscles are most reliably predicted using our techniques and b) reference value of the theoretically muscle activations for each muscle for comparison with EMG. It is a pre-requisite for objective C that will assess any differences between the normal and shoulder instability groups' muscle activity based on the static optimisation results.

This chapter 7 is based on the upper-limb models and on the inverse kinematics results of the Control Group (CG) dataset from chapter 6. For each repetition of each motion, the joint moment is calculated at every time step as detailed in the Methods section (5.2). The load is then further distributed between the different actuators (i.e. muscles) in order to compute the activations that would lead to each individual motion based on the chosen cost function. As there are more muscles crossing a joint than there are degrees of freedoms, leading to infinite possible combinations of muscle activities for each motion. This muscle redundancy defines an underdetermined system, and optimisation following a specific cost function minimising the activations allows to find unique solutions, as described in the Static Optimisation parts of the literature review (3.4.4) and methodology (5.2). The control quality check were performed as described in the methodology.

The results are presented in the form of average Root Mean Square Error (RMSE) values and output from correlation analyses, between the predicted muscle activation and measured EMG. Results are provided for the muscles of the model for which reference

experimental EMG data are available (middle-trapezius, infraspinatus, latissimus dorsi, deltoid posterior and anterior, and pectoralis major) and provide a baseline or reference of how accurate our predictions of muscle activations are using this pipeline for a given motion and muscle. The results are meaningful in the ability of the model to predict muscle activations based on individual kinematics in healthy individuals, which is a different approach than that of Chapter 6 that defined a normative muscle activation pattern for all possible normal kinematical variations of a given motion as discussed in the conclusion of the literature review.

7.2. Results

The results for a single repetition of a single participant are shown as an illustration of the intermediary steps of the Static Optimisation process across all repetitions of all sets (Fig. 7.1). The difference between the two waveforms is highlighted with a shaded area, and this difference is quantified using RMSE and correlation. All values are scaled to the maximum value encountered in the dataset. Therefore, the EMG data of the Deltoid Anterior (shown below) is scaled to the maximum value it had across all repetitions and motions, and the predicted activation is scaled to the maximum value of the predicted activation encountered across all repetitions and motions.

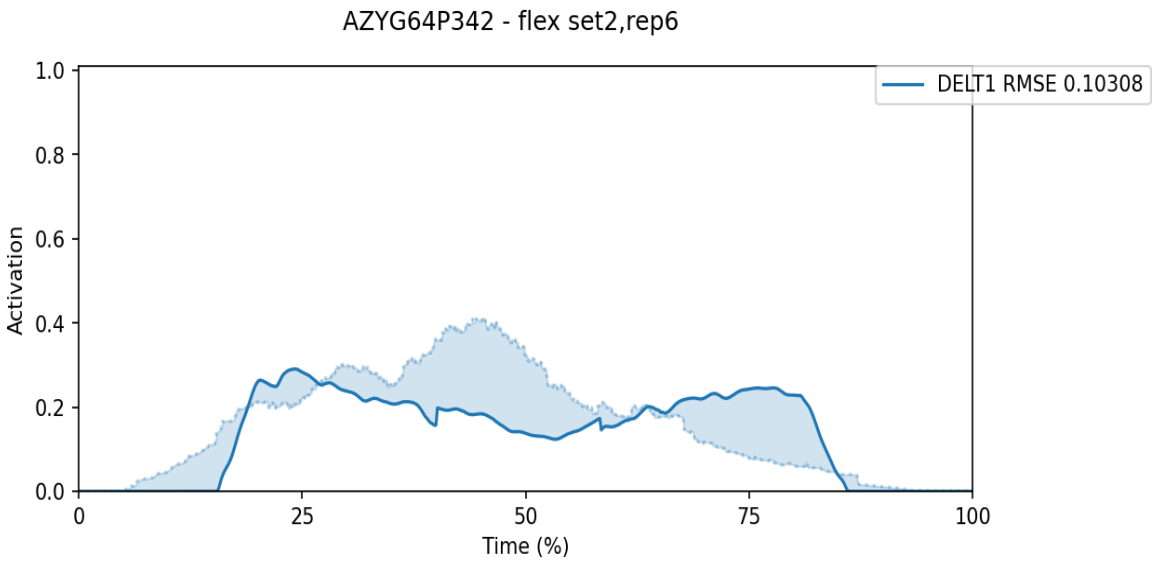

Fig. 7.1) Example based on one repetition of one motion of one participant: the blue solid line is the predicted activation from the static optimisation, the blue dotted line is the experimental EMG, the shaded area is the difference (graphical representation of the RMSE value that is shown in the top right legend).

7.2a. Root Mean Square Error results

The RMSE analysis of the Static Optimisation process on the Control Group dataset shows that some motions and muscles are better predicted than others. A graphical illustration of one high and one low score is presented below in Fig. 7.2.

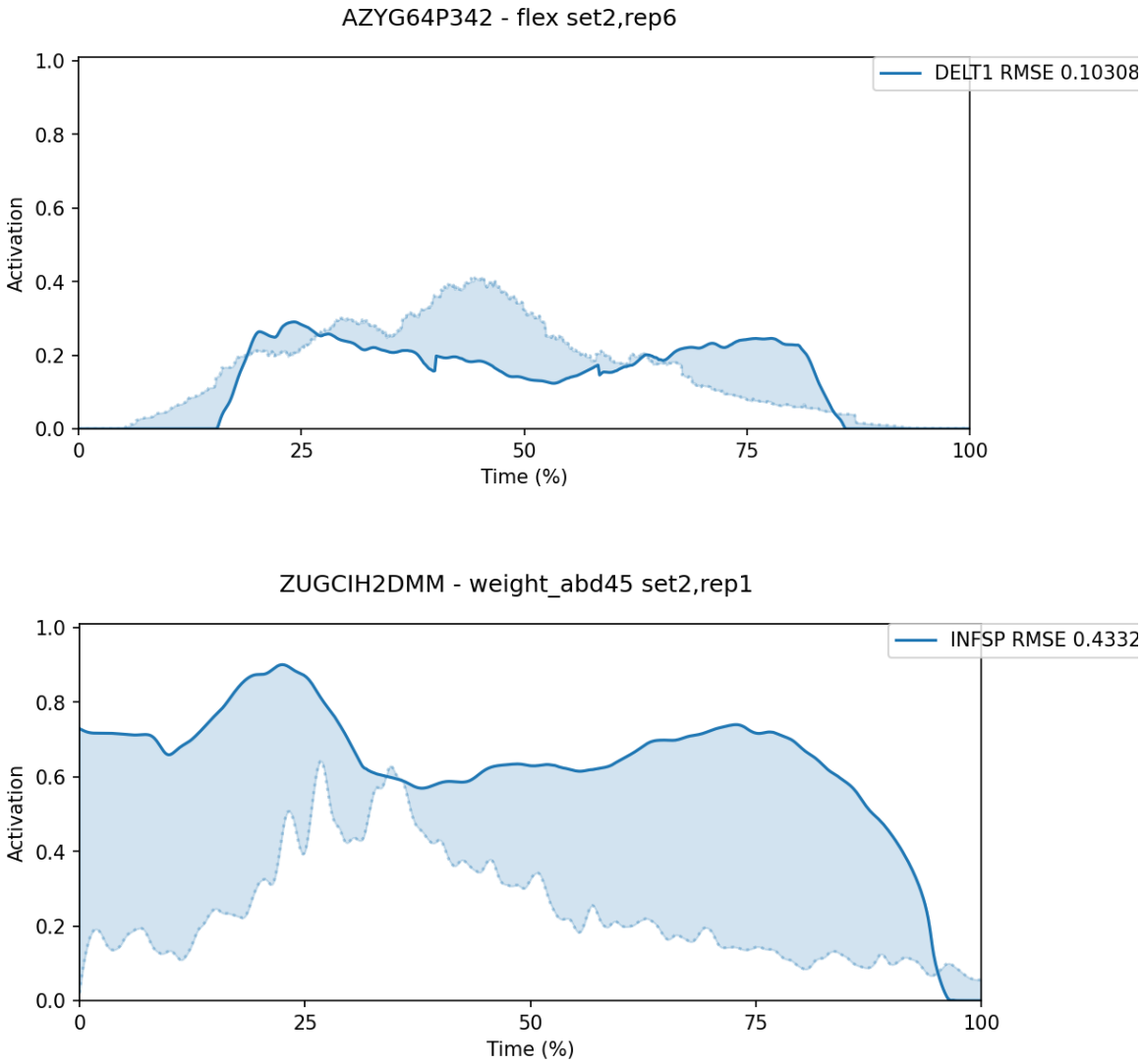

Fig. 7.2) Illustration of two the RMSE values between the static optimisation result (muscle activation prediction) and the experimental EMG. Top is a low value, meaning the prediction is in reasonable agreement with the experimental EMG, and more accurate than the bottom picture with a high value (which shaded area is increased).

Considering all the muscles, Table 7.1 below shows that the prediction of each unweighted motions is better (lowest average RMSE value) than its corresponding weighted motions.

The motions where activities are the most accurately predicted on average are the unweighted ones (the best being unweighted axial with RMS of 0.09), and the least accurately predicted are the weighted ones (worst being weighted abduction with a RMSE of 0.21).

The muscles Deltoid Posterior and Latissimus Dorsi (RMS 0.12 for both) and Pectoralis Major (RMS 0.13) are the most accurately predicted across all motion, while Infraspinatus (worst with RMS 0.20), Deltoid Anterior and Trapezius are the less accurately predicted.

The overall best predictions are found in Deltoid Posterior for axial rotation unweighted (best with RMS 0.05) and weighted, hand head and flexion, as well as pectoralis major for axial (unweighted) and hand head. The worse overall is Infraspinatus (worst with RMS 0.32) for weighted axial rotation, Trapezius and Deltoid anterior for weighted abduction.

Table 7.1) This table summarises the ability of our model to predict the experimental EMG in the control group. *Each value corresponds to the average* ***RMSE*** *(of all repetitions of all participants) between the waveforms of the predicted muscle activations (results from the Static Optimisation analysis) and of the experimental surface EMG. Green cells highlight the best predictions, and darker shades of green indicate lower errors.*

RMSE CG	**Trapezius Middle**	**Deltoid Anterior**	**Deltoid Posterior**	**Lat. Dorsi**	**Pect. Major**	**Infra**	**Average**
Flexion	0.13	0.13	0.11	0.10	0.14	0.13	0.12
Weight flexion	0.19	0.21	0.15	0.15	0.23	0.22	0.19
Abduction	0.19	0.17	0.13	0.13	0.09	0.15	0.14
Weight abduction	0.27	0.25	0.22	0.16	0.17	0.19	0.21
Abd45	0.10	0.11	0.05	0.07	0.05	0.18	0.09
Weight abd45	0.16	0.21	0.08	0.11	0.14	0.32	0.16
Hand head	0.14	0.11	0.07	0.13	0.06	0.20	0.11
Average	0.17	0.17	0.12	0.12	0.13	0.20	

The differences between muscles and motions, as well as their spread, are shown graphically in Fig 7.3. Some motions have lower average RMSE difference values than others, and within each motion the muscles have different RMSE values as well. No muscle

or motion has a systematically smaller spread. The plots for all motions are in Appendix Fig. 7.3 for reference.

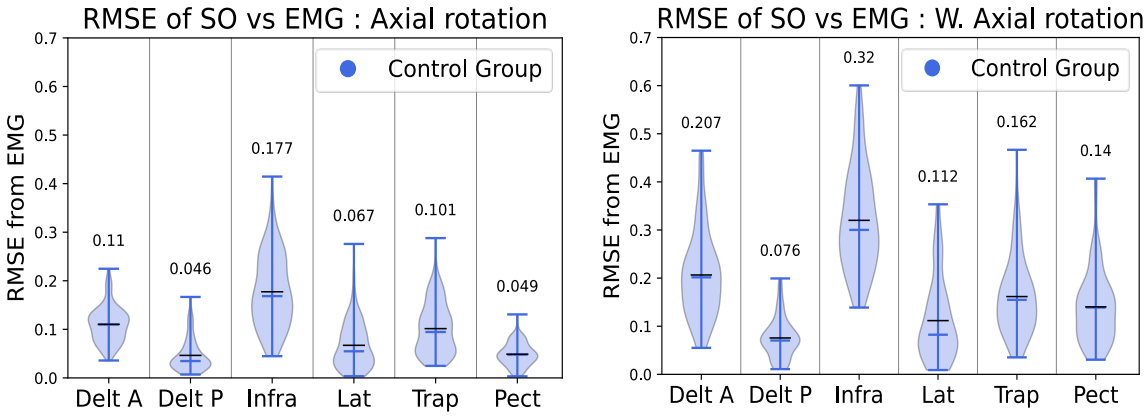

Fig 7.3) Showing the RMSE values of the predicted muscle activation from Static Optimisation versus the measured EMG, in the Control Group, of selected motions. Each violin plot has a line for the maximum, median, and minimum value. The mean value is shown as text above and as a black line on the plot. The shape extends to 1.5 times the inter-quartile range, showing the outlier points on either side of the distribution. Headings: Delt A = Deltoid Anterior, Delt P = Deltoid Posterior, Infra = Infraspinatus, Lat = Latissimus, Trap = Trapezius, Pect = Pectoralis Major.

7.2b. Correlation results

As RMSE only considers the amplitude of the difference between the measured EMG and predicted muscle activation, and does not take the shape of the waveforms into account, a non-amplitude correlation approach or correlation analysis was performed that measures the similarity between two signals. The results are first presented in the form of Pearson correlation coefficient values, which informs, on average, on how well each waveform of the experimental EMG matches that of the predicted activations (Table 7.2). The higher the value, the better the match.

Table 7.2) Summary of the waveform agreement between the predicted waveform of muscle activations and the experimental EMG. *Each value corresponds to the* ***Pearson correlation coefficient****, across all repetitions of all participants of the CG dataset. Darker cells highlight the best predictions (higher values).*

Correlation **measure** CG	**Trapezius Middle**	**Deltoid Anterior**	**Deltoid Posterior**	**Lat. Dorsi**	**Pect. Major**	**Infra**	**Average**
Flexion	0.21	0.57	0.06	0.1	0.31	0.43	0.28
Weight flexion	0.22	0.6	0.11	0.04	0.45	0.53	0.32
Abduction	0.2	0.53	0.24	-0.01	0.28	0.23	0.24
Weight abd	0.24	0.59	0.2	0.01	0.17	0.36	0.26
Abd45	-0.02	-0.04	0.07	0.09	0	0.42	0.09
Weight abd45	0.1	0.1	0.16	0.08	0.15	0.25	0.14
Hand head	0.21	0.57	-0.11	0.08	0.09	0.46	0.22
Average	0.17	0.42	0.1	0.06	0.21	0.38	

The Pearson coefficient analysis shows complementary results to those of the RMSE analysis. The predictions of the weighted motions have a better waveform agreement to the experimental EMG than the unweighted versions do. The best motions overall are the flexion weighted (0.32) and unweighted (0.26), and the worst motion is the unweighted axial rotation ("Abd45", 0.09).

On a per-muscle basis, across all motions, the best agreement is found in the Deltoid Anterior (0.42) and Infraspinatus (0.38) and the lowest agreement is found in the muscle Latissimus Dorsi (0.06) and Deltoid Posterior (0.1).

Overall, the best agreement is found in the Deltoid Anterior for the motion weighted abduction (0.59), flexion and hand-to-head (0.57). The lowest agreement is found in the muscle Pectoralis Major in the motion of unweighted axial rotation (0).

The table below illustrates the different cases of high and low agreement between RMSE and correlation measures.

RMSE: good match (low value) CORR: good match (high value) Deltoid Anterior, in motion Flexion 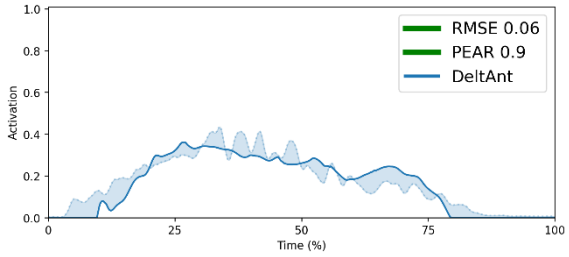	RMSE: poor match (high value) CORR: poor match (low value) Trapezius, in motion weighted abduction 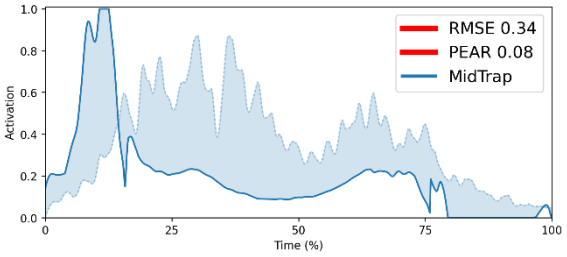
RMSE: good match (low value) CORR: poor match (high value) Deltoid Posterior, in motion Flexion 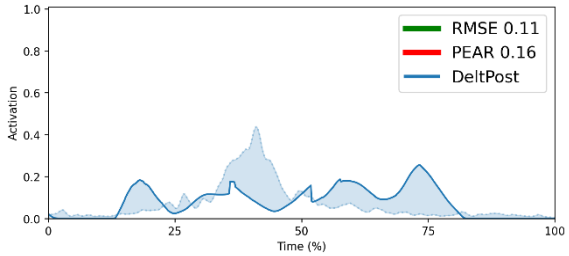	RMSE: poor match (high value) CORR: good match (high value) Infraspinatus, in motion w. axial rotation 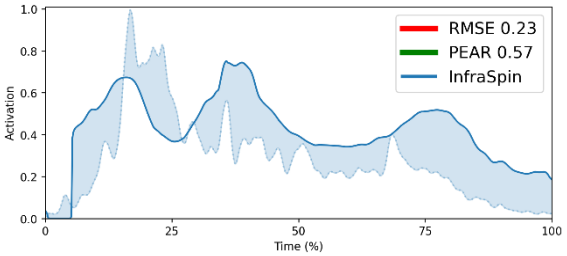

Fig. 7.4) Illustration of four RMSE and correlation values between the static optimisation result (muscle activation prediction) and the experimental EMG.

7.3. Discussion

The objective of this chapter was to use musculoskeletal modelling techniques to predict muscle activations in the healthy group, based on the kinematic data alone, and to define baselines of which muscles are most reliably predicted using our techniques as well as reference value for each muscle.

The results have been presented in the form of average Root Mean Square Error (RMSE) values and output from correlation analyses, between the predicted muscle activation and measured experimental EMG.

The results for RMSE value, in the CG dataset, show that the amplitude of muscle activity throughout the motion is more accurately predicted by the model in the unweighted motions than in weighted motions, which could be explained by the underlying assumption made in the cost function used which minimises muscle activations. This assumption might not hold true when weight is involved in prescribed motions used in this protocol, meaning that adding weight induces more co-contraction than the model predicts.

The most accurate prediction, based on RMSE values, was for the motion unweighted axial rotation which represents a very narrow range of motion and reduces the possible muscle activations to generate the motion.

The combined motion hand-to-head (unweighted) yielded an overall better accuracy than the (unweighted) physiological motions flexion and abduction, and the best predicted muscles (lowest RMSE) are also in hand-to-head motion. It might seem counter-intuitive at first that a combined motion is better predicted than simple physiological ones that require less joint and angle combinations and therefore can be expressed in simpler ways.

However, two elements could explain this result. A less restrictive motion performed in a more natural way could be better represented by our cost function, as the subjects might not have had the opportunity to optimise their control strategies for new and unfamiliar tasks. This specific motion has less range of motion in humeral elevation than the others (to the exception of axial rotation which yielded the best results), and might therefore be less impacted by the limitations of our model in defining scapular motion in high elevations as described in the Methods chapter. Additionally, it is possible that participants over-contracted as they reached full elevation.

The best predicted muscles across all motions are the Deltoid Posterior, as well as Latissimus Dorsi and Pectoralis Major that are both expected to have less activation and contribution overall which could explain why they have such low RMSE scores.

The less well predicted muscles overall are Deltoid Anterior and Trapezius. The normalisation has been done based on the highest value of each muscle across all motions for reasons detailed in the literature review, which differs from a conventional Maximum Voluntary Contraction approach) although both the experimental EMG and the predicted activities are normalised the same way so that to a) not impact the results and b) be repeatable. This less accurate prediction could be explained, for the Deltoid, by the way the muscle fibers are modelled that might not match the anatomical placement of the EMG used in the experimental setup. The Deltoid is a large muscle composed of many fibers, and, as seen in the literature review chapter, up to 19 segments organised in seven groups have been detected in this muscle (Brown et al. 2007). Muscles are typically modelled with fewer actuators than there are physiological muscle fibers or segments in order to match the moment arm at the joint level as it is the case in this study. Special care

can be given in the construction of the model in order to match specific muscle segments as it could be the case for the Deltoid. Therefore, the amplitude might differ, and this idea is further reinforced by the good results of the Deltoid Posterior.

The infraspinatus and trapezius are highly sensitive to the position of the scapula, which is a known limitation of our model and can explain the high RMSE showing a poor prediction.

Limitations of the RMSE analysis are illustrated in 7.3, as it only provides information on the overall match of the two waveforms and therefore does not allow to differentiate between one small area of large discrepancy and a continuous small difference. For this reason, the correlation analysis is conducted.

The results for the Pearson correlation analysis cast light on a different aspect of the difference between the EMG and the prediction and take the general shape of the waveform into account. Some of the results of the correlation measures are different to those of the RMSE. Participants might find it difficult to completely relax a muscle especially when repeating a motion despite the instructions and the resting time allowed as described in the Methodology chapter, and in addition a baseline noise might be present on the EMG. Therefore, the beginning and end of the motions are likely to have a larger impact on the correlation value (with the trend of the waveform being different) than on the RMSE value (as it is generally on small activations). In addition, the predicted activations can be under estimated mid-motion (at the peak) as participants could over activate their muscles, which can also have a significant impact on the correlation value.

A direct comparison to other studies is challenging due to variations in the movements conducted, number and selection of muscles measured, models and scaling methods, and

more importantly different populations, and therefore these results provide a novel and significant addition to the literature. However, the prediction of the correlation analyses is in accordance with the original publication (Wu, 2016) of the model that found a generally good agreement in the timing of activity or no activity from the result of static optimisation compared to surface EMG in a series of functional tasks, despite a highly different population used (six healthy adult males).

In summary, RMSE appears to present less limitations than correlation measures to assess the quality of prediction using the chosen methodology. The best (RMSE) predicted muscles are the Deltoid Posterior, Latissimus Dorsi and Pectoralis Major in unweighted motions, and more specifically in unweighted axial rotation. This chapter established a baseline of how accurately this specific modelling method predicts muscle activations in a series of normal motions, and the next chapter will investigate any existing difference in the prediction abilities of the Shoulder Instability dataset.

Chapter 8:
Differences in muscle activation prediction abilities between Control and Shoulder Instability groups

8.1. Introduction

The third and final objective of this PhD is to assess our ability to discriminate or classify two groups based on muscle control alone. Chapter 7 (objective B) defined a baseline of the difference to be expected between the predicted activations and the recorded EMG signals (for each muscle and motion) in a non-pathological group (control group "CG"). This current chapter applies the same methodology to the Shoulder Instability (SI) group, in other words using Static Optimisation based on the unique kinematics of each motion. The description, general strengths and weaknesses of this methodology have already been covered in the previous chapter.

The results of the Static Optimisation of the SI group are presented as a direct comparison to those of the CG group in section 1), in order to highlight any difference in the predictions across muscles and motions, based on a) RMSE values, and b) correlation measures. Statistical analyses are then performed in c) to calculate any significant differences between the model's ability to predict muscle activations in the two groups.

Finally, in section 2) **Static Optimisation and a statistical analysis are used on the subgroup of participants of the SI group that exhibited normal kinematics and muscle activity patterns** (referred to as "subset")**.** In chapter 6, a subgroup of the SI group was identified that has kinematics falling within the norm for specific motions, and normal muscle activity within these motions. This makes them virtually indistinguishable from a participant of the Control Group with the standard use of a motion capture and surface EMG systems following our protocol. This subset, that comprises a list of motions and muscles for the participant of the subgroup, is particularly interesting to analyse as it directly tests the main hypothesis which states that known pathological participants who

are kinematically indistinguishable from the norm can be differentiated on the basis of their muscle control alone. Therefore, the purpose of this chapter is to highlight any observable difference in the results in order to be able to identify pathological participants that would otherwise be considered to be within kinematical and EMG norms.

8.2. Differences between Control and Shoulder Instability groups

The intermediary results of the Static Optimisation analysis on the Shoulder Instability group – following a similar methodology to Chapter 7 on the Control Group - are available in the Appendix (Tables 8.01-2. Fig. 8.01). The following sections directly compare the results.

8.2a. RMSE analysis

Considering the two cohorts together the RMSE values that describe the difference between the predicted activation from SO and the experimental EMG are consistent with the previous analyses of each group individually. Table 8.1a shows where the model is best at predicting muscle activations considering all participants of the study (both groups), and table 8.1b shows which muscle and movement are more diagnostic, meaning the difference of accuracy of prediction between the two groups. The information is also presented in a single summary table in Appendix Table 8.1.

Table 8.1a) Average of the RMSE values of the two groups, showing where the model is best considering all participants of the study*. The lower the value, therefore the darker the cell, the better the prediction. Value: RMSE between predicted muscle activity (SO) and experimental EMG.*

	Trapezius	Delt. Ant	Delt. Post	Lat. Dorsi	Pect. Maj	Infraspin.	Total
Flexion	0.14	0.14	0.115	0.09	0.15	0.125	0.76
Weight flex.	0.19	0.23	0.155	0.13	0.24	0.21	1.16
Abduct	0.20	0.19	0.14	0.12	0.095	0.15	0.90
Weight abd.	0.27	0.26	0.23	0.135	0.16	0.195	1.25
Abd45	0.11	0.115	0.055	0.06	0.065	0.17	0.58
Weight abd45	0.16	0.215	0.09	0.09	0.16	0.295	1.01
Hand head	0.145	0.125	0.075	0.12	0.07	0.17	0.71
Total per muscle	0.1735	0.18	0.125	0.105	0.135	0.19	0.91
Total	1.38	1.46	0.99	0.85	1.08	1.51	

The overall model's ability to predict muscle activities, considering both groups (in the column "Total"), is best in all unweighted tasks than in all weighted tasks, and therefore each activity is better predicted in its unweighted version. The best overall motion considering all muscles being unweighted axial rotation, and the worst being weighted

abduction. The model also yields more accurate results (row “Total”) in estimating the activities of the latissimus dorsi (best), deltoid posterior and pectoralis major, and oppositely it has less accurate results with the muscles infraspinatus (worst), trapezius and deltoid anterior.

Table 8.1b) Difference of the RMSE value of both groups (SI-CG), showing which muscle and movements are more diagnostic*. In green, the prediction is better for the CG group than for the SI group (positive values). In blue, the prediction is better for the SI group than for the CG group (negative values). Values: RMSE between predicted muscle activity (SO) and experimental EMG. Column and row "Total" are colored with a heatmap showing the largest difference in dark.*

	Trapezius	Delt. Ant	Delt. Post	Lat. Dorsi	Pect. Maj	Infraspin.	Total
Flexion	0.01	0.02	0.01	-0.02	0.02	-0.01	0.03
Weight flex.	0.00	0.04	0.01	-0.04	0.02	-0.02	0.01
Abduct	0.02	0.04	0.02	-0.02	0.01	0.00	0.07
Weight abd.	0.00	0.02	0.02	-0.05	-0.02	0.01	-0.02
Abd45	0.02	0.01	0.01	-0.02	0.03	-0.02	0.03
Weight abd45	0.00	0.01	0.02	-0.04	0.04	-0.05	-0.02
Hand head	0.01	0.03	0.01	-0.02	0.02	-0.06	-0.01
Total per muscle	0.01	0.02	0.01	-0.03	0.01	-0.02	0.00
Total	0.07	0.19	0.11	-0.24	0.13	-0.17	

On a per motion basis considering all the muscles (column "Total") the model is consistently better at predicting the Control Group than the Shoulder Instability group in all physiological unweighted motions (except "hand to head"), and was better at predicting

the Shoulder Instability group than the Control Group in all weighted motions (except "Flexion"). The highest differences were found in motion unweighted flexion (CG better than SI by 0.03 RMSE on average) and weighted abduction (SI better than CG by 0.07 RMSE on average).

On a per muscle basis considering all the motions, the model is better at predicting in the Control Group all the muscles except latissimus dorsi and infraspinatus (which were better predicted in SI group). The highest difference was found in muscles deltoid anterior and pectoralis major (CG better than SI by 0.19 and 0.13 RMSE respectively) and latissimus dorsi (SI better than CG by 0.24 RMSE on average)

Overall, the highest RMSE difference between the two groups:

- where CG prediction was better than SI (0.04 difference) shows Deltoid Anterior in weighted flexion, Pectoralis Major in weighted axial rotation and Deltoid Anterior in Abduction.
- where SI prediction was better than CG shows Infraspinatus in Hand head (0.06 difference), Latissimus Dorsi in weighted abduction (0.05 difference) and Infraspinatus in weighted axial rotation (0.05 difference).

The spread of the data presented in Fig. 8.1) indicates that no muscle or motion has a systematically different spread in one group or the other. It presents the data for the motions that show the highest difference between groups. The plots for all motions are in Appendix Fig. 8.1).

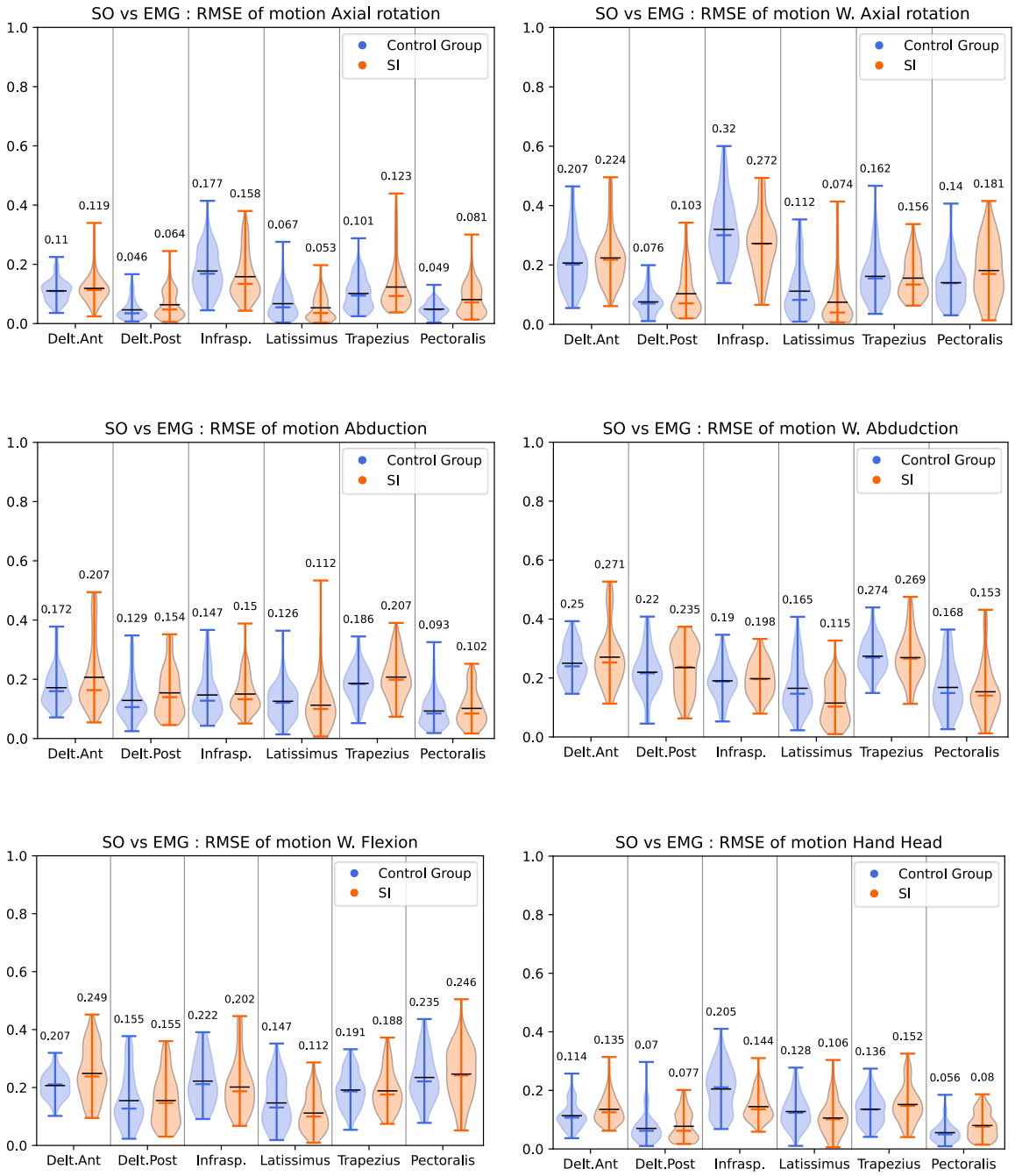

Fig. 8.1) plot comparison of the RMSE difference between the SI and CG groups. Each value is the average RMSE between predicted muscle activity (SO) and experimental EMG. Each violin plot has a line for the maximum, median, and minimum value. The mean value is shown as text above and as a black line on the plot. The shape extends to 1.5 times the inter-quartile range, showing the outlier points on either side of the distribution.

8.2b. Correlation analysis

The correlation measure estimates the degree of correlation of the waveforms of the prediction and experimental EMG for a given muscle in a specific motion, and is introduced in chapter 7. It presents a much larger spread than the RMSE analysis.

The full table is in Appendix Table 8.2, and the spread is shown below in Fig. 8.2, with the full plot available in Appendix Fig. 8.2.

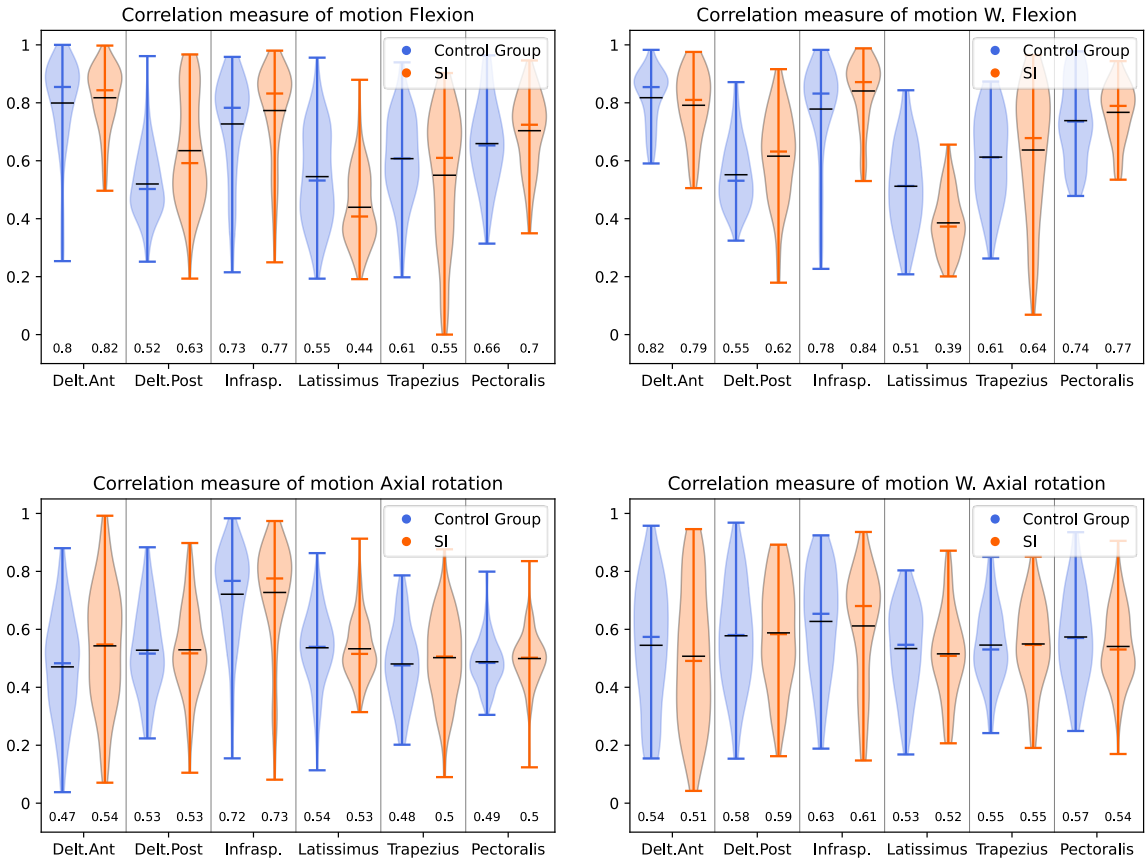

*Fig. 8.2) plot comparison of the **Pearson correlation measure** difference between the SI and CG groups. Each value is the average measure between predicted muscle activity (SO) and experimental EMG. Higher values represent a better prediction. Each violin plot has a line for the maximum, median, and minimum value. The mean value is shown as text below and as a black line on the plot. The shape extends to 1.5 times the inter-quartile range, showing the outlier points on either side of the distribution.*

8.2c. Statistical differences

i) RMSE permutation tests

Statistical differences are found between the two groups. Table 8.2 shows the statistically significant differences between the prediction of muscle activity in the Control and the Shoulder Instability group, per motion and muscle, based on the RMSE value.

Table 8.2) Result from the permutation tests with SI and CG based on the RMSE values. *The cells in green represent the situations where the null hypothesis has been rejected and the alternative hypothesis has been accepted, meaning that SI changes the accuracy of prediction of the Static Optimisation. It emphasises the fact that there are differences between the two groups for a given muscle in a given motion, in the way our model predicts the muscle activities.*

	Mid-Trap	Delt-Ant	Delt-Post	Lat-Dorsi	Pec-Major	Infra-Spin	Total Row
Flexion	TRUE	TRUE		TRUE	TRUE	TRUE	5
Abduction	TRUE	TRUE	TRUE				3
Axial Rot.	TRUE		TRUE	TRUE	TRUE	TRUE	5
Hand head	TRUE	TRUE		TRUE	TRUE	TRUE	5
W.Abduction				TRUE			1
W.Axial Rot.			TRUE	TRUE	TRUE	TRUE	4
W.Flexion		TRUE		TRUE			2
TotalCol	4	4	3	6	4	4	

In line with the previous sections, there are more muscles exhibiting a statistical difference between unweighted motions than their weighted version. Considering all the muscles, the motions where the most statistically significant results are found are flexion, axial rotation and hand-to-head (5 out of 6 muscles). The muscle Latissimus dorsi was found statistically significant in all motions except abduction. Weighted abduction and weighted

flexion have the smallest number of muscles with a statistically significative difference with 2 and 1 respectively.

ii) Correlation permutation tests

Statistical differences are found based on the results from the correlation measure, and are summarised in Table 8.3) below.

***Table 8.3) Result from the permutation tests with SI and CG based on the Pearson correlation measures**. The cells in green represent the situations where the null hypothesis has been rejected and the alternative hypothesis has been accepted, meaning that SI changes the accuracy of prediction of the Static Optimisation. It emphasises the fact that there are differences between the two groups for a given muscle in a given motion, in the way our model predicts the muscle activities.*

	Mid-Trap	Delt-Ant	Delt-Post	Lat-Dorsi	Pec-Major	Infra-Spin	Total Row
Flexion	TRUE		TRUE	TRUE	TRUE	TRUE	5
Abduction	TRUE		TRUE	TRUE	TRUE		4
Axial Rot.		TRUE					1
Hand head			TRUE	TRUE	TRUE	TRUE	4
W.Abduction					TRUE	TRUE	2
W.Axial Rot.							0
W.Flexion			TRUE	TRUE		TRUE	3
TotalCol	2	1	4	4	4	4	

Similarly to the results based on the RMSE value, unweighted motions present more muscles with statistical differences on average, apart from the motion hand to head. Pectoralis major, Deltoid Posterior, Latissimus Dorsi and Infraspinatus are found different between the two groups in the most motions (four out of seven).

8.3. Static Optimisation on SI participants with normal kinematics

Differences have been reported, in section 2, in the way the model estimates the muscle activations between the Control and the Shoulder Instability groups. This section 3 focuses

on the subgroup of the Shoulder Instability group displaying kinematics and EMG that are within the norm (as defined in Chapter 6) for some motions and muscles ("subset"), and are therefore virtually indistinguishable while being known participants of the shoulder instability group. Three different approaches are used to attempt to discriminate between those two groups as summarised graphically in Fig. 8.3. The results from the Static Optimisation of the subset are compared to those of the Control Group, based on a) RMSE values, and b) correlation measures. Statistical analyses using permutation tests are then conducted in c) to identify any difference between those two groups (control group and subgroup).

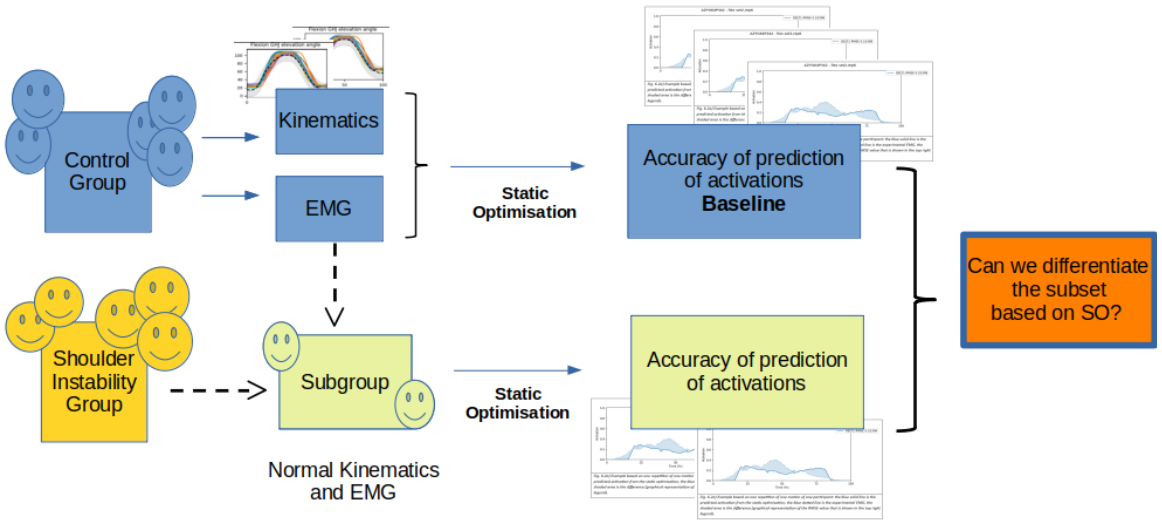

Fig. 8.3) Summary of the pipeline, showing the subgroup of the Shoulder Instability group that exhibits normal kinematics and muscle activity ("subset"), as well as the static optimisation analyses. The control group (blue) defines the normal kinematics, emg, and accuracy of prediction. The shoulder instability group (orange) has a subgroup of participants (green) that exhibit normal kinematics and emg for specific motions and muscles (vertical dotted arrow, "subset"). The final step is comparing the accuracy of prediction of the control group to that of the subset using the results of Static Optimisation (SO).

8.3a. RMSE analysis

Considering the baseline of abilities of our model to predict muscle activities in normal participants (objective B in Chapter 7 using Static Optimisation), the following results assess differences between the Control Group and the Subset, based on the RMSE values.

Table 8.4 presents the results of the RMSE tests. For each motion and muscle, the two-standard deviations RMSE (of the difference between predicted activation and EMG) was calculated in the Control Group. Each motion and muscle of the subset was tested against this two-standard deviations of the norm of prediction of the Control Group (RMSE). More than half (6/11) participants of the subgroup had at least one muscle falling outside across the motions. Differences are mainly found in muscles Pectoralis Major and Latissimus Dorsi, in the motions Axial rotation weighted and unweighted.

Table 8.4) This table shows, for each motion identified as normal of the subgroup, the number of times that a muscles' RMSE value (average of all repetitions) falls outside of the two standard deviations of the baseline of our prediction*. The individual muscles are also mentioned in each cell. In blue are the cells where Pectoralis Major was identified.*

RMSE outside of norm in subset	Flexion	Abduction	Axial rotation	Hand to head	Flexion with weight	Abduction with weight	Axial rotation with weight	Total
0WL1RZ767E							0	0.0% (0/6)
7SJS0JZX3A	16.667% (1/6) ['DeltAnt']	33.333% (2/6) ['DeltAnt', 'DeltPost']	16.667% (1/6) ['PecMajor']	0		16.667% (1/6) ['DeltAnt']	33.333% (2/6) ['LatDorsi', 'PecMajor']	19.444% (7/36)
26MIB6XDC6			16.667% (1/6) ['PecMajor']		0		16.667% (1/6) ['PecMajor']	11.111% (2/18)
905G3EUHWJ			0				0	0.0% (0/12)
CL966HXS0C			0					0.0% (0/6)
FEH3JSLARJ							0	0.0% (0/6)
HACIMVVX5A			16.667% (1/6) ['DeltAnt']				0	8.333% (1/12)
TKTEK8R7A0			66.667% (4/6) ['DeltAnt', 'DeltPost',				16.667% (1/6) ['DeltPost']	41.667% (5/12)

			'MidTrap', 'PecMajor']					
WWO521323K			0				0	0.0% (0/12)
WX3800CYC3	0				16.667% (1/6) ['InfraSpin']		33.333% (2/6) ['DeltAnt', 'DeltPost']	16.667% (3/18)
YRG37Y39YS			0				16.667% (1/6) ['PecMajor']	8.333% (1/12)
Total column	1/6 = 17%	2/6 = 33%	7/24 = 29%	0	1/6 = 17%	1/6 = 17%	7/30 = 23%	

Two participants of the subgroup exhibit overall high scores across all tested motions with ~20% and ~42% of the muscles identified as being outside of the norm when considering average RMSE values. Across all participants of the subgroup, two motions have more frequently identified muscles, namely weighted axial rotation (5/10 participants) and unweighted axial rotation (4/8 participants).

In the Shoulder Instability group, 10/15 participants had normal kinematics in weighted axial rotation, and all of those had normal EMG for Pectoralis Major and Latissimus Dorsi (from Table 6.6 in Chapter 6). When compared to the **two-standard deviations of the difference between predicted activation and EMG**, the Pectoralis Major was found abnormal in 3/10 participants and the Latissimus Dorsi in 1/10.

In the Shoulder Instability group, 8/10 participants had normal kinematics in unweighted axial rotation, and all of those had normal EMG for Pectoralis Major and Latissimus Dorsi. When compared to the two-standard deviations of the difference between predicted activation and EMG, the Pectoralis Major was found abnormal in 3/10 participants, and the Latissimus Dorsi in 0/10.

Therefore, in our dataset, **Pectoralis Major is differentiable 3/10 times in both weighted and unweighted axial rotation using the two-standard deviations of RMSE of SO, even when the Kinematics and EMG appear normal.**

Figure 8.4 below illustrates the differentiation of a participant of the subgroup.

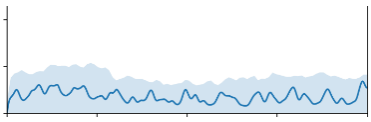

EMG (blue line) of a SI participant with normal kinematics and EMG, within the two standard deviations of the EMG norm (shaded blue)

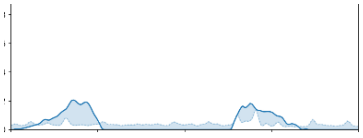

SO (blue line) of a healthy participant (Pectoralis Major in weighted Axial), which accuracy (shaded blue) is within the two standard deviations of the RMSE-SO norm (not indicated).

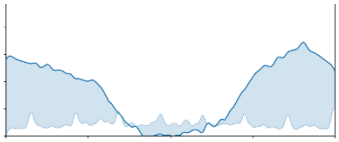

SO (blue line) of the subset belonging to a participant of the subgroup (Pectoralis Major in weighted Axials), which accuracy (shaded blue) is outside of the two standard deviations of the RMSE-SO norm (not indicated).

Fig. 8.4) Graphical illustration of the differentiation of a participant from the subgroup based on the accuracy of the static optimisation when both kinematics and EMG are normal (i.e. belong to the subset).

The same test has been performed on the Control and Shoulder Instability groups, in order to provide the Figure 8.5 below that allows us to observe the spread of the data as well as to summarise the findings. The higher values mean that more muscles (across all motions) were predicted differently than the baseline that was established in Chapter 2 with the normal dataset. As differences have already been shown between the Control group and the Shoulder Instability group, higher values are expected in the SI group. The main takeaway is that participants from the subgroup (red) also exhibit high values compared to the control group (blue), which indicates that they can be differentiated on the basis of their muscle control, while they couldn't be separated from the blue dots on the basis of their kinematics or EMG data alone.

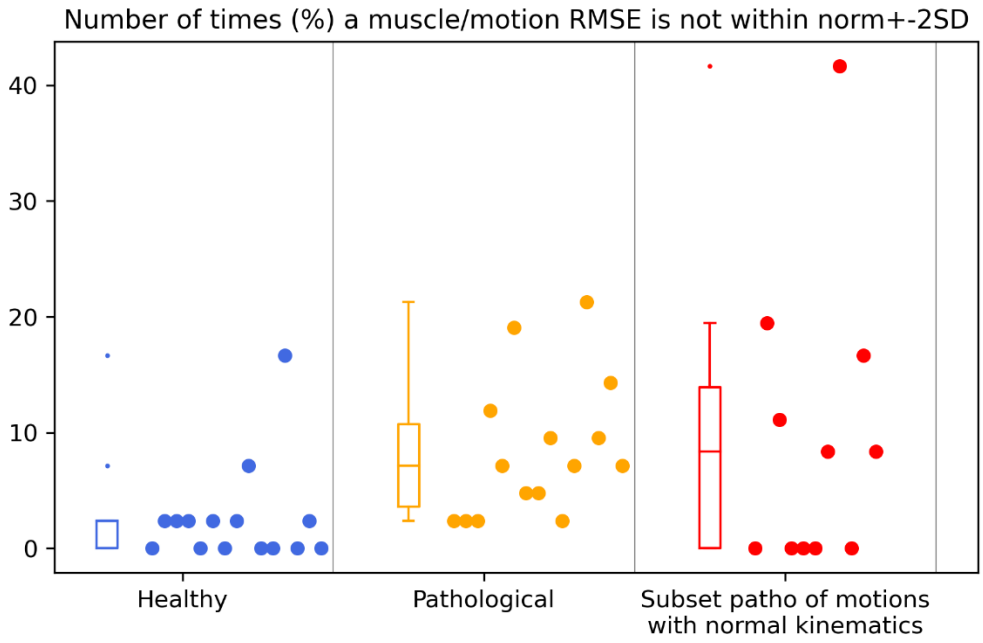

Fig. 8.5) Each dot represents a participant from the Control (blue), Shoulder Instability minus Subset (orange) or Subset (red) group. The subset is only comprised of the normal motions and muscles of the SI group (subgroup). For each dot representing a participant, a zero value on the Y axis means that across all motions, all the muscles are predicted within two-standard deviations of the baseline. Any increment on Y is a percentage of the number of muscles across motions. 19% means that out of the 6 muscles across 7 motions (42 combinations), a muscle was not within the two-standard deviations of the baseline 8 times.

8.3b. Correlation analysis

The same comparison to the two standard deviations of the norm is done based on the correlation analysis. Correlation measures are provided in Appendix Table 8.4. It shows less differentiation in comparison to the RMSE approach.

To compare and summarise these approaches, each test has been done also to the Control and Shoulder Instability group and summarised in Figure 8.6 below. The RMSE approach intuitively differentiates the Control Group from the Shoulder Instability group better than the correlation analysis. More importantly, the subgroup (in red) appears to have differences as well. The next section covers a statistical analysis of each approach.

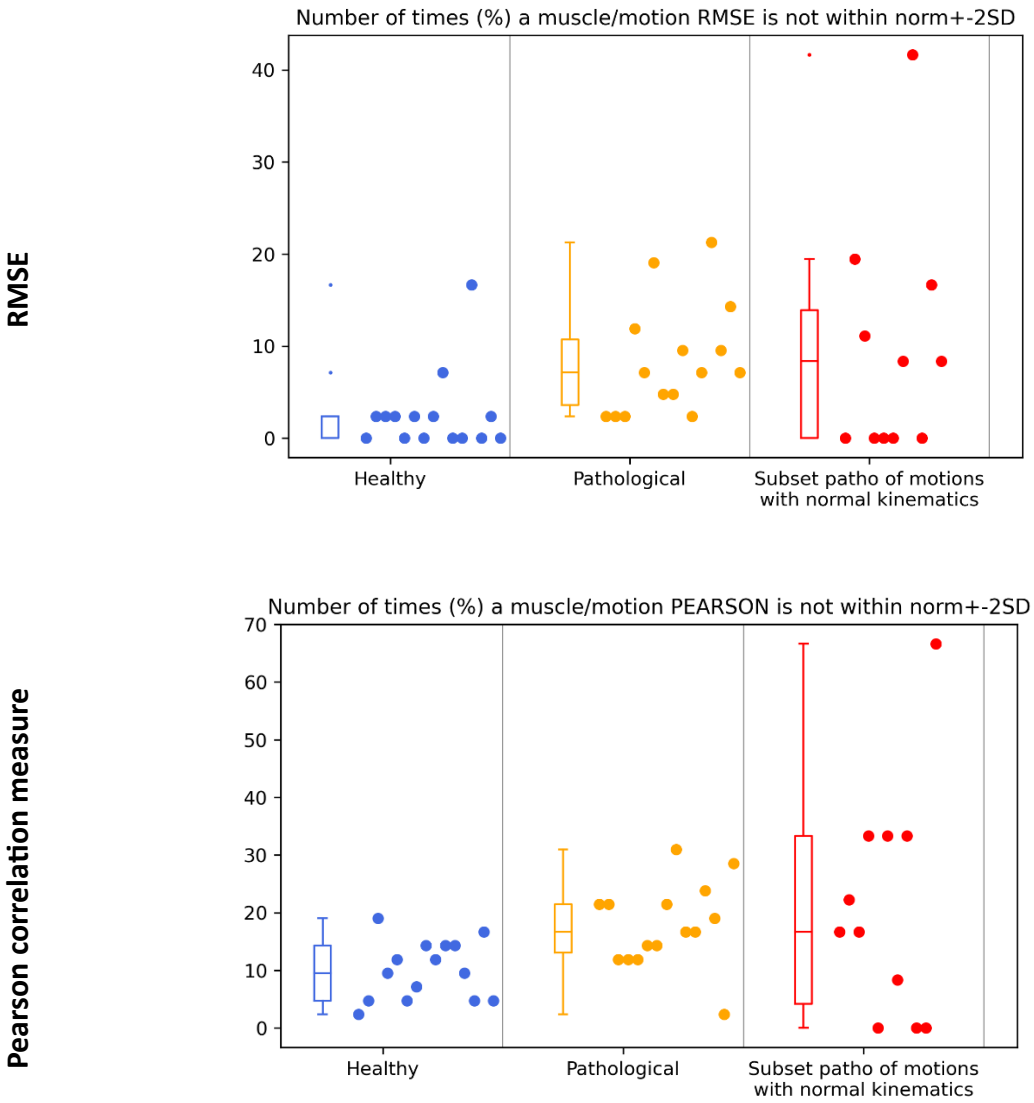

Fig. 8.6) Each dot represents a participant from the Control (blue), Shoulder Instability minus subset (orange) or Subset (red) group. The subset is only comprised of the normal motions and muscles of the SI group (subgroup). For each dot representing a participant, a zero value on the Y axis means that across all motions, all the muscles are predicted within two-standard deviations of the baseline. Top plot is based on RMSE, and bottom plot on correlation measure. For each point, any increment on Y is a percentage of the number of muscles across motions. 19% means that for this participant out of the 6 muscles across 7 motions (42 combinations), a muscle was not within the two-standard deviations of the baseline 8 times.

8.3c. Statistical analysis

This section performs permutation tests as described in section 2.c). For each approach (RMSE and correlation measure), the permutation tests are performed on each muscle, motion and participant of the subset. Therefore, the probability of the difference between predicted activation and EMG of each motion and muscle from the subset (that has normal kinematics and EMG) is tested to verify if it is likely to belong to the Control Group or not. In other words, even if the kinematics and EMG are normal, this analysis tests if there is a statistical difference in the way muscle activity is predicted using static optimisation. These results are complementary to those of the two-standard deviation tests from the previous section.

i) RMSE permutation tests

Table 8.4 presents the results of the permutation tests based on the RMSE values, in other words testing if the RMSE value of each muscle and motion of the subset (that has normal kinematics and EMG) is likely to belong to the Control Group.

All participants (11/11) from the subgroup have at least one muscle in one motion whose prediction is statistically different from that of the Control Group. Differences are mainly found in the motions Axial rotation unweighted (8/8, i.e. every motion that had normal kinematics and EMG) and weighted (9/10).

Within those two motions, the muscles in Pectoralis Major (found 6/8 and 6/10 times in axial unweighted and weighted respectively), Latissimus Dorsi (5/8 and 6/10 times) and Deltoid Posterior (5/8 and 5/10 times) appear the most often.

Table 8.4) Each cell with data corresponds to the motion that was identified as having normal kinematics for a given participant of the subgroup*. The value is a ratio and a percentage of how many times a muscle had a p-value <0.05 rejecting the null hypothesis (of the two-tailed test) that there was no difference between all repetitions of this participant and all repetitions of the normal group for this given motion and muscle,* ***based on the RMSE value****.*

Permutations on subset	Flexion	Weight Flexion	Abduction	Weight Abd.	Axial rotation	W. axial rotation	Hand head	Total Row
0WL1RZ767E						PecMajor		1 / 6 = 16.7%
7SJS0JZX3A	DeltAnt DeltPost InfraSpin		DeltAnt DeltPost	DeltAnt DeltPost MidTrap	DeltAnt DeltPost InfraSpin LatDorsi PecMajor	DeltPost InfraSpin LatDorsi PecMajor	DeltAnt DeltPost LatDorsi	20 / 36 = 55.6%
26MIB6XDC6		InfraSpin LatDorsi PecMajor			DeltAnt DeltPost InfraSpin LatDorsi PecMajor	DeltAnt DeltPost InfraSpin LatDorsi PecMajor		13 / 18 = 72.2%
905G3EUHWJ					DeltPost 'LatDorsi MidTrap PecMajor	DeltPost LatDorsi		6 / 12 = 50.0%
CL966HXS0C					DeltAnt MidTrap PecMajor			3 / 6 = 50.0%
FEH3JSLARJ						MidTrap		1 / 6 = 16.7%
HACIMVVX5A					DeltAnt DeltPost LatDorsi MidTrap PecMajor	DeltAnt PecMajor		7 / 12 = 58.3%
TKTEK8R7A0					DeltAnt DeltPost InfraSpin MidTrap PecMajor	DeltPost InfraSpin LatDorsi MidTrap		9 / 12 = 75.0%
WWO521323K					DeltAnt InfraSpin MidTrap	0 / 6 = 0% []		3 / 12 = 25.0%
WX3800CYC3	DeltPost InfraSpin LatDorsi MidTrap PecMajor	DeltPost InfraSpin MidTrap PecMajor				DeltAnt DeltPost LatDorsi PecMajor		13 / 18 = 72.2%
YRG37Y39YS					InfraSpin LatDorsi	InfraSpin LatDorsi PecMajor		5 / 12 = 41.7%
Total Column	**8/16 = 50%**	7/16 = 43.8%	2 / 6 = 33.3%	3 / 6 = 50.0%	**31/48 = 64.6%**	26/60 = 43.3%	3 / 6 = 50.0%	

ii) Correlation permutation tests

Appendix Table 8.5 presents the results of the permutation tests based on the correlation measures. The main motions and muscles identified are similar to the RMSE. To ease the comparison, the results are summarised and presented together in the table 8.5 below.

The Pectoralis Major in the motion unweighted Axial rotation is more often identified as being statistically different based on RMSE or correlation measure than the other muscles, motions, and methods.

Table 8.5) Results from the permutation tests, identifying muscles and motions of the subset (normal kinematics and EMG of the shoulder instability group) that do not statistically belong to the control group*. First column is the value on which the statistical analysis is performed. Second column shows how many participants of the subgroup had at least one muscle in one motion with statistical differences. Third column shows how many motions had at least one muscle with statistical differences, among the motions that had normal kinematics and emg. Fourth column shows the detail of the muscles most often identified. Legend: Pectoralis Major ("Pec"), Latissimus Dorsi ("Lat"),*

Permutations based on	Number of participants of subgroup with statistical changes in at least one motion / number of participants in the subgroup	Motions most identified / number of motions with normal kinematics and emg	Muscles most identified in this motion, across participants
RMSE	11/11	Axial rotation (8/8)	**Pec (6/8) = 75%**
			Lat (5/8) = 63%
		Weight axial rotation (9/10)	Pec (6/10) = 60%
			Lat (6/10) = 60%
Correlation	11/11	Axial rotation (8/8)	Pec (1/8) = 13%
			Lat (2/8) = 25%
		Weight axial rotation (9/10)	Pec (1/10) = 10%
			Lat (3/10) = 30%

8.4. Discussion

The third and final objective of this PhD was to a) assess our ability to discriminate or classify two groups based on muscle pattern alone and b) more specifically investigate, using our model, participants from the SI group that had motion and muscle activities indistinguishable from the norm from Chapter 6.

Considering the two cohorts together informed on the overall abilities of the model to predict muscle activations in a range of individuals belonging to both groups, as well as on the differences in prediction that can exist between the two groups. With no surprise, behaviours that were common to each group individually (based on the RMSE value) remained, namely that unweighted motions are better predicted than weighted motions in general, and that several muscles (such as the Pectoralis Major, Latissimus Dorsi, and Deltoid Posterior) are better predicted compared to others (such as the Infraspinatus, Trapezius and Deltoid Anterior). This could be explained by the tendency, in both groups when using weights, to co-contract more than anticipated by the model that minimises muscle activations.

Comparing the RMSE values between groups shows that the Control Group is better predicted than the Shoulder Instability group in all unweighted motions (to the exception of hand-to-head) when considering all muscles. From a per-muscle perspective, the main anatomical actors of the motions, namely Deltoid (Anterior and Posterior) and Trapezius are consistently found better predicted in the CG group in unweighted motions. This may be as if the SI group, in general, is prioritising stability over efficiency when using no weight (as covered in the section 3.1.3 and 3.2.3 of the literature review and discussed in

Chapter 6), which is less well represented by our cost function and is a non-surprising result.

Additionally, the Shoulder Instability group is better predicted than the Control Group in weighted motions abduction and axial rotation, when considering all muscles. This could mean that when using weights, the SI group has a tendency not co-contract as much as CG, also maybe to prioritise stability, although those results largely are due to two main muscles only: the Latissimus Dorsi and the Infraspinatus.

The correlation analyses provided additional information and the results differed from those of RMSE. They presented more limitations, a larger spread, and less difference than RMSE in during the statistical analysis.

Combining these results, the muscles that exhibited the most difference in the prediction ability of their muscle activity between the Control and Shoulder Instability groups are the Pectoralis Major and Latissimus Dorsi, in unweighted motions. As discussed in Chapter 6 during the comparison of the EMG of both groups, unweighted tasks might be more likely to exhibit differences in muscle activities, as higher degrees of contractions could show as weight is increased, reducing the differences.

The tendency to prioritise stability over efficiency in unweighted motions can be an important information to consider in the assessment and diagnosis of Shoulder Instability patients.

The results of Static Optimisation on the Shoulder Instability participants that had normal kinematics and EMG (subgroup) showed clear patterns, however generalisations from this subgroup have to be considered carefully as any more detailed explanation should be the subject of a series of case studies which is out of the scope of this study.

First, the two-standard deviations of the baseline established in Chapter 7 on the Control Group was used to compare the results to the subset (list of normal motions and muscles from the subgroup) using a) RMSE and b) correlation measure. RMSE showed the most differences, and seems to be better able to discriminate between those two groups. **Based on the RMSE** values alone, the SI group and the subset exhibit clear differences with the CG. Both the SI group as a whole and the subset have muscles for which the average RMSE (across all repetitions) is higher than those of the CG. **The motion showing the most difference is axial rotation** (weighted and unweighted) in both the subset and the SI group when compared to CG, and **the muscle that appears the most is Pectoralis major.**

These results are further reinforced by **the permutation tests**, that show a higher average percentage of muscles with statistically significant results across all motions for each participant, and also highlight **the motion of unweighted axial rotation** as being the one with the most significant number of muscles in the subset, and Pectoralis Major and Latissimus Dorsi as being the most often identified muscles.

In the motion of axial rotation, the positioning of the arm at 45° of abduction mostly relies on muscle activities to keep the head of the humerus centred in the glenoid fossa. This is due to the glenohumeral ligaments providing less support anteriorly in this distinctive position, and more specifically the superior glenohumeral and coracohumeral ligaments that have a lesser tension, as well as the GH joint being less congruent below the 60-90 degrees of elevation threshold defining the “closed pack” position (Manske, 2016), allowing more anterior displacement of the humeral head which has to be compensated by non-soft tissues. In addition, while performing the rotations in this position, the muscles have clearly identified roles of internal or external rotators, which is not the case

when larger ranges of motion are involved and that the muscles can change their role during the course of motion as seen in the literature review. It might make the identification of the muscle patterning easier.

It is essential to emphasise again that these results are based on this specific dataset, following this specific methodology, and that it does not allow to conclude generalities on which muscles are most likely to be used for discrimination between groups in general, due to the diversity of the clinical presentations and the number of possible compensatory muscle patterns. The identification of the motion unweighted axial rotation as having the most significant results is however an indication of a non-normal patterning, regardless of the compensatory combination used. Nonetheless, it is interesting to note that the Pectoralis Major and Latissimus Dorsi are both actors of medial rotation which is the direction of instability defined by the superior glenohumeral and coracohumeral ligaments mentioned above. It is also worth noting that, in Chapter 1, within the unweighted axial rotation motions of the subgroup identified as normal, the muscles that had normal EMG (8/11 times) were Pectoralis Major, Latissimus Dorsi and Deltoid Posterior.

In other words, high values (directly compared to the norm with RMSE, or identified via permutation tests of RMSE or correlation measure), based on the SO results, across all muscles in unweighted axial rotation, appear to be able to indicate of not belonging to the Control Group, even when those participants have perfectly normal kinematics, and even when the EMG were shown as normal. Similarly, high values across all motions distinguish - in our datasets - both the SI group and subset from the CG.

9. General discussion

The results of Chapter 6 (objective A) showed differences in both kinematics and EMG patterns between the two groups. While most research characterising the motion of shoulder instability patients focuses on scapular position and motion both at rest and during motion across different clinical presentations (Paletta et al. 1997, Illyes and Kiss 2006, Ogston and Ludewig 2007, Struyf et al. 2011), an interesting finding of chapter 6 was that the overall arm position of the groups (i.e. thoraco-humeral angles) appears too similar to be differentiated by the naked eye (and virtually indistinguishable or with limited results from normal in flexion and abduction) which aligns with the findings from Jaggi et. al (2012), while providing new evidence specific to this age group. Yet statistically significant differences were found in the 3D kinematic and EMG patterns, which identify different movement strategies in shoulder instability individuals and emphasise the importance of Motion Capture and EMG technologies in clinical assessments. The difference in movement strategy across the shoulder-girdle joints and associated muscles may be due to SI participants prioritising stability over efficiency as was found by Illyes and Kiss (2006) in a study on multidirectional instability covering an older age group. Further work through a longitudinal study will be needed to identify if these differences can predict those at risk of future instability. The Shoulder Instability group presented in this study can therefore be differentiated from CG based on both 3D motion capture and EMG data. These results provide new evidence that following an episode of instability, young people exhibit differences that are both quantifiable and statistically significant when compared to an age and sex matched control group, which aligns with the findings of

research based on the adult population (Leroux et al. 2015). This data may help future research to identify meaningful patterns, differences or modification in kinematics and muscle activity patterns.

The kinematics observed provided no clear differences between the weighted and unweighted motions in the RMSE and SPM analyses, and taking into account the risks of dislocation of this specific population, it is not recommended to use low or self-selected weights (no difference), or to increase the weight (unsafe) to emphasise kinematic differences that could be expected with higher loads and discriminate the populations in future studies using this methodology. There is no clear consensus in the literature regarding the kinematics of shoulder instability patients, and most studies do not cover the age range of the cohort presented in this thesis or do not perform the motions in a similar way. However, moderate evidence of a decreased upward rotation of the scapula (similar to the findings of chapter 6, and to Kobayashi, 2022) and of an increased upward scapula rotation (opposite to the findings of chapter 6) are described in a literature review by Spanhove (2021) during motions of arm elevation in the scapular plane, which is different from the motion of frontal elevation in the sagittal plane of the protocol of this current study.

In addition to the motions performed being different to other studies, several aspects can impact the kinematic results of this study:

- The virtual markers defined in the model, that match the anatomical ones placed on the participants and are used for the inverse kinematics, are very few on the thorax in the form of a single cluster on the sternum. Although this does not impact the angles or calculations of the kinematic chain as defined in the model, this can sometimes have the

consequence of overestimating trunk inclination when only the upper torso would be moving, and that could impact the interpretation of the thoraco-humeral angles that are meant to represent what a clinician would be seeing, i.e. the global angle between the torso and the arm. A possible solution for this would be adding markers on the pelvis to have the option to estimate the full position of the trunk in the model, which can also help with visual representations in the forms of biofeedback.

- The timing of the tasks carried out was not constrained during data collection. The only information provided during the demonstration was an indication of the expected time each motion should take. This was decided to allow some freedom in the execution and hopefully provide a more natural and representative motion, but it inherently allows for more variability.

- The chosen methodology to track the motion of the scapula, using an acromion cluster and a single calibration, has limitations that were discussed in the methodology chapter. While it can have an impact more specifically in higher ranges of motion, it is a chosen compromise to increase practicality for further clinical use.

The EMG results showed that weighted tasks exhibited less difference between the two groups with the SPM analysis, and it is therefore recommended to assess this specific SI group in unweighted motions. This is consistent with the kinematic recommendations. Some findings, such as increased activity of the posterior deltoid, infraspinatus and triceps muscles, and decreased activity of the deltoid anterior in the SI group are in accordance with previously published studies (Illyes 2007, Spanhove 2021). Some findings in chapter 6 such as the increased activity of the biceps muscle are contrary to other studies (Illyes 2007). Special care needs to be given to standardising the protocols across studies in

future publications to prevent the contradiction of some results found today in the literature preventing consensus on muscle patterns (Struyf, 2014) as discussed in 3.2.2 of the literature review.

Kinematic RMSE and SPM showed similar differences in angles between the two groups. Therefore they both appear to be a way to discriminate, with arguments for and against each (ease of use with a single number for RMSE, identification of the time of the differences for SPM). However in this population EMG benefits from SPM analysis that allows a better differentiation in unweighted motions, and its use is increasingly recommended for upper limb EMG analysis (Kobayashi, 2022).

Whereas additional information on the deeper muscles of the shoulder that have an important role in stability could be useful in understanding the complex muscle patterns, the use of fine-wire EMG is highly impractical in routine assessment and also has its own limitations.

The muscle patterns are complex. The results show no obvious over- or under-contraction through any of the motions assessed that could be easily detectable by clinical observation alone, which is consistent with the findings of Jaggi et al. (2012) and Lewis and Bayley (2004), and supports the standardisation of the use of electromyography in clinical assessments. Muscle patterns appear to be grouped by position and function. Further analyses of synergies and Principal Component Analysis might inform on these complex behaviours.

The protocol used in this study was able to assess differences in movement and muscle activity patterns of young people with and without instability. Using this pipeline, the SI group can be differentiated through a) their kinematics when modelling physiological

joints (a kinematic chain comprising an unrestricted scapula), and through b) their muscle control using surface EMG. We recommend assessing shoulder instability participants matching our inclusion criteria in unweighted motions and tasks. The fact that both groups can be differentiated is consistent with what current literature suggests (Lawton, 2022), while adding valuable information with objective kinematic and electromyography data that focuses on this age group and that uses physiological motions that would allow repeatability across future studies.

In addition to the group comparison, a **subgroup of shoulder instability participants** was identified that had at least one motion and muscle virtually indistinguishable from the norm. The most common normal motions were axial rotation at 45° abduction weighted and unweighted. Within these motions, the most common normal muscles were Pectoralis Major, Latissimus Dorsi and Deltoid Posterior. **Subgroup** refers to the list of participants from the SI group that had normal motions and muscles. **Subset** refers to the normal motions and muscles themselves, independently of which participant of the subgroup they belong to. This information serves for objective C.

In Chapter 7 (objective B), the upper limb rigid body model with a free moving scapula has predicted muscle activations in the healthy group. The results showed that the model yields consistent results, in the way that unweighted motions are always better predicted than weighted motions. It provides confidence in the reliability of the model and therefore in its use in our study as opposed to having varying results per participant. A baseline with reference values for each muscle of what would be expected from a healthy participant using the chosen methodology has also been defined and served for objective C in Chapter 8. This baseline could help follow-on research if based on a similar methodology. It is

difficult to compare the accuracy of prediction of muscle activations (using static optimisation) with other studies, given the variability in model parameters and protocols. For example, Erademir et al. (2006) reviews studies using different models of the arm and shoulder and highlights differences in joint definitions and degrees of freedoms. The parameters to be optimised also vary and can be based on muscle stresses (Karlsson and Peterson, 1992), muscle activations (Delp et al. 2007, Kaufman et al. 1991), energy consumption (Praagman et al. 2006) or fatigue (Nieminen et al. 1995). Motions also differ and can range from slight variations in the plane of motion to different movements such as wheelchair-related activities (van Drongelen et al. 2005). However, the accuracy of prediction found in this thesis is in accordance with the agreement in the timing of activations between static optimisation and surface EMG found by Wu (2016) in an adult population. Among the existing differences in protocols, the scaling of the surface EMG data is often performed using a maximum voluntary contraction which differs from what was done in this study for safety reasons as discussed in the methods chapter (5.1). Consequently, the results add novel information on the expected ratio of activity between muscles and muscle groups in healthy young people.

While the goal was to define a baseline using this specific setup, the difference in the accuracy of the model to predict some muscles hold our attention, which does not impact the next objective and is therefore not part of the limitations. The model was chosen in part for the simplicity of the way the muscles were defined, with fewer lines of action (or muscle fibres) in large muscles compared to other models. However, muscles are usually defined with priority given to matching experimental moment arms, and not to matching the anatomical line of action that best represents a single surface EMG. Each muscle fibre being independent, it is possible that some model fibre(s) or segments of a same muscle

could be more representative of the anatomical experimental muscle than others. This could be the basis for either a) optimising the selection of one or several muscle fibres to find better matches between the predicted and experimental activations, or b) defining new model with this in mind.

The correlation results would provide useful information on a case-by-case basis, and would allow to show a difference in timing that might highlight compensatory behaviours for a given participant in a given motion. However, this study of group comparison showed to be of limited value in the overall quantification of the model's abilities to predict muscle activations in order to establish a baseline.

Lastly, Chapter 8 (objective C) had several parts. The first part of this objective was to compare the results between the two groups to highlight the differences in our model's prediction abilities, which could then be used as discriminators. The use of average RMSE values as well as non-parametric statistical analyses showed high probability of differences in the ability of the model to predict the muscle activations between the two groups, in specific muscles and motions.

Today our understanding of the control of the shoulder girdle in shoulder instability is based on the general paradigm that co-contractions constrain motion as a function of the degree of instability (Seyres et al. 2024, Shumway-Cook and Woollacott, 2007). In other words, in positions where the shoulder is most unstable and the ratio of shear over compressive forces increases, co-contraction is likely to increase as an attempted compensatory mechanism. The glenohumeral stability has been investigated in single planes of motion (Ameln et al. 2018) and across functional tasks in adults (Marchi et al. 2014). This behaviour and associated specific co-contraction patterns may change over

time as the ability to maintain stability is improved and the kinematics and ranges of motion consequently increase. **This has implications in rehabilitation in general and more specifically of shoulder instability, as it demonstrates that there is no universally ideal or normative movement pattern (Mulla 2023, Bateman et al. 2015, Liaghat et al. 2022), and that muscle activity patterns can be assessed taking the unique kinematics and anatomical features of each subject into account, which is the objective of Chapter 8.** The results of this chapter add value to the general understanding of control and co-contraction issues in the way that the prediction of the model, based on a cost function that minimises muscle forces, explains the following points:

- CG is better predicted than SI in unweighted motions (as SI tends to contract more than CG for stability purposes).
- CG and SI are better predicted in unweighted motions (tendency for both groups, in weighted motions, to co-contract more than represented by the cost function).
- SI is better predicted than CG in weighted motions (with a load, SI appears to contract less than CG for stability. This is in line with the results of Illyes 2007 and Illyes 2009 that found a reduced EMG activity during rapid throwing motions which also increase mechanical stress).

Therefore, SI appears to have a narrower range of co-contraction than CG, as represented below in Fig. 9.1, and this new finding could help further research and help guide subsequent rehabilitation protocols.

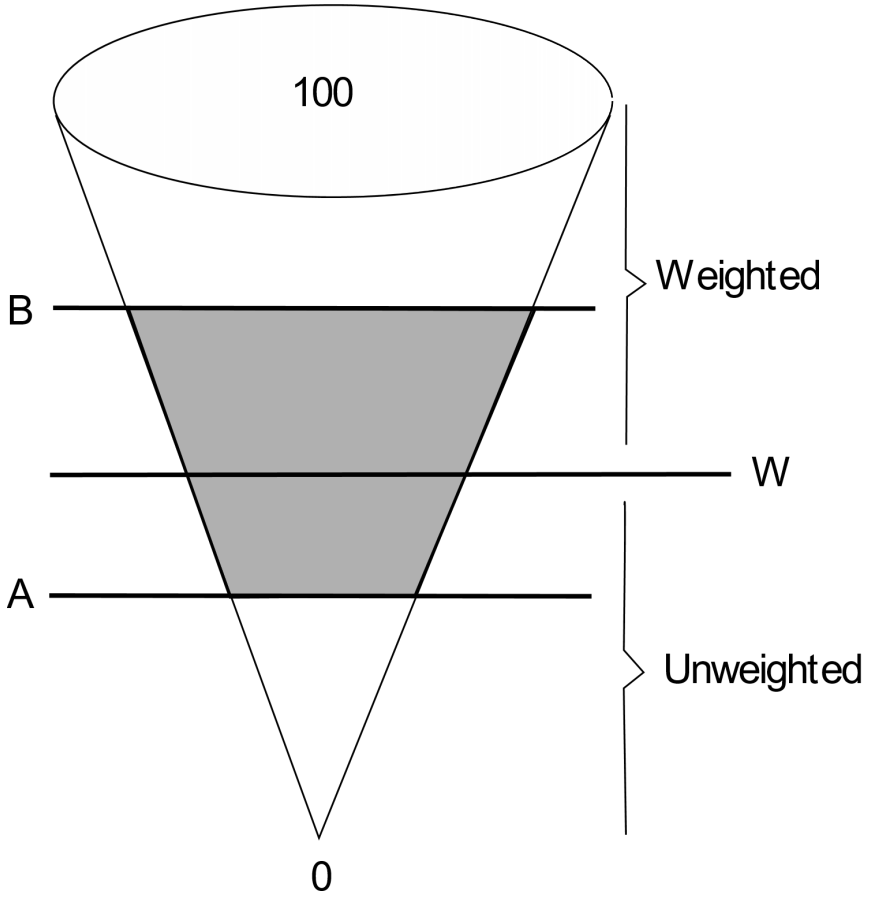

Fig. 9.1) Cone figure representing the estimated potential range of co-activations of the SI and CG groups. The cone illustrates the co-contraction of the muscles of the shoulder girdle, from no muscle activated (base) to all muscle fully activated (top). The illustrated range of co-activations of SI is the shaded area, while the full cone represents the range of CG. SI tends to co-contract more than CG in unweighted motions (line A), and to co-contract less than CG in weighted motions (line B). Line W separates the case where weight is used during motion (above) to the case where no weight is used (below). The model's prediction of muscle forces is based on an assumption of minimisation of activation, therefore in each category (Weight/No weight) the lower activations are better predicted: CG in unweighted motions, and SI in weighted motions.

The second part of objective C (chapter 8) answers the following hypothesis: “some shoulder instability patients may be kinematically indistinguishable (i.e., they fall within the norm) from a healthy control group, but can be differentiated on the basis of their muscle control”.

Objective A identified a subgroup of SI participants that are virtually indistinguishable from normal Kinematics and EMG in some motions (subset). Objective B defined a baseline of reference values of the ability of our model to predict muscle activations.

RMSE, correlation values and non-parametric statistical analyses were used to answer the hypothesis. Those analyses provided information suggesting strongly that some participants of the subset did not belong to the normal group. Specifically, the muscles Pectoralis Major and Latissimus Dorsi in the motions of axial rotation weighted and unweighted were found different between these groups. In other words, the results indicated that, **even given normal kinematics and EMG data, their muscle control does not fall within the expected values of predictions that assume a strategy of minimisation of effort**. This could serve as important information in the classification of Shoulder Instability in the future.

Some limitations have become apparent in this study, some of which are already mentioned or discussed in the previous chapters, and some of which were deliberately chosen in order to keep the pipeline simple, common to all participants, and with potential clinical applications in mind. While they do not undermine or contradict the results of this work that presented a way to discriminate two groups, it should be acknowledged that the small sample size in the Shoulder Instability group (5 Traumatic and 10 Atraumatic) might not be representative of the large diversity of clinical

presentations that exist. It therefore does not allow definitive statistical conclusions on this pathology, which means that the results should not be generalised and need to be taken as an indication and guide for future studies described in the next section. Other limitations are included in the discussion below.

10. General conclusion and further study

The purpose of this general conclusion is to bring together parts of the discussions from the previous chapters in order to summarise and recommend further work based on this PhD.

Current evidence available on shoulder instability makes general assumptions about the basic components of motor control (Shumway et al. 2012; Philp et al. 2022). This has led to numerous attempts to provide classification systems that fail to cover the large variety of clinical presentations that can exist across different age groups.

Most of the available information that can be used from a clinical point of view is based on clinical scales or function (Bateman et al. 2018, Rouleaux et al. 2010). In addition, only limited high quality normative data derived from technologies such as electromyography or motion capture is available that could be used as objective reference values across the spectrum of presentations and ages. As a consequence our general understanding of fundamental control is lacking in this pathology, and current knowledge is focused on the observable fundamental deficits (Spanhove 2021, Struyf 2014, Jaggi 2012). Possible interventions are therefore rather speculative as they address the symptoms and not necessarily the cause which is reflected in the lack of consensus on the true clinical outcome of shoulder instability (Barlow et al. 2018, Warby et al. 2013, Harris et al. 2013, Coughlin et al. 2018).

The motivation behind this study was to use objective data and modelling techniques to explore ways to investigate the underlying motor control in a personalised way, and therefore present new options and tools to approach and understand this complex

pathology. In other words, to look more broadly at our current understanding of shoulder girdle muscle control and co-contraction.

The technologies used, motion capture and EMG, started having regular uses in lower limb for the care of complex patients around 20 years ago. Their use in upper limb remains limited mainly due to the complexity of the kinematics of the shoulder girdle and of its underlying muscle control. In shoulder instability, the muscles likely to present impaired patterning might already be known based on the clinical presentation. The literature review could have helped make specific hypothesis (such as, for example, the suspicion of involvement of the Deltoid Anterior in physiological motions (Hundza, 2006), or a recent systematic review providing moderate evidence for prolonged or higher rotator muscle activity (Spanhove, 2021)), and consequently a limited number of participants would have allowed to perform powered statistical analyses to test these hypotheses.

However, in this work, it was chosen not to use too many prior assumptions about the findings or results (i.e. about the impaired muscles), but instead it was chosen to explore the whole dataset providing equal importance to all motions, muscles, and participants. Such exploratory approach was preferred so as to establish a methodology from which further work could benefit. Follow-up studies might therefore be more hypothesis driven on the basis of this work. The aim of this work was to demonstrate a novel method for quantifying muscle function in young people presenting with shoulder instability using musculoskeletal modeling techniques. The first step in this method was to understand this pathology better, and then the next was to lay the ground work to potentially improve individual clinical assessment and outcome prediction in the future.

The literature review showed that there was little to no reference data for young people presenting with Shoulder Instability, **which defined objective A.** Upon completion of chapter 6, normative data were presented that were clearly distinguishable from the pathological population and that can serve for further studies.

The literature review also showed the important role of compensatory mechanisms, from a kinematic and muscle activity point of view, as well as the possible limitations that can represent normal reference data when assessing those patients. **This defined objectives B and C, covered in chapter 7 and 8 respectively, and the hypothesis was made that some shoulder instability patients might be kinematically indistinguishable from a healthy control group, but can be differentiated on the basis of their muscle control.**

Given the complexity and the variability in shoulder instability presentations, this work did not aim to identify individual muscles (which would have required a specific study on each individual case). Instead, this work aimed to provide information on the overall likeliness of impairment of the muscle activity profiles. A subset of participants was identified that had both kinematics and EMG falling within the norm in some tasks. The model provided for some participants a strong indication of impaired muscle control behaviours. In essence, this approach removes a limitation of the variability of the kinematics which exist in the upper limb and consequently it broadens the experimental EMG accepted norm. It does so by comparing the ensemble of the experimental muscle activities to the predicted ones assuming a strategy of minimisation of efforts based on the unique kinematics of a given participant.

The chapters of this PhD demonstrate an accessible and personalised pipeline that investigates muscle control in shoulder instability participants in a way that is complementary to the conventional approach of reference data, and provides a new insight on muscle patterns. The results of both studies (objective A and objectives B and C) also advocate for the streamlining of the use of modelling based on individual kinematics in clinical settings, to assess both joint angles and muscle control in this population.

Further study

This research is an initial step towards improving the clinical outcome of shoulder instability patients. It is also a groundwork for longer term goals in upper limb biomechanics in general, such as streamlining technology into clinical practice. Recommendations for further research is presented in this section, some of which are already in progress.

Further research in adult population would allow covering a less specific pathological population and exploring any potential differences between children and adults using the same methodology. This could therefore provide an accurate comparison with existing literature whose variability has been discussed in the literature review. Validation through longitudinal study may identify patterns that could be predictors of poor or good long term clinical outcomes. In addition, a very broad range of upper limb pathologies could potentially benefit from the approach of either of the two studies presented in this thesis, and therefore different clinical populations could be tested.

The accuracy of prediction of muscle activations of the model could be improved. Whilst the model used in this study showed a consistent behaviour with similarly consistent results that allowed us to discriminate two groups, fundamental changes in the model or in a different one would allow different information to be gained that could be beneficial in single participant evaluations.

As an example of a follow-on study, the aim could be to test for biomarkers of disease mechanisms or predictors of clinical recovery by characterising the role of the deep shoulder muscles in the stability of the GH joint in shoulder instability patients. This information could be gained by incorporating more realistic movements into the models

such as the sliding of the humeral head in the glenoid and using joint reaction analyses and muscle activation data from static optimisation. Patients could be characterised based on this stability in a longitudinal study and an automated pipeline could be used as a clinical assessment tool.

Additionally, using different algorithms to estimate muscle forces (optimisers and cost functions) could allow to better match the experimental EMG. In other words, it could better estimate muscle patterning leading to specific motions, and this in turn could be used to differentiate and improve shoulder instability classification systems. Extensive work has been done in the recent years on Principal Component Analysis and synergies, which could be complementary information and clues on the way the neuromuscular system work.

Clinical use has always been kept in mind throughout this work. One of the important points is information dissemination. It would be useful to initially evaluate through a survey the best way to translate the information to clinicians with different experience who deal in different settings with relevant upper limb patients. It would define standardised clinical reports the same way it is done for the lower-limb. This work demonstrated that mechanical models add clinical value by helping characterise and interpret kinematics and muscle control. This work provided novel information on the control strategies adopted for particular movements that an individual might demonstrate, which could be used to inform both patients and clinicians by providing quantitative information. With a real-time compatible approach to evaluate muscle patterns, there is also great potential in the use of biofeedback technologies in both clinical assessment and rehabilitation. Following up with the discussion on the challenges that clinicians and patients face quantifying muscle control and when objectifying proprioception in general (3.2.3), a complementary study could have the aim of investigating the effect of biofeedback on muscle control in shoulder instability patients. A clinical trial with a control group would allow assessing their ability to modify (re-train) their acquired activation patterns and therefore the way they perform motions. It

could be done by using automated models to provide simplified overview of either the cocontraction pattern or the joint reaction forces in real time. This would enable clinicians to guide the retraining towards a clinical goal that is patient specific, and as such serve as a clinical tool.

In general, the consistent use of biomechanical models and standardised protocols in order to provide feedback on a fundamental and yet subconscious aspect of the motor function could not only empower patients and clinicians but could also be opening the way to a wider application in different patient populations.

11. Bibliography

Ackland DC, Richardson M, Pandy MG. Axial rotation moment arms of the shoulder musculature after reverse total shoulder arthroplasty. J Bone Joint Surg Am. 2012 Oct 17;94(20):1886-95. doi: 10.2106/JBJS.J.01861. PMID: 23079881.

Ackland DC, Pak P, Richardson M, Pandy MG. Moment arms of the muscles crossing the anatomical shoulder. J Anat. 2008 Oct;213(4):383-90. doi: 10.1111/j.1469-7580.2008.00965.x. Epub 2008 Aug 6. PMID: 18691376; PMCID: PMC2644775.

Ager AL, Borms D, Deschepper L, Dhooghe R, Dijkhuis J, Roy JS, Cools A. Proprioception: How is it affected by shoulder pain? A systematic review. J Hand Ther. 2020 Oct-Dec;33(4):507-516. doi: 10.1016/j.jht.2019.06.002. Epub 2019 Aug 31. PMID: 31481340.

Ameln DJD, Chadwick EK, Blana D, Murgia A. The Stabilizing Function of Superficial Shoulder Muscles Changes Between Single-Plane Elevation and Reaching Tasks. IEEE Trans Biomed Eng. 2019 Feb;66(2):564-572. doi: 10.1109/TBME.2018.2850522. Epub 2018 Jun 25. PMID: 29993505.

Anderson FC, Pandy MG. Static and dynamic optimization solutions for gait are practically equivalent. J Biomech. 2001 Feb;34(2):153-61. doi: 10.1016/s0021-9290(00)00155-x. PMID: 11165278.

Ansanello Netto W, Zanca GG, Saccol MF, Zatiti SCA, Mattiello SM. Scapular muscles weakness in subjects with traumatic anterior glenohumeral instability. Physical Therapy in Sport. 2018 Sep;33:76–81.

Baker, Richard, Jennifer L. McGinley, Michael H. Schwartz, Sarah Beynon, Adam Rozumalski, H. Kerr Graham, and Oren Tirosh. 'The Gait Profile Score and Movement Analysis Profile'. *Gait & Posture* 30, no. 3 (October 2009): 265–69. https://doi.org/10.1016/j.gaitpost.2009.05.020.

Barden JM, Balyk R, Raso VJ, Moreau M, Bagnall K. Atypical shoulder muscle activation in multidirectional instability. Clinical Neurophysiology. 2005 Aug;116(8):1846–57.

Barlow JD, Grosel T, Higgins J, Everhart JS, Magnussen RA. Surgical treatment outcomes after primary vs recurrent anterior shoulder instability. Journal of Clinical Orthopaedics and Trauma [Internet]. 2018 Oct [cited 2019 Feb 19]; Available from: https://linkinghub.elsevier.com/retrieve/pii/S0976566218303916

Bateman M, Osborne SE, Smith BE. Physiotherapy treatment for atraumatic recurrent shoulder instability: Updated results of the Derby Shoulder Instability Rehabilitation Programme. Journal of Arthroscopy and Joint Surgery 2019;6:35-41. https://doi.org/10.1016/j.jajs.2019.01.002

Bateman M, Jaiswal A, Tambe AA. Diagnosis and management of atraumatic shoulder instability. Journal of Arthroscopy and Joint Surgery. 2018 May;5(2):79–85.

Bateman M, Smith BE, Osborne SE, Wilkes SR. Physiotherapy treatment for atraumatic recurrent shoulder instability: early results of a specific exercise protocol using pathology-specific outcome measures. Shoulder Elbow. 2015 Oct;7(4):282-8. doi: 10.1177/1758573215592266. Epub 2015 Jul 3. PMID: 27582989; PMCID: PMC4935133.

Belli Italo, Sagar Joshi, J. Micah Prendergast, Irene Beck, Cosimo Della Santina, Luka Peternel, and Ajay Seth. 'Does Enforcing Glenohumeral Joint Stability Matter? A New Rapid Muscle Redundancy Solver Highlights the Importance of Non-Superficial Shoulder Muscles'. BioRxiv, 1 January 2023, 2023.07.11.548542. https://doi.org/10.1101/2023.07.11.548542.

Bourgain, M., Hybois, S., Thoreux, P., Rouillon, O., Rouch, P., & Sauret, C. (2018). Effect of shoulder model complexity in upper-body kinematics analysis of the golf swing. Journal of Biomechanics, 75, 154–158. doi:10.1016/j.jbiomech.2018.04.025

Brilakis E, Avramidis G, Malahias M-A, Stathellis A, Deligeorgis A, Chiotis I, et al. Long-term outcome of arthroscopic remplissage in addition to the classic Bankart repair for the management of recurrent anterior shoulder instability with engaging Hill–Sachs lesions. Knee Surgery, Sports Traumatology, Arthroscopy [Internet]. 2018 Oct 29 [cited 2019 Feb 19]; Available from: http://link.springer.com/10.1007/s00167-018-5261-3

Brown, J.M.M., J.B. Wickham, D.J. McAndrew, and X.-F. Huang. "Muscles within Muscles: Coordination of 19 Muscle Segments within Three Shoulder Muscles during Isometric Motor Tasks." Journal of Electromyography and Kinesiology 17, no. 1 (February 2007): 57–73. https://doi.org/10.1016/j.jelekin.2005.10.007.

Brownson P, Donaldson O, Fox M, Rees JL, Rangan A, Jaggi A, Tytherleigh-Strong G, McBernie J, Thomas M, Kulkarni R. BESS/BOA Patient Care Pathways: Traumatic anterior shoulder instability. Shoulder Elbow. 2015 Jul;7(3):214-26. doi: 10.1177/1758573215585656. Epub 2015 May 26. Erratum in: Shoulder Elbow. 2016 Jan;8(1):71. doi: 10.1177/1758573215607822. PMID: 27582981; PMCID: PMC4935160.

Burkhart SS, Morgan CD, Ben Kibler W. The disabled throwing shoulder: spectrum of pathology part III: the SICK scapula, scapular dyskinesis, the kinetic chain, and rehabilitation. Arthroscopy: The Journal of Arthroscopic & Related Surgery. 2003 Jul;19(6):641–61.

Burkhart SS, De Beer JF. Traumatic glenohumeral bone defects and their relationship to failure of arthroscopic Bankart repairs: significance of the inverted-pear glenoid and the humeral engaging Hill-Sachs lesion. Arthroscopy. 2000 Oct;16(7):677-94. doi: 10.1053/jars.2000.17715. PMID: 11027751.

Burkhead WZ Jr, Rockwood CA Jr. Treatment of instability of the shoulder with an exercise program. J Bone Joint Surg Am. 1992 Jul;74(6):890-6. PMID: 1634579.

Christensen HW. Precision and accuracy of an electrogoniometer. J Manipulative Physiol Ther. 1999 Jan;22(1):10-4. doi: 10.1016/s0161-4754(99)70099-0. PMID: 10029943.

Clarkson, Hazel M. Musculoskeletal Assessment: Joint Motion and Muscle Testing. 3rd ed. Philadelphia: Wolters Kluwer/Lippincott Williams & Wilkins Health, 2013.

Cleland, Joshua, Shane Koppenhaver, and Frank H. Netter. Netter's Orthopaedic Clinical Examination: An Evidence-Based Approach. 2nd ed. Philadelphia, Pa: Saunders/Elsevier, 2011.

Codman, E. A. The Shoulder: Rupture of the Supraspinatus Tendon and Other Lesions in or about the Subacromial Bursa. Malabar, Fla: R.E. Kreiger, 1934

Constant, C. R., and A. H. Murley. "A Clinical Method of Functional Assessment of the Shoulder." Clinical Orthopaedics and Related Research, no. 214 (January 1987): 160–64.

Coughlin RP, Bullock GS, Shanmugaraj A, Sell TC, Garrigues GE, Ledbetter L, et al. Outcomes After Arthroscopic Rotator Interval Closure for Shoulder Instability: A Systematic Review. Arthroscopy: The Journal of Arthroscopic & Related Surgery. 2018 Nov;34(11):3098-3108.e1.

Criswell, E., and J.R. Cram. Cram's Introduction to Surface Electromyography. G - Reference,Information and Interdisciplinary Subjects Series. Jones & Bartlett Learning, 2011.

Deitch, C.T. Mehlman, S.L. Foad, A. Obbehat, M. Mallory Traumatic anterior shoulder dislocation in adolescents Am J Sports Med, 31 (5) (2003), pp. 758-763

Digo, Elisa, Stefano Pastorelli, and Laura Gastaldi. 2022. "A Narrative Review on Wearable Inertial Sensors for Human Motion Tracking in Industrial Scenarios" Robotics 11, no. 6: 138. https://doi.org/10.3390/robotics11060138

Delp SL, Anderson FC, Arnold AS, Loan P, Habib A, John CT, Guendelman E, Thelen DG. OpenSim: open-source software to create and analyze dynamic simulations of movement. IEEE Trans Biomed Eng. 2007 Nov;54(11):1940-50. doi: 10.1109/TBME.2007.901024. PMID: 18018689.

Dufour, Michel, Michel Pillu, Karine Langlois, and Santiago Del Valle Acedo. Biomécanique fonctionnelle: membres, tête, tronc. 2e éd. Issy-les-Moulineaux: Elsevier Masson, 2017.

Dumont GD, Russell RD, Robertson WJ. Anterior shoulder instability: a review of pathoanatomy, diagnosis and treatment. Current Reviews in Musculoskeletal Medicine. 2011 Dec;4(4):200–7.

Ehrig RM, Taylor WR, Duda GN, Heller MO. A survey of formal methods for determining the centre of rotation of ball joints. J Biomech. 2006;39(15):2798-809. doi: 10.1016/j.jbiomech.2005.10.002. Epub 2005 Nov 15. PMID: 16293257.

Erdemir A, McLean S, Herzog W, van den Bogert AJ. Model-based estimation of muscle forces exerted during movements. Clin Biomech (Bristol, Avon). 2007 Feb;22(2):131-54. doi: 10.1016/j.clinbiomech.2006.09.005. Epub 2006 Oct 27. PMID: 17070969.

Ernstbrunner L, Francis-Pester FW, Fox A, Wieser K, Ackland DC. Patients with recurrent anterior shoulder instability exhibit altered glenohumeral and scapulothoracic joint kinematics during upper limb movement: A prospective comparative study. Clin Biomech (Bristol, Avon). 2022 Dec;100:105775. doi: 10.1016/j.clinbiomech.2022.105775. Epub 2022 Oct 1. PMID: 36242953.

Friston, K.J., Holmes, A.P., Worsley, K.J., Poline, J.-.-P., Frith, C.D. and Frackowiak, R.S.J. (1994), Statistical parametric maps in functional imaging: A general linear approach. Hum. Brain Mapp., 2: 189-210. https://doi.org/10.1002/hbm.460020402

Garner BA, Pandy MG. Musculoskeletal model of the upper limb based on the visible human male dataset. Comput Methods Biomech Biomed Engin. 2001 Feb;4(2):93-126. doi: 10.1080/10255840008908000. PMID: 11264863.

Goetti P, Denard PJ, Collin P, Ibrahim M, Hoffmeyer P, Lädermann A. Shoulder biomechanics in normal and selected pathological conditions. EFORT Open Rev. 2020 Sep 10;5(8):508-518. doi: 10.1302/2058-5241.5.200006. PMID: 32953136; PMCID: PMC7484714.

Gomberawalla MM, Sekiya JK. Rotator Cuff Tear and Glenohumeral Instability: A Systematic Review. Clinical Orthopaedics and Related Research®. 2014 Aug;472(8):2448–56.

Gosling John, Philip Harris, John Humpherson, Ian Whitmore, and Peter Willan. Human Anatomy, Color Atlas and Textbook + Student Consult Online Access. Place of publication not identified: Elsevier, 2016.

Gu, Chenyu, Weicong Lin, Xinyi He, Lei Zhang, and Mingming Zhang. 'IMU-Based Motion Capture System for Rehabilitation Applications: A Systematic Review'. Biomimetic Intelligence and Robotics 3, no. 2 (1 June 2023): 100097. https://doi.org/10.1016/j.birob.2023.100097.

Guala A, Rial P, Mendoza L, RIal W, Perezlindo L, De Azcuénaga M. Arthroscopic Bankart Repair after Anterior Traumatic Shoulder Dislocation in Workers. Orthopaedic Journal of Sports Medicine. 2018 Dec;6(12_suppl5):2325967118S0020.

Griffin J, Jaggi A, Daniell H, Chester R. A systematic review to compare physiotherapy treatment programmes for atraumatic shoulder instability. Shoulder Elbow. 2023 Aug;15(4):448-460. doi: 10.1177/17585732221080730. Epub 2022 Feb 18. PMID: 37538527; PMCID: PMC10395403.

Harris JD, Gupta AK, Mall NA, Abrams GD, McCormick FM, Cole BJ, et al. Long-Term Outcomes After Bankart Shoulder Stabilization. Arthroscopy: The Journal of Arthroscopic & Related Surgery. 2013 May;29(5):920–33.

Hayes K, Callanan M, Walton J, Paxinos A, Murrell GAC. Shoulder Instability: Management and Rehabilitation. Journal of Orthopaedic & Sports Physical Therapy. 2002 Oct;32(10):497–509.

Hettrich CM, Cronin KJ, Raynor MB, Wagstrom E, Jani SS, Carey JL, et al. Epidemiology of the Frequency, Etiology, Direction, and Severity (FEDS) system for classifying glenohumeral instability. Journal of Shoulder and Elbow Surgery. 2019 Jan;28(1):95–101.

Hicks JL, Uchida TK, Seth A, Rajagopal A, Delp SL. Is my model good enough? Best practices for verification and validation of musculoskeletal models and simulations of movement. J Biomech Eng. 2015 Feb 1;137(2):020905. doi: 10.1115/1.4029304. Epub 2015 Jan 26. PMID: 25474098; PMCID: PMC4321112.

Hughes PC, Taylor NF, Green RA. Most clinical tests cannot accurately diagnose rotator cuff pathology: a systematic review. Aust J Physiother. 2008;54(3):159-70. doi: 10.1016/s0004-9514(08)70022-9. PMID: 18721119.

Hundza SR, Zehr EP. Muscle activation and cutaneous reflex modulation during rhythmic and discrete arm tasks in orthopaedic shoulder instability. Exp Brain Res. 2007 May;179(3):339-51. doi: 10.1007/s00221-006-0793-z. Epub 2006 Nov 30. PMID: 17136525.

Hurov, Jack. “Anatomy and Mechanics of the Shoulder: Review of Current Concepts.” Journal of Hand Therapy 22, no. 4 (October 2009): 328–43. https://doi.org/10.1016/j.jht.2009.05.002.

Hettrich CM, Cronin KJ, Raynor MB, Wagstrom E, Jani SS, Carey JL, et al. Epidemiology of the Frequency, Etiology, Direction, and Severity (FEDS) system for classifying glenohumeral instability. Journal of Shoulder and Elbow Surgery. 2019 Jan;28(1):95–101.

Illyes A, Kiss RM. Electromyographic analysis in patients with multidirectional shoulder instability during pull, forward punch, elevation and overhead throw. Knee Surgery, Sports Traumatology, Arthroscopy 2007;15:624-631.

Illyes A, Kiss J, Kiss RM. Electromyographic analysis during pull, forward punch, elevation and overhead throw after conservative treatment or capsular shift at patient with

multidirectional shoulder joint instability. J Electromyogr Kinesiol. 2009 Dec;19(6):e438-47. doi: 10.1016/j.jelekin.2008.09.008. Epub 2008 Dec 4. PMID: 19062304.

Illyes A, Kiss RM. Kinematic and muscle activity characteristics of multidirectional shoulder joint instability during elevation. Knee Surg Sports Traumatol Arthrosc. 2006 Jul;14(7):673-85. doi: 10.1007/s00167-005-0012-7. Epub 2005 Dec 14. PMID: 16362361.

Jaeger A, Braune C, Welsch F, Sarikaya Y, Graichen H. Postoperative functional outcome and stability in recurrent traumatic anteroinferior glenohumeral instability: comparison of two different surgical capsular reconstruction techniques. Archives of Orthopaedic and Trauma Surgery. 2004 May 1;124(4):226–31.

Jaggi A, Noorani A, Malone A, Cowan J, Lambert S, Bayley I. Muscle activation patterns in patients with recurrent shoulder instability. Int J Shoulder Surg. 2012 Oct;6(4):101-7. doi: 10.4103/0973-6042.106221. PMID: 23493512; PMCID: PMC3590699.

Jaspers E, Feys H, Bruyninckx H, Cutti A, Harlaar J, Molenaers G et al. The reliability of upper limb kinematics in children with hemiplegic cerebral palsy. Gait & Posture 2011;33:568-575. https://doi.org/10.1016/j.gaitpost.2011.01.011

Johnson LB, Sumner S, Duong T, Yan P, Bajcsy R, Abresch RT, de Bie E, Han JJ. Validity and reliability of smartphone magnetometer-based goniometer evaluation of shoulder abduction--A pilot study. Man Ther. 2015 Dec;20(6):777-82. doi: 10.1016/j.math.2015.03.004. Epub 2015 Mar 17. PMID: 25835780.

Karduna, Andrew R, Phil W McClure, and Lori A Michener. “Scapular Kinematics: Effects of Altering the Euler Angle Sequence of Rotations.” Journal of Biomechanics, 2000, 6.

Katolik, Leonid I., Anthony A. Romeo, Brian J. Cole, Nikhil N. Verma, Jennifer K. Hayden, and Bernard R. Bach. “Normalization of the Constant Score.” Journal of Shoulder and Elbow Surgery 14, no. 3 (May 2005): 279–85. https://doi.org/10.1016/j.jse.2004.10.009.

Karlsson D, Peterson B. Towards a model for force predictions in the human shoulder. J Biomech. 1992 Feb;25(2):189-99. doi: 10.1016/0021-9290(92)90275-6. PMID: 1733994.

Kaufman KR, An KW, Litchy WJ, Chao EY. Physiological prediction of muscle forces--I. Theoretical formulation. Neuroscience. 1991;40(3):781-92. doi: 10.1016/0306-4522(91)90012-d. PMID: 2062441.

Klintberg IH, Cools AM, Holmgren TM, Holzhausen AC, Johansson K, Maenhout AG, Moser JS, Spunton V, Ginn K. Consensus for physiotherapy for shoulder pain. Int Orthop. 2015 Apr;39(4):715-20. doi: 10.1007/s00264-014-2639-9. Epub 2014 Dec 31. PMID: 25548127.

Kobayashi, Kotono, Jun Umehara, Todd C Pataky, Masahide Yagi, Tetsuya Hirono, Yasuyuki Ueda, and Noriaki Ichihashi. ‘Application of Statistical Parametric Mapping for Comparison of Scapular Kinematics and EMG’. Journal of Biomechanics 145 (December 2022): 111357. https://doi.org/10.1016/j.jbiomech.2022.111357.

Kocher MS. Editorial Commentary: Shoulder Instability Outcome Reporting Requires Standardization. Arthroscopy: The Journal of Arthroscopic & Related Surgery. 2018 Apr;34(4):1295–6.

Konrad, P. The ABC of EMG, A Practical Introduction to Kinesiological Electromyography; Noraxon Inc.: Scottsdale, AZ, USA, 2005

Kuechle DK, Newman SR, Itoi E, Morrey BF, An KN. Shoulder muscle moment arms during horizontal flexion and elevation. J Shoulder Elbow Surg. 1997 Sep-Oct;6(5):429-39. doi: 10.1016/s1058-2746(97)70049-1. PMID: 9356931.

Kuhn JE. A new classification system for shoulder instability. Br J Sports Med. 2010 Apr;44(5):341-6. doi: 10.1136/bjsm.2009.071183. PMID: 20371559.

Kuroda, T. Sumiyoshi, J. Moriishi, K. Maruta, N. Ishige The natural course of atraumatic shoulder instability J Shoulder Elbow Surg, 10 (2) (2001), pp. 100-104

Lawton, S. Choudhury, P. Mansat, R.H. Cofield, A.A. Stans Pediatric shoulder instability: presentation, findings, treatment, and outcomesJ Pediatr Orthop B, 22 (1) (2002), pp. 52-61

Lazarides AL, Duchman KR, Ledbetter L, Riboh JC, Garrigues GE. Arthroscopic Remplissage for Anterior Shoulder Instability: A Systematic Review of Clinical and Biomechanical Studies. Arthroscopy: The Journal of Arthroscopic & Related Surgery. 2019 Feb;35(2):617–28.

Le Loet, Xavier, and Olivier Vittecoq. “The Sternocostoclavicular Joint: Normal and Abnormal Features.” Joint Bone Spine 69, no. 2 (March 2002): 161–69. https://doi.org/10.1016/S1297-319X(02)00362-7

Lempereur M, Brochard S, Leboeuf F, Rémy-Néris O. Validity and reliability of 3D marker based scapular motion analysis: a systematic review. J Biomech. 2014 Jul 18;47(10):2219-30. doi: 10.1016/j.jbiomech.2014.04.028. Epub 2014 May 1. PMID: 24856913.

Lehman, Gregory J. “Biomechanical Assessments of Lumbar Spinal Function. How Low Back Pain Sufferers Differ from Normals. Implications for Outcome Measures Research. Part i: Kinematic Assessments of Lumbar Function.” Journal of Manipulative and Physiological Therapeutics 27, no. 1 (January 2004): 57–62. https://doi.org/10.1016/j.jmpt.2003.11.007.

Leroux, D. Ogilvie-Harris, C. Veillette, J. Chahal, T. Dwyer, A. Khoshbin, et al. The epidemiology of primary anterior shoulder dislocations in patients aged 10 to 16 years Am J Sports Med, 43 (9) (2015), pp. 2111-2117

Levin MF, Kleim JA, Wolf SL. What do motor "recovery" and "compensation" mean in patients following stroke? Neurorehabil Neural Repair. 2009 May;23(4):313-9. doi: 10.1177/1545968308328727. Epub 2008 Dec 31. PMID: 19118128.

Levine WN, Sonnenfeld JJ, Shiu B. Shoulder Instability. Clinics in Sports Medicine. 2018 Apr;37(2):161–77.

Lewis JS. Rotator cuff tendinopathy/subacromial impingement syndrome: is it time for a new method of assessment? Br J Sports Med. 2009 Apr;43(4):259-64. doi: 10.1136/bjsm.2008.052183. Epub 2008 Oct 6. PMID: 18838403.

Lewis A, Kitamura T, Bayley JI. (ii) The classification of shoulder instability: new light through old windows! Current Orthopaedics. 2004 Apr;18(2):97–108.

Liaghat B, Skou ST, Søndergaard J, Boyle E, Søgaard K, Juul-Kristensen B. Short-term effectiveness of high-load compared with low-load strengthening exercise on self-reported function in patients with hypermobile shoulders: a randomised controlled trial. Br J Sports Med. 2022 Jun 1;56(22):1269–76. doi: 10.1136/bjsports-2021-105223. Epub ahead of print. PMID: 35649707; PMCID: PMC9626913.

Lin YC, Dorn TW, Schache AG, Pandy MG. Comparison of different methods for estimating muscle forces in human movement. Proc Inst Mech Eng H. 2012 Feb;226(2):103-12. doi: 10.1177/0954411911429401. PMID: 22468462.

Lirio-Romero C, Torres-Lacomba M, Gómez-Blanco A, Acero-Cortés A, Retana-Garrido A, de la Villa-Polo P, Sánchez-Sánchez B. Electromyographic biofeedback improves upper extremity function: a randomized, single-blinded, controlled trial. Physiotherapy. 2021 Mar;110:54-62. doi: 10.1016/j.physio.2020.02.002. Epub 2020 Feb 15. PMID: 32718746.

Longo, Umile Giuseppe, Alessandra Berton, Nicola Papapietro, Nicola Maffulli, and Vincenzo Denaro. “Biomechanics of the Rotator Cuff: European Perspective.” In Medicine and Sport Science, edited by N. Maffulli, 57:10–17. Basel: KARGER, 2011. https://doi.org/10.1159/000328870.

Ludewig PM, Phadke V, Braman JP, Hassett DR, Cieminski CJ, LaPrade RF. Motion of the shoulder complex during multiplanar humeral elevation. J Bone Joint Surg Am. 2009 Feb;91(2):378-89. doi: 10.2106/JBJS.G.01483. PMID: 19181982; PMCID: PMC2657311.

Ludewig PM, Saini G, Hellem A, Kahnert EK, Rezvanifar SC, Braman JP, Staker JL. Changing our Diagnostic Paradigm Part II: Movement System Diagnostic Classification. Int J Sports Phys Ther. 2022 Jan 1;17(1):7-17. doi: 10.26603/001c.30177. PMID: 35024204; PMCID: PMC8720248.

Lugo, Roberto, Peter Kung, and C. Benjamin Ma. “Shoulder Biomechanics.” European Journal of Radiology 68, no. 1 (October 2008): 16–24. https://doi.org/10.1016/j.ejrad.2008.02.051.

Maitland’s Peripheral Manipulation. Management of Neuromusculoskeletal Disorders-Volume 2. (Churchill Livingstone, 2013)

Magee, David J. Orthopedic Physical Assessment. St. Louis, Mo.: Saunders Elsevier, 2006.

Magermans DJ, Chadwick EK, Veeger HE, van der Helm FC. Requirements for upper extremity motions during activities of daily living. Clin Biomech (Bristol, Avon). 2005 Jul;20(6):591-9. doi: 10.1016/j.clinbiomech.2005.02.006. PMID: 15890439.

Makki D, Duodu J, Nixon M. Prevalence and pattern of upper limb involvement in cerebral palsy. Journal of Children's Orthopaedics. 2014 May;8(3):215–9.

Manske, Robert. (2016). Fundamental Orthopedic Management for the Physical Therapist Assistant, 4th ed.

Mantovani G, Ng KC, Lamontagne M. Regression models to predict hip joint centers in pathological hip population. Gait Posture. 2016 Feb;44:48-54. doi: 10.1016/j.gaitpost.2015.11.001. Epub 2015 Nov 10. PMID: 27004632.

Marchi J, Blana D, Chadwick EK. Glenohumeral stability during a hand-positioning task in previously injured shoulders. Med Biol Eng Comput. 2014 Mar;52(3):251-6. doi: 10.1007/s11517-013-1087-9. Epub 2013 May 24. PMID: 23702698.

Matsumura, Aoi, Atsushi Ueda, and Yasuo Nakamura. 'A New Method of Estimating Scapular Orientation during Various Shoulder Movements: A Comparison of Three Non-Invasive Methods'. Journal of Electromyography and Kinesiology 44 (February 2019): 46–55. https://doi.org/10.1016/j.jelekin.2018.11.007.

McClure PW, Michener LA. Staged Approach for Rehabilitation Classification: Shoulder Disorders (STAR–Shoulder). Physical Therapy. 2015 May 1;95(5):791-800.

McFarland EG, Kim TK, Park HB, Neira CA, Gutierrez MI. The effect of variation in definition on the diagnosis of multidirectional instability of the shoulder. J Bone Joint Surg Am. 2003 Nov;85(11):2138-44. doi: 10.2106/00004623-200311000-00011. PMID: 14630842.

McMahon PJ, Jobe FW, Pink MM, Brault JR, Perry J. Comparative electromyographic analysis of shoulder muscles during planar motions: anterior glenohumeral instability versus normal. J Shoulder Elbow Surg. 1996 Mar-Apr;5(2 Pt 1):118-23. doi: 10.1016/s1058-2746(96)80006-1. PMID: 8742875.

Merletti R, Hermens H. Introduction to the special issue on the SENIAM European Concerted Action. Journal of Electromyography and Kinesiology : Official Journal of the International Society of Electrophysiological Kinesiology. 2000 Oct;10(5):283-286. DOI: 10.1016/s1050-6411(00)00019-5. PMID: 11018437.

Millard M, Uchida T, Seth A, Delp SL. Flexing computational muscle: modeling and simulation of musculotendon dynamics. J Biomech Eng. 2013 Feb;135(2):021005. doi: 10.1115/1.4023390. PMID: 23445050; PMCID: PMC3705831.

Monnet T, Desailly E, Begon M, Vallée C, Lacouture P. Comparison of the SCoRE and HA methods for locating in vivo the glenohumeral joint centre. J Biomech. 2007;40(15):3487-92. doi: 10.1016/j.jbiomech.2007.05.030. Epub 2007 Jul 13. PMID: 17631297.

Morris AD, Kemp GJ, Frostick SP. Shoulder electromyography in multidirectional instability. J Shoulder Elbow Surg. 2004 Jan-Feb;13(1):24-9. doi: 10.1016/j.jse.2003.09.005. PMID: 14735069.

Morrison, David S., Brad S. Greenbaum, and Andy Einhorn. “SHOULDER IMPINGEMENT.” Orthopedic Clinics of North America 31, no. 2 (April 2000): 285–93. https://doi.org/10.1016/S0030-5898(05)70148-6.

Mulla DM, Keir PJ. Neuromuscular control: from a biomechanist's perspective. Front Sports Act Living. 2023 Jul 5;5:1217009. doi: 10.3389/fspor.2023.1217009. PMID: 37476161; PMCID: PMC10355330.

Nicholson, Kristen F., R. Tyler Richardson, Elizabeth A. Rapp, R. Garry Quinton, Kert F. Anzilotti, and James G. Richards. ‘Validation of a Mathematical Approach to Estimate Dynamic Scapular Orientation’. Journal of Biomechanics 54 (March 2017): 101–5. https://doi.org/10.1016/j.jbiomech.2017.01.025.

Nieminen H, Takala EP, Niemi J, Viikari-Juntura E. Muscular synergy in the shoulder during a fatiguing static contraction. Clin Biomech (Bristol, Avon). 1995 Sep;10(6):309-317. doi: 10.1016/0268-0033(95)00041-i. PMID: 11415572.

Nikooyan AA, Veeger HE, Chadwick EK, Praagman M, Helm FC. Development of a comprehensive musculoskeletal model of the shoulder and elbow. Med Biol Eng Comput. 2011 Dec;49(12):1425-35. doi: 10.1007/s11517-011-0839-7. Epub 2011 Oct 29. PMID: 22038240; PMCID: PMC3223593.

Nikooyan AA, van der Helm FC, Westerhoff P, Graichen F, Bergmann G, Veeger HE. Comparison of two methods for in vivo estimation of the glenohumeral joint rotation center (GH-JRC) of the patients with shoulder hemiarthroplasty. PLoS One. 2011 Mar 31;6(3):e18488. doi: 10.1371/journal.pone.0018488. PMID: 21483808; PMCID: PMC3069111.

Noorani A, Goldring M, Jaggi A, Gibson J, Rees J, Bateman M, Falworth M, Brownson P. BESS/BOA patient care pathways: Atraumatic shoulder instability. Shoulder Elbow. 2019 Feb;11(1):60-70. doi: 10.1177/1758573218815002. Epub 2018 Dec 10. PMID: 30719099; PMCID: PMC6348586.

Ogston JB, Ludewig PM. Differences in 3-dimensional shoulder kinematics between persons with multidirectional instability and asymptomatic controls. Am J Sports Med. 2007 Aug;35(8):1361-70. doi: 10.1177/0363546507300820. Epub 2007 Apr 9. PMID: 17420507.

Paletta GA Jr, Warner JJ, Warren RF, Deutsch A, Altchek DW. Shoulder kinematics with two-plane x-ray evaluation in patients with anterior instability or rotator cuff tearing. J Shoulder Elbow Surg. 1997 Nov-Dec;6(6):516-27. doi: 10.1016/s1058-2746(97)90084-7. PMID: 9437601.

Palmer K, Walker-Bone K, Linaker C, Reading I, Kellingray S, Coggon D, Cooper C. The Southampton examination schedule for the diagnosis of musculoskeletal disorders of the upper limb. Ann Rheum Dis. 2000 Jan;59(1):5-11. doi: 10.1136/ard.59.1.5. PMID: 10627419; PMCID: PMC1752977.

Papi E, Bull AMJ, McGregor AH. Alteration of movement patterns in low back pain assessed by Statistical Parametric Mapping. J Biomech. 2020 Feb 13;100:109597. doi: 10.1016/j.jbiomech.2019.109597. Epub 2019 Dec 24. PMID: 31928738; PMCID: PMC7001037.

Pataky TC, Vanrenterghem J, Robinson MA (2016). Region-of-interest analyses of one-dimensional biomechanical trajectories: bridging 0D and 1D methods, augmenting statistical power. PeerJ 4: e2652, doi.org/10.7717/peerj.2652.

Pearl ML, Harris SL, Lippitt SB, Sidles JA, Harryman DT 2nd, Matsen FA 3rd. A system for describing positions of the humerus relative to the thorax and its use in the presentation of several functionally important arm positions. J Shoulder Elbow Surg. 1992 Mar;1(2):113-8. doi: 10.1016/S1058-2746(09)80129-8. Epub 2009 Feb 19. PMID: 22959048.

Philp F., A. Faux-Nightingale, S. Woolley, E. de Quincey, A. Pandyan, Evaluating the clinical decision making of physiotherapists in the assessment and management of paediatric shoulder instability, Physiotherapy 115 (2022) 46-57. https://www.sciencedirect.com/science/article/pii/S0031940621007173.

Philp F, Faux-Nightingale A, Woolley S, de Quincey E, Pandyan A. Evaluating the clinical decision making of physiotherapists in the assessment and management of paediatric shoulder instability. Physiotherapy. 2022 Jun;115:46-57. doi: 10.1016/j.physio.2021.12.330. Epub 2021 Dec 24. PMID: 35184006.

Pizzari, T., J. Wickham, L. Watson, M. Zika, and S. Hill. 'Altered Muscle Activation Patterns in Multidirectional Shoulder Instability during Dynamic Abduction'. Journal of Science and Medicine in Sport 12 (January 2009): S4. https://doi.org/10.1016/j.jsams.2008.12.011.

Praagman M, Chadwick EK, van der Helm FC, Veeger HE. The relationship between two different mechanical cost functions and muscle oxygen consumption. J Biomech. 2006;39(4):758-65. doi: 10.1016/j.jbiomech.2004.11.034. PMID: 16439246.

Preece SJ, Jones RK, Brown CA, Cacciatore TW, Jones AK. Reductions in co-contraction following neuromuscular re-education in people with knee osteoarthritis. BMC Musculoskelet Disord. 2016 Aug 27;17(1):372. doi: 10.1186/s12891-016-1209-2. PMID: 27568007; PMCID: PMC5002319.

Rab, George T. "Shoulder Motion Description: The ISB and Globe Methods Are Identical." Gait & Posture 27, no. 4 (May 2008): 702–5. https://doi.org/10.1016/j.gaitpost.2007.07.003.

Rab G, Petuskey K, Bagley A. A method for determination of upper extremity kinematics. Gait Posture. 2002 Apr;15(2):113-9. doi: 10.1016/s0966-6362(01)00155-2. PMID: 11869904.

Rapp, Elizabeth A., R. Tyler Richardson, Stephanie A. Russo, William C. Rose, and James G. Richards. 'A Comparison of Two Non-Invasive Methods for Measuring Scapular Orientation in Functional Positions'. Journal of Biomechanics 61 (August 2017): 269–74. https://doi.org/10.1016/j.jbiomech.2017.07.032.

Robinson CM, Howes J, Murdoch H, Will E, Graham C. Functional outcome and risk of recurrent instability after primary traumatic anterior shoulder dislocation in young patients. J Bone Joint Surg Am. 2006 Nov;88(11):2326-36. doi: 10.2106/JBJS.E.01327. PMID: 17079387.

Robinson Mark A., Jos Vanrenterghem, Todd C. Pataky, Statistical Parametric Mapping (SPM) for alpha-based statistical analyses of multi-muscle EMG time-series, Journal of Electromyography and Kinesiology, Volume 25, Issue 1, 2015, Pages 14-19, ISSN 1050-6411, https://doi.org/10.1016/j.jelekin.2014.10.018.

Roelker SA, Caruthers EJ, Hall RK, Pelz NC, Chaudhari AMW, Siston RA. Effects of Optimization Technique on Simulated Muscle Activations and Forces. J Appl Biomech. 2020 Jul 14;36(4):259-278. doi: 10.1123/jab.2018-0332. PMID: 32663800.

Rocourt, Marianne H.H., Lorenz Radlinger, Fabian Kalberer, Shahab Sanavi, Nicole S. Schmid, Michael Leunig, and Ralph Hertel. "Evaluation of Intratester and Intertester Reliability of the Constant-Murley Shoulder Assessment." Journal of Shoulder and Elbow Surgery 17, no. 2 (March 2008): 364–69. https://doi.org/10.1016/j.jse.2007.06.024.

Rouleau DM, Faber K, MacDermid JC. Systematic review of patient-administered shoulder functional scores on instability. Journal of Shoulder and Elbow Surgery. 2010 Dec;19(8):1121–8.

Sahrom S, Wilkie JC, Nosaka K, Blazevich AJ. Comparison of methods of derivation of the yank-time signal from the vertical ground reaction force-time signal for identification of movement-related events. J Biomech. 2021 Jan 22;115:110048. doi: 10.1016/j.jbiomech.2020.110048. Epub 2020 Sep 19. PMID: 33272585.

Saul KR, Hu X, Goehler CM, Vidt ME, Daly M, Velisar A, Murray WM. Benchmarking of dynamic simulation predictions in two software platforms using an upper limb musculoskeletal model. Comput Methods Biomech Biomed Engin. 2015;18(13):1445-58. doi: 10.1080/10255842.2014.916698. Epub 2014 Jul 4. PMID: 24995410; PMCID: PMC4282829.

Scott B, Seyres M, Philp F, Chadwick EK, Blana D. Healthcare applications of single camera markerless motion capture: a scoping review. PeerJ. 2022 May 26;10:e13517. doi: 10.7717/peerj.13517. PMID: 35642200; PMCID: PMC9148557.

Seyres, Martin, Neil Postans, Robert Freeman, Anand Pandyan, Edward K. Chadwick, and Fraser Philp. 'Children and Adolescents with All Forms of Shoulder Instability Demonstrate Differences in Their Movement and Muscle Activity Patterns When Compared to Age- and Sex-Matched Controls'. Journal of Shoulder and Elbow Surgery, March 2024, S1058274624001617. https://doi.org/10.1016/j.jse.2024.01.043.

Seth A, Matias R, Veloso AP and Delp SL. A biomechanical model of the scapulothoracic joint to accurately capture scapular kinematics during shoulder movements. PLOS ONE. (2015)

Shields DW, Jefferies JG, Brooksbank AJ, Millar N, Jenkins PJ. Epidemiology of glenohumeral dislocation and subsequent instability in an urban population. Journal of Shoulder and Elbow Surgery. 2018 Feb;27(2):189–95.23, no. 4 (5 December 2008): 313–19. https://doi.org/10.1177/1545968308328727.

Shumway-Cook, M.H. Woollacott, Motor control: translating research into clinical practice, Lippincott Williams & Wilkins, 2012

Soslowsky, L. J., E. L. Flatow, L. U. Bigliani, R. J. Pawluk, G. A. Ateshian, and V. C. Mow. "Quantitation of in Situ Contact Areas at the Glenohumeral Joint: A Biomechanical Study." Journal of Orthopaedic Research 10, no. 4 (July 1992): 524–34. https://doi.org/10.1002/jor.1100100407.

Spanhove V, Calders P, Berckmans K, Palmans T, Malfait F, Cools A, De Wandele I. Electromyographic Muscle Activity and Three-Dimensional Scapular Kinematics in Patients With Multidirectional Shoulder Instability: A Study in the Hypermobile Type of the Ehlers-Danlos Syndrome and the Hypermobility Spectrum Disorders. Arthritis Care Res (Hoboken). 2022 May;74(5):833-840. doi: 10.1002/acr.24525. Epub 2022 Mar 24. PMID: 33253470.

Spanhove V, Van Daele M, Van den Abeele A, Rombaut L, Castelein B, Calders P et al. Muscle activity and scapular kinematics in individuals with multidirectional shoulder instability: A systematic review. Ann Phys Rehabil Med 2021;64:101457. 10.1016/j.rehab.2020.10.008

Speciali, Danielli S., Elaine M. Oliveira, Jefferson R. Cardoso, João C. F. Correa, Richard Baker, and Paulo R. G. Lucareli. 'Gait Profile Score and Movement Analysis Profile in Patients with Parkinson's Disease during Concurrent Cognitive Load'. *Brazilian Journal of Physical Therapy* 18, no. 4 (August 2014): 315–22. https://doi.org/10.1590/bjpt-rbf.2014.0049.

Stokdijk M, Nagels J, Rozing PM. The glenohumeral joint rotation centre in vivo. J Biomech. 2000 Dec;33(12):1629-36. doi: 10.1016/s0021-9290(00)00121-4. PMID: 11006387.

Stokes DJ, McCarthy TP, Frank RM. Physical Therapy for the Treatment of Shoulder Instability. Phys Med Rehabil Clin N Am. 2023 May;34(2):393-408. doi: 10.1016/j.pmr.2022.12.006. Epub 2023 Feb 26. PMID: 37003660.

Struyf F., Cagnie B., Cools A., Baert I., Van Brempt J., Struyf P., and Meeus M.. 'Scapulothoracic Muscle Activity and Recruitment Timing in Patients with Shoulder Impingement Symptoms and Glenohumeral Instability'. Journal of Electromyography and Kinesiology 24, no. 2 (April 2014): 277–84. https://doi.org/10.1016/j.jelekin.2013.12.002.

Struyf F, Nijs J, Baeyens JP, Mottram S, Meeusen R. Scapular positioning and movement in unimpaired shoulders, shoulder impingement syndrome, and glenohumeral instability. Scand J Med Sci Sports. 2011 Jun;21(3):352-8. doi: 10.1111/j.1600-0838.2010.01274.x. Epub 2011 Mar 8. PMID: 21385219.

Thelen DG. Adjustment of muscle mechanics model parameters to simulate dynamic contractions in older adults. J Biomech Eng. 2003 Feb;125(1):70-7. doi: 10.1115/1.1531112. PMID: 12661198.

Thomas SC, Matsen FA. An approach to the repair of avulsion of the glenohumeral ligaments in the management of traumatic anterior glenohumeral stability. JBJS 1989;71A: 506-13.

Uhthoff HK, Sarkar K. An algorithm for shoulder pain caused by soft-tissue disorders. Clin Orthop Relat Res. 1990 May;(254):121-7. PMID: 2182249.

Ustun TB, Chatterji S, Kostanjsek N, Rehm J, Kennedy C, Epping-Jordan J, Saxena S, von Korff M, Pull C; WHO/NIH Joint Project. Developing the World Health Organization Disability Assessment Schedule 2.0. Bull World Health Organ. 2010 Nov 1;88(11):815-23. doi: 10.2471/BLT.09.067231. Epub 2010 May 20. PMID: 21076562; PMCID: PMC2971503.

Vanmechelen I, Desloovere K, Haberfehlner H, Martens B, Vermeulen JR, Buizer AI, Aerts JM, Feys H, Monbaliu E. Altered upper limb kinematics in individuals with dyskinetic cerebral palsy in comparison with typically developing peers - A statistical parametric mapping study. Gait Posture. 2023 Jun 17:S0966-6362(23)00159-5. doi: 10.1016/j.gaitpost.2023.06.010. Epub ahead of print. PMID: 37344269.

Van Drongelen S, van der Woude LH, Janssen TW, Angenot EL, Chadwick EK, Veeger DH. Glenohumeral contact forces and muscle forces evaluated in wheelchair-related activities of daily living in able-bodied subjects versus subjects with paraplegia and tetraplegia. Arch Phys Med Rehabil. 2005 Jul;86(7):1434-40. doi: 10.1016/j.apmr.2005.03.014. PMID: 16003677.

Veeger, H.E.J., and F.C.T. van der Helm. "Shoulder Function: The Perfect Compromise between Mobility and Stability." Journal of Biomechanics 40, no. 10 (January 2007): 2119–29. https://doi.org/10.1016/j.jbiomech.2006.10.016.

Vinti, Mariaconceta. “Caractérisation biomécanique et physiologique de la cocontraction spastique dans la parésie spastique.” PhD diss., Arts Et Métiers ParisTech, 2012. https://tel.archives-ouvertes.fr/pastel-00913644/.

Walker, David R., Aimee M. Struk, Scott A. Banks, and Thomas W. Wright. “Scapulohumeral Rhythm in Shoulders with Reverse Shoulder Arthroplasty.” Journal of Shoulder and Elbow Surgery 24, no. 4 (April 2015): e113. https://doi.org/10.1016/j.jse.2014.11.012.

Warby S, Pizzari T, Ford J, Hahne A, Watson L. The effect of exercise-based management for multidirectional instability of the glenohumeral joint: A systematic review. Journal of Science and Medicine in Sport. 2013 Dec;16:e9–10.

Warby SA, Ford JJ, Hahne AJ, Watson L, Balster S, Lenssen R, Pizzari T. Comparison of 2 Exercise Rehabilitation Programs for Multidirectional Instability of the Glenohumeral Joint: A Randomized Controlled Trial. Am J Sports Med. 2018 Jan;46(1):87-97. doi: 10.1177/0363546517734508. Epub 2017 Oct 19. PMID: 29048942.

Watson L, Balster S, Lenssen R, Hoy G, Pizzari T. The effects of a conservative rehabilitation program for multidirectional instability of the shoulder. Journal of Shoulder and Elbow Surgery. 2018 Jan;27(1):104–11.

Wattananon P, Kongoun S, Chohan A, Richards J. The use of statistical parametric mapping to determine altered movement patterns in people with chronic low back pain. J Biomech. 2023 May;153:111601. doi: 10.1016/j.jbiomech.2023.111601. Epub 2023 Apr 25. PMID: 37126886.

Weel H, Tromp W, Krekel PR, Randelli P, van den Bekerom MPJ, van Deurzen DFP. International survey and surgeon’s preferences in diagnostic work-up towards treatment of anterior shoulder instability. Archives of Orthopaedic and Trauma Surgery. 2016 Jun;136(6):741–6.

Wilcox, Reg B., Arslanian, Linda E., and Millet, Peter J. “Rehabilitation Following Total Shoulder Arthroplasty.” Journal of Orthopaedic and Sports Physical Therapy, December 2005. https://doi.org/10.2519/jospt.2005.2000.

Williams S, Schmidt R, Disselhorst-Klug C, Rau G. An upper body model for the kinematical analysis of the joint chain of the human arm. J Biomech. 2006;39(13):2419-29. doi: 10.1016/j.jbiomech.2005.07.023. Epub 2005 Sep 12. PMID: 16159659.

Winter, David A. Biomechanics and Motor Control of Human Movement. 4th ed. Hoboken, N.J: Wiley, 2009.

Wu G, van der Helm FC, Veeger HE, Makhsous M, Van Roy P, Anglin C, Nagels J, Karduna AR, McQuade K, Wang X, Werner FW, Buchholz B; International Society of Biomechanics. ISB recommendation on definitions of joint coordinate systems of various joints for the

reporting of human joint motion--Part II: shoulder, elbow, wrist and hand. J Biomech. 2005 May;38(5):981-992. doi: 10.1016/j.jbiomech.2004.05.042. PMID: 15844264.

Wu W, Lee PVS, Bryant AL, Galea M, Ackland DC. Subject-specific musculoskeletal modeling in the evaluation of shoulder muscle and joint function. J Biomech. 2016 Nov 7;49(15):3626-3634. doi: 10.1016/j.jbiomech.2016.09.025. Epub 2016 Sep 23. PMID: 28327299.

12. Appendix

Appendix Chapter 5 Methods

Appendix Table 5.2, clusters of the experimental marker set	
Placement illustration	Description of cluster placement
	Sternal marker cluster Positioned using double sided tape on the anterior aspect of the thorax, approximately one finger width below the sternal notch. Placement was below the sterno-clavicular joint and in keeping with the midline of the body. The antero-superior border of the thorax is defined by the insicura jugularis (IJ) point and the antero-inferior border is defined Processes Xiphoideus (PX) point. For participants with breast tissue, a more superior placement of the sternal cluster may have been required, not exceeding the antero-superior border of the thorax. In this case, adequate visibility of the marker cluster was ensured prior to identification of virtual markers. The inferior edge of the cluster was marked.
	Acromion marker cluster Positioned using double sided tape on the flat surface of the acromion. Secure to the acromion with extra tape. Following identification of the acromioclavicular joint, posterior palpation identified the flattest area of the acromion. The base of the cluster was marked.

Appendix Table 5.3, illustration of the anatomical and virtual markers	
Landmarks illustration	Description of landmarks
	THORAX SEGMENT C7 Spinous Process (C7) C7 can be seen with flexion of the head and protrudes more dorsally than C6 and T1. With extension of the head C6 disappears first and C7 remains palpable for longer. T8 Spinous Process (T8) From either the proximal or distal reference points (below) Alternate with two palpating fingers and count from cranial to caudal to the 8th thoracic vertebrae Reference points: T3 / T4 spinous process in line with spina scapulae T7 spinous process in line with angulus inferior scapula Insicura Jungularis (IJ) Manubrium sterni is proximally bounded by the incisura jungularis. Cranial bowl-shaped limitation of the manubrium sterni (deepest point). Palpation/ identification of the point should be done from superior to inferior. Processus Xiphoideus (PX)

	Most caudal point of the sternum in keeping with the midline.
	CLAVICLE SEGMENT Art. Sternoclavicularis (SC) Located bilaterally from the IJ, course from cranio-medial to caudo-lateral. (protraction and retraction of the shoulder facilitate palpation) Art. Acromioclavicularis (AC) Front: follow the front of the acromion to medial until a discrete notch is felt (V-shaped to open anterior). Back: follow the top of the spina scapula and the back of the clavicle laterally to where the two bone pieces meet. A little further to the lateral side is the dorsal boundary of the AC joint.
	Scapula segment Processus Coracoideus (PC) In the fossa infraclavicularis (ventral) from medial to lateral palpation until one feels a medial, bony structure (only the top and medial side can be palpated). See CLAVICLE SEGMENT Palpation of the PC may be facilitated by protracting the shoulder girdle Trigonum Scapulae (TS) Origin of the spina scapulae in line with the spinous process of T3 on the medial scapula edge. (spina goes to the latero-cranial). Palpate the midpoint of the triangular

	surface on the medial border of the scapula in line with the scapular spine Angulus Inferior (AI) Follow the medial edge of the scapula caudally (most caudal point of the scapula, location at the level of the spinous process of T7) Angulus Acromialis (AA) Follow the spina scapulae, from mid-caudal to latero-cranial until kink is felt in the dorso-lateral edge of the acromion (this rear corner is rectangular). Most laterodorsal point of the scapula
	HUMERUS SEGMENT Glenohumeral rotation centre (GH) Calculated via regression – with the participant's arm in abduction ask them to rotate their arm in a circular motion. Forearm in **supinated** position Lateral Epicondyle (LE) Palpable on the distal lateral side of the humerus (slight passive flexion of the elbow facilitates palpation). Medial Epicondyle (ME) Palpable on the distal medial side of the humerus (slight passive flexion elbow).
	FOREARM SEGMENT

	Forearm in **prone** position – palpation should be done from distal to proximal Radial Styloid (RS) Most caudal-antero point on the radial styloid Lateral edge of the radius leads distally into a depression. Palpate slightly proximal to the depression and the radial styloid is the palpable protrusion. Palpation easiest with radial deviation. Ulnar Styloid (US) Most caudal-postero point on the ulnar styloid. Medial edge of the ulna leads distally into a depression. Palpate slightly proximal to the depression and the ulna styloid is the palpable protrusion. Palpation easiest with ulna deviation.
	HAND SEGMENT Styloid process of 3rd Metacarpal (MC3) Follow the third metacarpal on its dorsal side from distal to proximal. The small bone elevation on the base is the styloid process. Palpation easiest with maximum palmar flexion. (os capitatum lies in depression just proximal to styloid process of the 3rd Metacarpal) Distal head of 2nd Metacarpophalangeal joint (MCP2) Palpate just distal to the 2nd metacarpophalangeal joint (these joints are easy to palpate on the dorso-lateral side in light flexion position or with longitudinal traction).

	Distal head of 3rd Metacarpophalangeal joint (MCP3) Palpate just distal to the 3rd metacarpophalangeal joint (these joints are easy to palpate on the dorso-lateral side in light flexion position or with longitudinal traction). Distal head of 5th Metacarpophalangeal joint (MCP5) Palpate just distal to the 5th metacarpophalangeal joint (these joints are easy to palpate on the dorso-lateral side in light flexion position or with longitudinal traction).

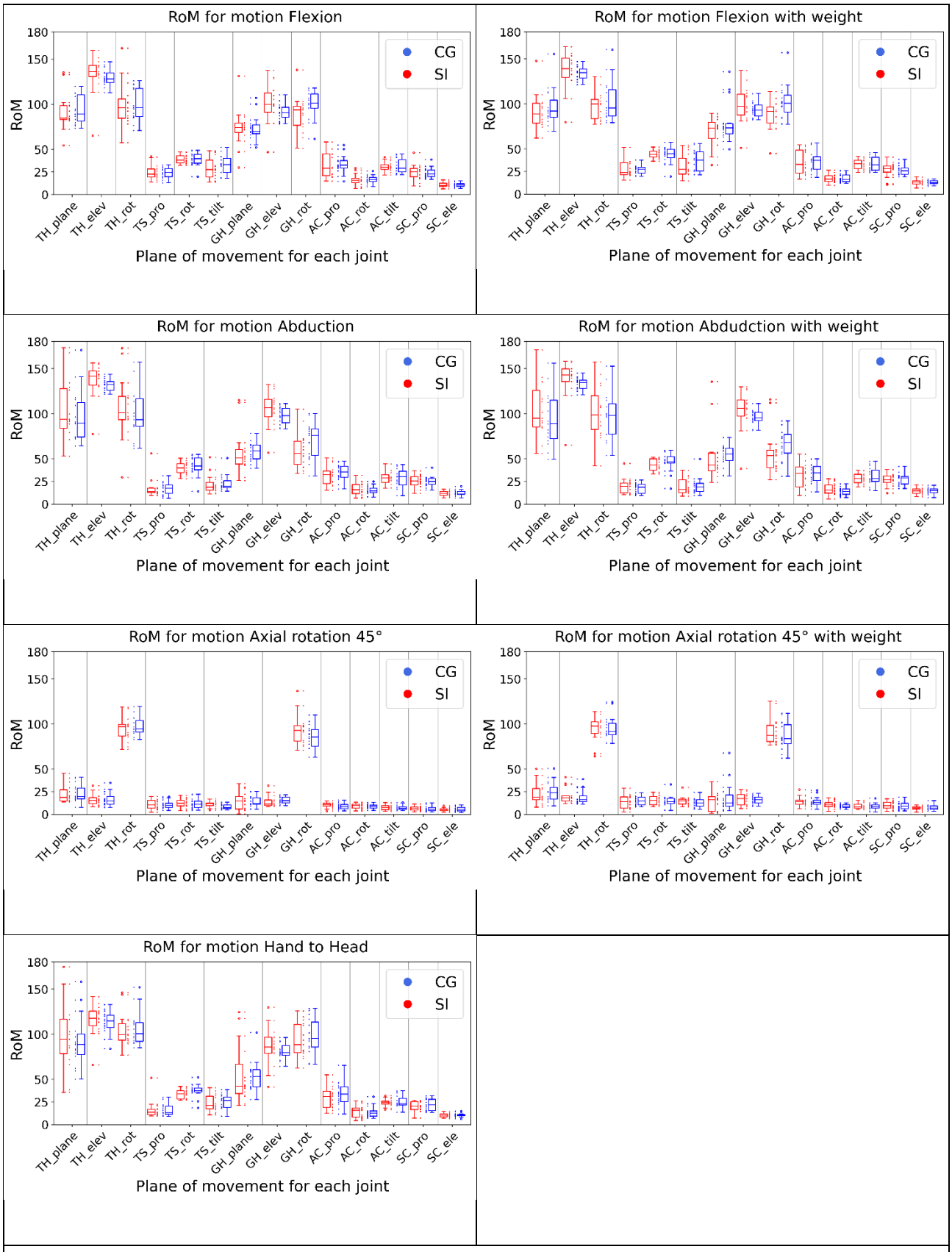

Appendix Fig. 6.2) RoM per group: Shoulder Instability group (SI) vs Control Group (CG).

The boxes extend from the first to third quartile, with a line at the median. The whiskers extend to 1.5 times the inter-quartile range. Flier points are above the whiskers. Headings: TH = thoracohumeral, TS = thoracoscapular, GH = glenohumeral, AC = acromioclavicular, SC = sternoclavicular, elev = elevation, rot = rotation, pro = protraction.

Appendix Chapter 7 (Objective B)

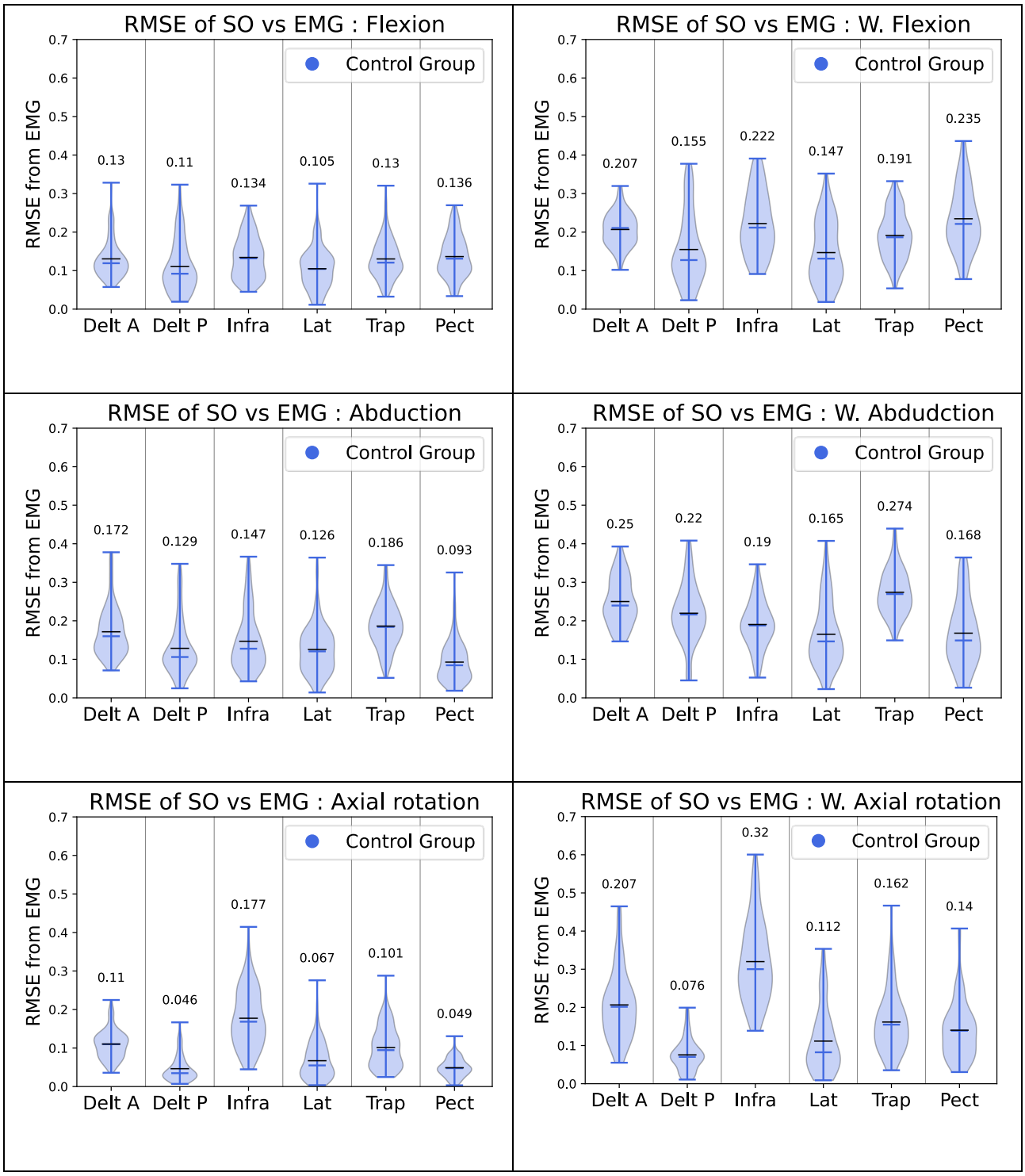

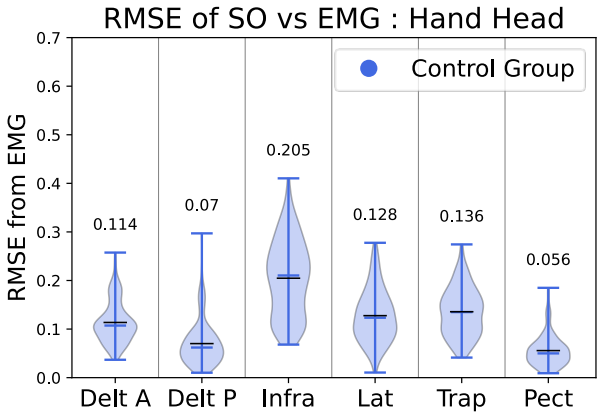

Appendix Fig 7.3) Showing the RMSE values of the predicted muscle activation from Static Optimisation versus the measured EMG, in the Control Group. Each violin plot has a line for the maximum, median, and minimum value. The mean value is shown as text above and as a black line on the plot. The shape extends to 1.5 times the inter-quartile range, showing the outlier points on either side of the distribution. Headings: Delt A = Deltoid Anterior, Delt P = Deltoid Posterior, Infra = Infraspinatus, Lat = Latissimus, Trap = Trapezius, Pect = Pectoralis Major.

Appendix Table 6.5) Identifying the participants from the CGI group that have motion across all angles of the model indistinguishable from normal kinematics, at each time step.

Participants from SI group	Flexion	Abduction	Axial rotation 45	Hand Head	Flexion with weight	Abduction with weight	Axial rotation 45 with weight
0WL1RZ767E	TRUE	TRUE	TRUE	TRUE	TRUE	TRUE	TRUE
7SJS0JZX3A			TRUE		TRUE	TRUE	
7X0AGZUZFG		TRUE	TRUE	TRUE			TRUE
26MIB6XDC6		TRUE	TRUE	TRUE	TRUE	TRUE	TRUE
905G3EUHWJ							
B6SNJ3SBIW	TRUE	TRUE	TRUE		TRUE		
CL966HXS0C	TRUE	TRUE	TRUE		TRUE	TRUE	TRUE
FEH3JSLARJ		TRUE	TRUE				TRUE
HACIMVVX5A	TRUE		TRUE		TRUE		TRUE
PJ3URGRTWJ		TRUE	TRUE	TRUE			TRUE
S6IRQQNB3G			TRUE				TRUE
TKTEK8R7A0							TRUE
WWO521323K			TRUE		TRUE		TRUE
WX3800CYC3		TRUE	TRUE	TRUE			
YRG37Y39YS	TRUE	TRUE	TRUE		TRUE	TRUE	

Appendix Chapter 8 (Objective C)

Static Optimisation on SI – standalone (RMSE and Pearson correlation coefficient)

Appendix table 8.01) This table summarises the ability of our model to predict the experimental EMG in the Shoulder Instability group. Each value corresponds to the average **RMSE** (of all repetitions of all participants) between the waveforms of the predicted muscle activations (results from the Static Optimisation analysis) and of the experimental surface EMG. Green cells highlight the best predictions, and grey cells highlight best predictions overall.

RMSE SI	Trapezius Middle	Deltoid Anterior	Deltoid Posterior	Lat. Dorsi	Pect. Major	Infra	Average
Flexion	0.14	0.15	0.12	0.08	0.16	0.123	0.13
Weight flexion	0.19	0.25	0.16	0.11	0.25	0.20	0.19
Abduction	0.21	0.21	0.15	0.11	0.10	0.15	0.16
Weight abduction	0.27	0.27	0.24	0.11	0.15	0.20	0.21
Abd45	0.12	0.12	0.06	0.05	0.08	0.16	0.1
Weight abd45	0.16	0.22	0.10	0.07	0.18	0.27	0.17
Hand head	0.15	0.14	0.08	0.11	0.08	0.14	0.12
Average	0.18	0.20	0.13	0.09	0.14	0.18	

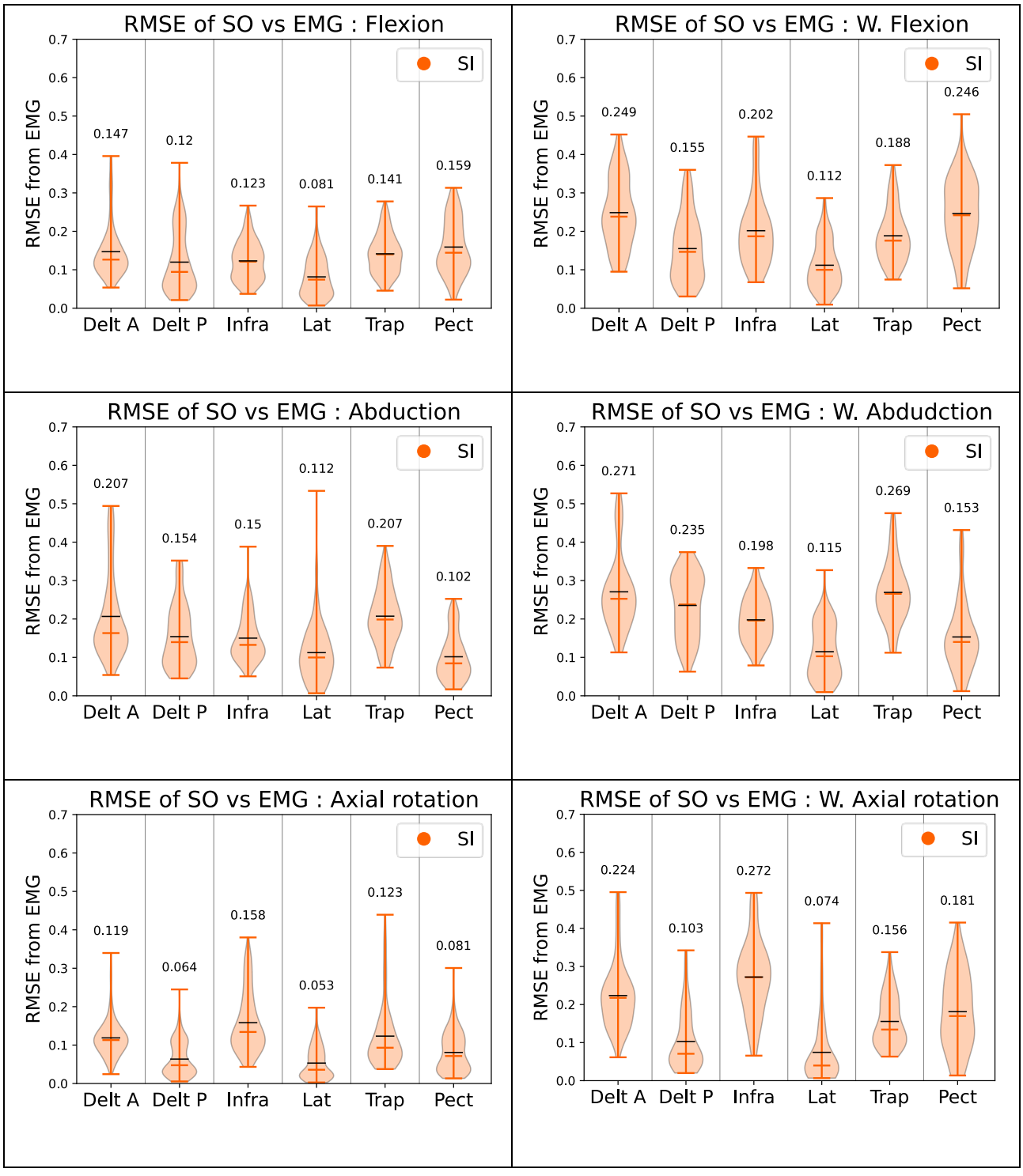
RMSE of SO vs EMG : Flexion
RMSE from EMG
SI
0.147
0.12
0.123
0.081
0.141
0.159
Delt A
Delt P
Infra
Lat
Trap
Pect
RMSE of SO vs EMG : W. Flexion
RMSE from EMG
SI
0.249
0.155
0.202
0.112
0.188
0.246
Delt A
Delt P
Infra
Lat
Trap
Pect
RMSE of SO vs EMG : Abduction
RMSE from EMG
SI
0.207
0.154
0.15
0.112
0.207
0.102
Delt A
Delt P
Infra
Lat
Trap
Pect
RMSE of SO vs EMG : W. Abdudction
RMSE from EMG
SI
0.271
0.235
0.198
0.115
0.269
0.153
Delt A
Delt P
Infra
Lat
Trap
Pect
RMSE of SO vs EMG : Axial rotation
RMSE from EMG
SI
0.119
0.064
0.158
0.053
0.123
0.081
Delt A
Delt P
Infra
Lat
Trap
Pect
RMSE of SO vs EMG : W. Axial rotation
RMSE from EMG
SI
0.224
0.103
0.272
0.074
0.156
0.181
Delt A
Delt P
Infra
Lat
Trap
Pect

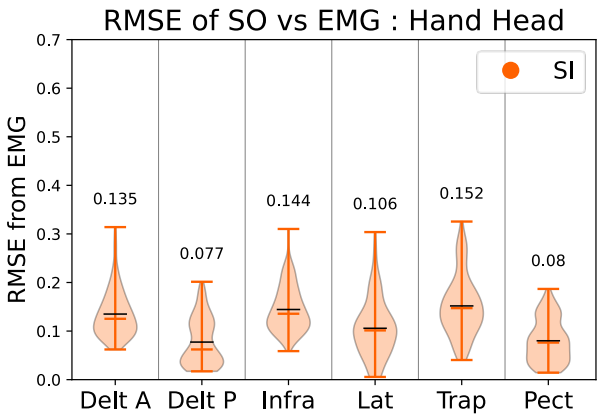

Appendix Fig. 8.01) Showing the RMSE values of the predicted muscle activation from Static Optimisation versus the measured EMG, in the Shoulder Instability group. Each violin plot has a line for the maximum, median, and minimum value. The mean value is shown as text above and as a black line on the plot. The shape extends to 1.5 times the inter-quartile range, showing the outlier points on either side of the distribution. Headings: Delt A = Deltoid Anterior, Delt P = Deltoid Posterior, Infra = Infraspinatus, Lat = Latissimus, Trap = Trapezius, Pect = Pectoralis Major.

*Appendix Table 8.02) Summary of the waveform agreement between the predicted waveform of muscle activations and the experimental EMG, in the Shoulder Instability group. Each value corresponds to the **Pearson correlation coefficient**, across all repetitions of all participants of the SI dataset. Darker cells highlight the best predictions.*

Correlation **measure** CG	**Trapezius Middle**	**Deltoid Anterior**	**Deltoid Posterior**	**Lat. Dorsi**	**Pect. Major**	**Infra**	**Average**
Flexion	0.11	0.6	0.27	-0.09	0.39	0.52	0.3
Weight flexion	0.27	0.55	0.23	-0.19	0.51	0.64	0.34
Abduction	0.08	0.57	0.36	-0.06	0.12	0.24	0.22
Weight abduction	0.31	0.56	0.24	0	0	0.47	0.26
Abd45	0.02	0.1	0.07	0.08	0.02	0.43	0.12
Weight abd45	0.11	0.03	0.18	0.05	0.09	0.22	0.11
Hand head	0.16	0.55	0.02	-0.03	0.04	0.54	0.21
Average	0.15	0.42	0.2	-0.03	0.17	0.44	

Appendix Table 8.1) highlighting RMSE difference between the SI and CG groups. Value: average RMSE between predicted muscle activity (SO) and experimental EMG. In green, the prediction is better for the CG group than for the SI group. In blue, the prediction is better for the SI group than for the CG group. The totals (column and row) with shades of grey represent the combination of both groups, and the darker the cell, the better the prediction overall. The totals (column and row) with shades of grey

	Trapezius		Deltoid Anterior		Deltoid Posterior		Lat. Dorsi		Pect. Major		Infraspin.		Total group		Total
	CG	SI	CG	SI	CG	SI	CG	SI	CG	SI	CG	SI	CG	SI	
Flexion	0.13	0.14	0.13	0.15	0.11	0.12	0.10	0.08	0.14	0.16	0.13	0.12	0.75	0.77	1.51
Weight flex.	0.19	0.19	0.21	0.25	0.15	0.16	0.15	0.11	0.23	0.25	0.22	0.20	1.16	1.15	2.31
Abduct	0.19	0.21	0.17	0.21	0.13	0.15	0.13	0.11	0.09	0.10	0.15	0.15	0.85	0.93	1.78
Weightabd.	0.27	0.27	0.25	0.27	0.22	0.24	0.16	0.11	0.17	0.15	0.19	0.20	1.27	1.24	2.51
Abd45	0.10	0.12	0.11	0.12	0.05	0.06	0.07	0.05	0.05	0.08	0.18	0.16	0.55	0.60	1.15
Weightabd45	0.16	0.16	0.21	0.22	0.08	0.10	0.11	0.07	0.14	0.18	0.32	0.27	1.06	1.01	2.03
Hand head	0.14	0.15	0.11	0.14	0.07	0.08	0.13	0.11	0.06	0.08	0.20	0.14	0.70	0.69	1.40
Avg. group	0.17	0.177	0.17	0.19	0.12	0.13	0.12	0.09	0.13	0.14	0.20	0.18	0.90	0.91	
Avg. global	0.35		0.36		0.25		0.21		0.27		0.378				

CG and SI- RMSE

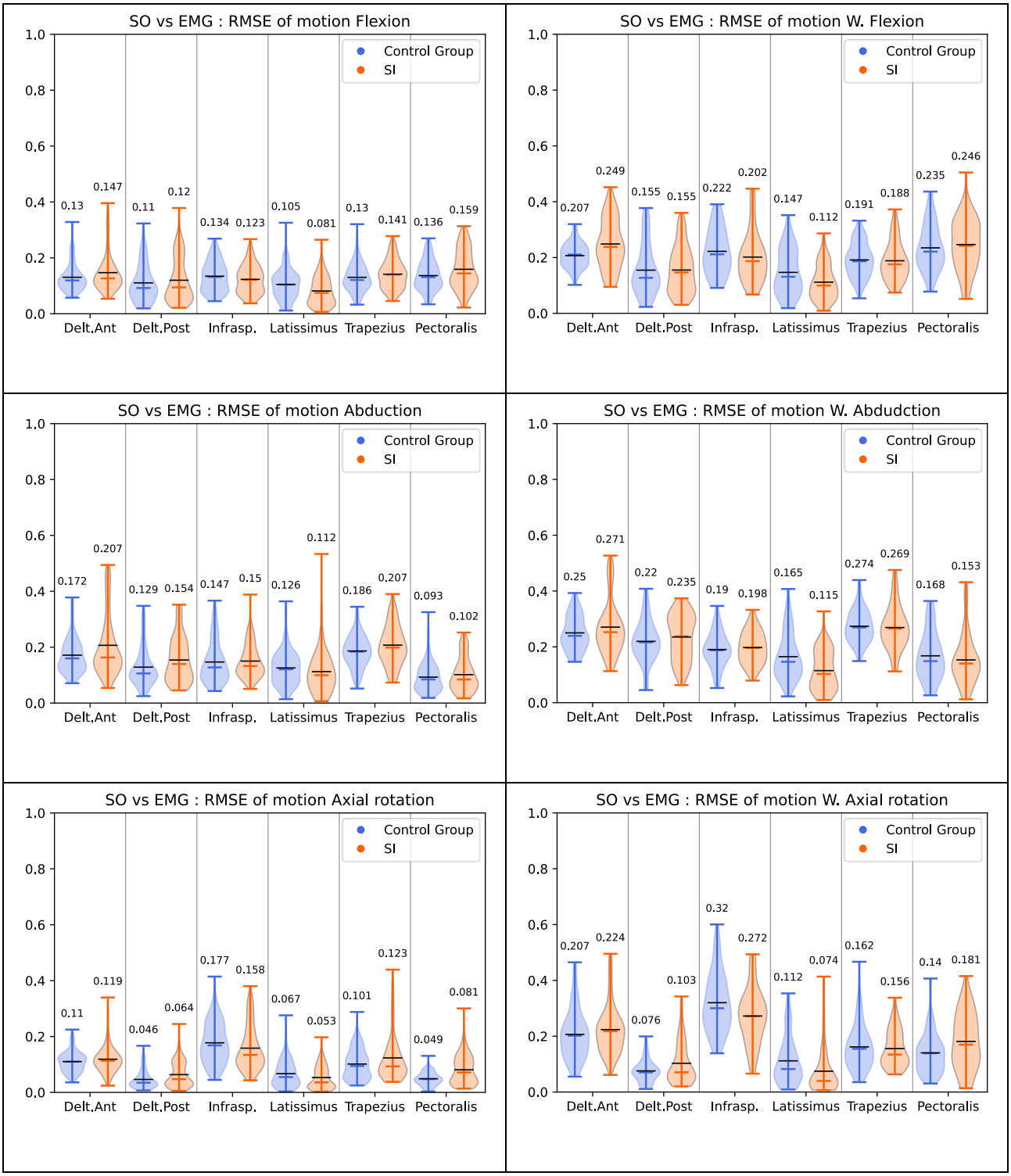

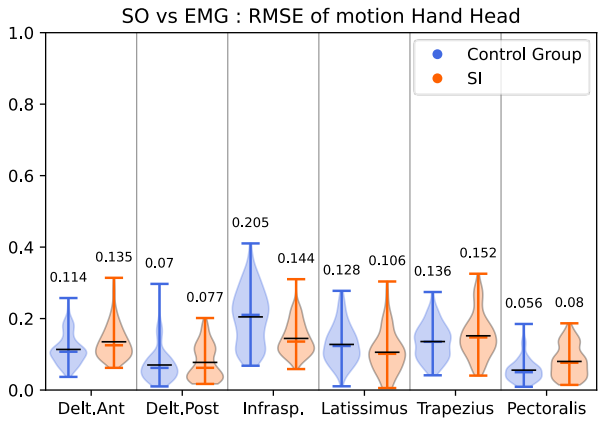

Appendix Fig. 8.1) plot comparison of the RMSE difference between the SI and CG groups. Each value is the average RMSE between predicted muscle activity (SO) and experimental EMG

Each violin plot has a line for the maximum, median, and minimum value. The mean value is shown as text above and as a black line on the plot. The shape extends to 1.5 times the inter-quartile range, showing the outlier points on either side of the distribution.

CG and SI- Pearson correlation coefficient

*Appendix Table 8.2) highlighting **Pearson correlation coefficient** difference between the SI and CG groups. Value: measure between predicted muscle activity (SO) and experimental EMG. In green, the prediction is better (higher value) for the CG group than for the SI group. In blue, the prediction is better for the SI group than for the CG group. The totals (column and row) with shades of grey represent the combination of both groups, and the darker the cell, the better the prediction overall.*

	Trapezius		Deltoid Anterior		Deltoid Posterior		Lat. Dorsi		Pect. Major		Infraspin		Average per group		Average
	CG	SI	CG	SI	CG	SI	CG	SI	CG	SI	CG	SI	CG	SI	
Flexion	0.21	0.11	0.57	0.6	0.06	0.27	0.1	-0.09	0.31	0.39	0.43	0.52	0.28	0.3	0.29
Weight Flex.	0.22	0.27	0.6	0.55	0.11	0.23	0.04	-0.19	0.45	0.51	0.53	0.64	0.33	0.33	0.33
Abduction	0.2	0.08	0.53	0.57	0.24	0.36	-0.01	-0.06	0.28	0.12	0.23	0.24	0.25	0.22	0.23
Weight Abd.	0.24	0.31	0.59	0.56	0.2	0.24	0.01	0	0.17	0	0.36	0.47	0.26	0.26	0.26
Axial	-0.02	0.02	-0.04	0.1	0.07	0.07	0.09	0.08	0	0.02	0.42	0.43	0.09	0.12	0.1
Weight Axial	0.1	0.11	0.1	0.03	0.16	0.18	0.08	0.05	0.15	0.09	0.25	0.22	0.14	0.11	0.13
Hand head	0.21	0.16	0.57	0.55	-0.11	0.02	0.08	-0.03	0.09	0.04	0.46	0.54	0.21	0.21	0.21
Avg. group	0.17	0.15	0.42	0.42	0.1	0.2	0.06	-0.03	0.21	0.17	0.38	0.44	0.22	0.22	
Avg. global	0.32		0.84		0.3		0.03		0.38		0.82				

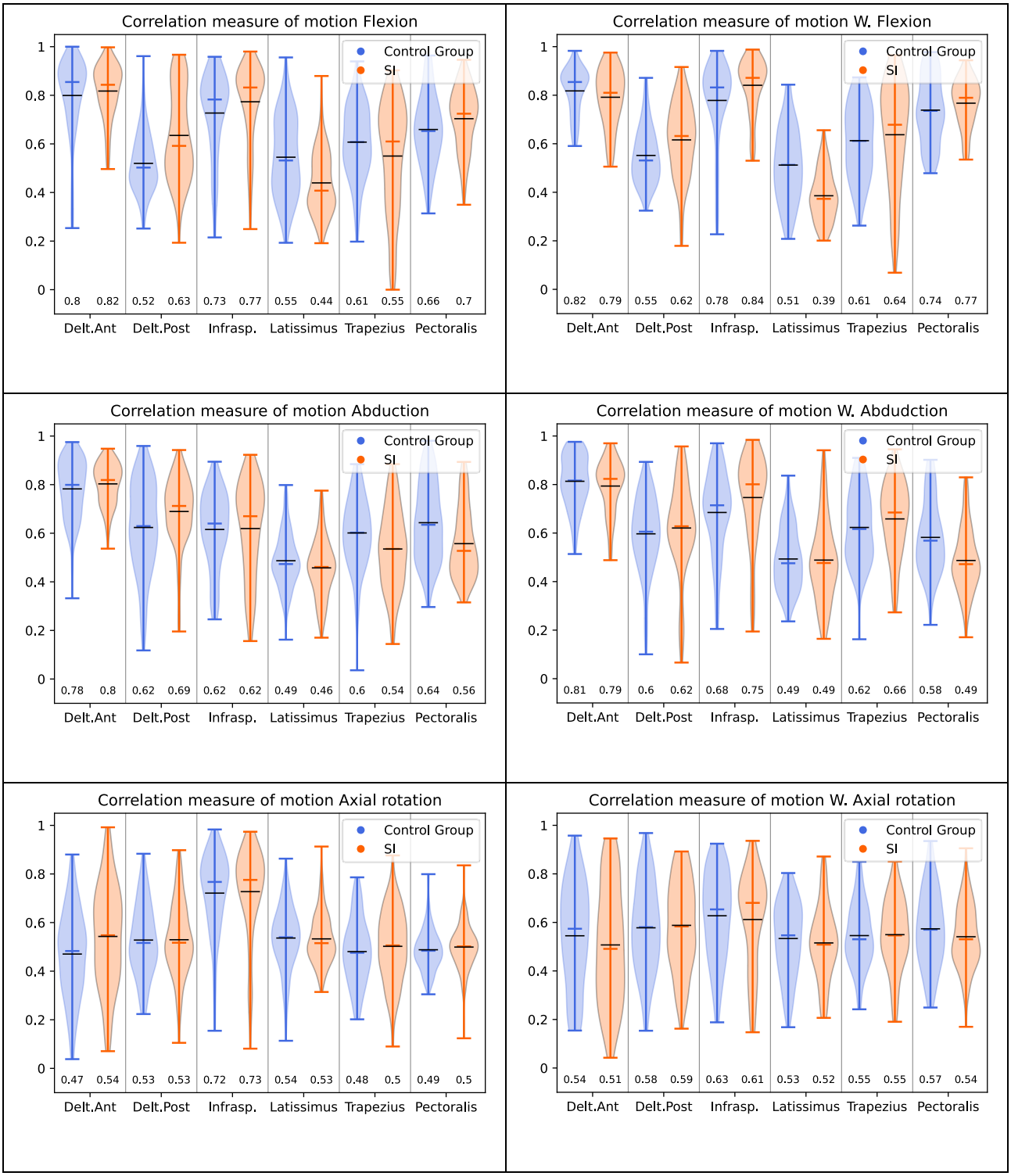
Correlation measure of motion Flexion
Control Group
SI
0.8 0.82 0.52 0.63 0.73 0.77 0.55 0.44 0.61 0.55 0.66 0.7
Delt.Ant Delt.Post Infrasp. Latissimus Trapezius Pectoralis
Correlation measure of motion W. Flexion
Control Group
SI
0.82 0.79 0.55 0.62 0.78 0.84 0.51 0.39 0.61 0.64 0.74 0.77
Delt.Ant Delt.Post Infrasp. Latissimus Trapezius Pectoralis
Correlation measure of motion Abduction
Control Group
SI
0.78 0.8 0.62 0.69 0.62 0.62 0.49 0.46 0.6 0.54 0.64 0.56
Delt.Ant Delt.Post Infrasp. Latissimus Trapezius Pectoralis
Correlation measure of motion W. Abdudction
Control Group
SI
0.81 0.79 0.6 0.62 0.68 0.75 0.49 0.49 0.62 0.66 0.58 0.49
Delt.Ant Delt.Post Infrasp. Latissimus Trapezius Pectoralis
Correlation measure of motion Axial rotation
Control Group
SI
0.47 0.54 0.53 0.53 0.72 0.73 0.54 0.53 0.48 0.5 0.49 0.5
Delt.Ant Delt.Post Infrasp. Latissimus Trapezius Pectoralis
Correlation measure of motion W. Axial rotation
Control Group
SI
0.54 0.51 0.58 0.59 0.63 0.61 0.53 0.52 0.55 0.55 0.57 0.54
Delt.Ant Delt.Post Infrasp. Latissimus Trapezius Pectoralis

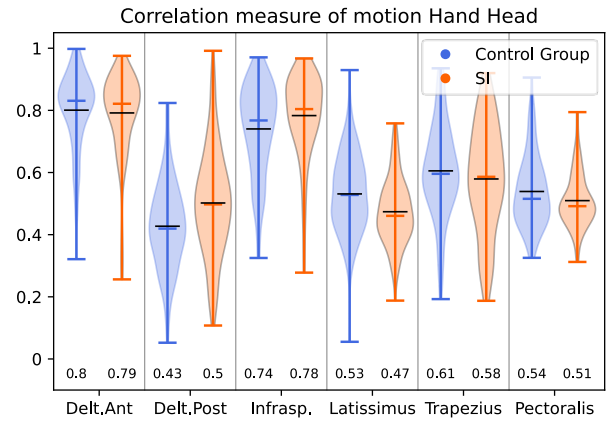

Appendix Fig. 8.2) plot comparison of the Pearson correlation measure difference between the SI and CG groups. Each value is the Pearson correlation measure between predicted muscle activity (SO) and experimental EMG. Higher values represent a better prediction.

Each violin plot has a line for the maximum, median, and minimum value. The mean value is shown as text below and as a black line on the plot. The shape extends to 1.5 times the inter-quartile range, showing the outlier points on either side of the distribution.

CG and Subset- correlation two standard deviations

*Appendix Table 8.4) This table shows, for each motion identified as normal of the subset, the number of times that a muscles' **Pearson correlation measure** (average of all repetitions) falls outside of the two standard deviations of the baseline of our prediction. The individual muscles are also mentioned in each cell. In blue are the cells where Pectoralis Major was identified.*

RMSE outside of norm in subset	Flexion	Abduction	Axial rotation	Hand to head	Flexion with weight	Abduction with weight	Axial rotation with weight	Total
0WL1RZ767E							16.7% (1/6) ['DeltAnt']	16.7% (1/6)
7SJS0JZX3A	50.0% (3/6) ['DeltAnt', 'DeltPost', 'MidTrap']	0	16.7% (1/6) ['InfraSpin']	33.3% (2/6) ['DeltAnt', 'MidTrap']		16.7% (1/6) ['PecMajor']	16.7% (1/6) ['DeltAnt']	22.2% (8/36)
7X0AGZUZFG								
26MIB6XDC6			0		16.667% (1/6) ['LatDorsi']		33.3% (2/6) ['DeltAnt', 'LatDorsi']	16.7% (3/18)
905G3EUHWJ			16.7% (1/6) ['DeltAnt']				50.0% (3/6) ['DeltAnt', 'DeltPost', 'InfraSpin']	33.3% (4/12)
B6SNJ3SBIW								
CL966HXS0C			0					0.0% (0/6)
FEH3JSLARJ							33.3% (2/6) ['DeltAnt', 'DeltPost']	33.3% (2/6)
HACIMVVX5A			16.7% (1/6) ['MidTrap']				0	8.3% (1/12)
PJ3URGRTWJ								
S6IRQQNB3G								
TKTEK8R7A0			50.0% (3/6) ['DeltAnt', 'LatDorsi', 'MidTrap']				16.7% (1/6) ['LatDorsi']	33.3% (4/12)
WWO521323K			0				0	0.0% (0/12)
WX3800CYC3	0				0		0	0.0% (0/18)
YRG37Y39YS			50.0% (3/6) ['DeltAnt', 'InfraSpin', 'PecMajor']				83.3% (5/6) ['DeltAnt', 'DeltPost', 'InfraSpin', 'LatDorsi', 'PecMajor']	66.7% (8/12)

CG and Subset- correlation permutations

*Appendix Table 8.5) Each cell with data corresponds to the motion that was identified as having normal kinematics for a given participant of the subgroup. The value is a ratio and a percentage of how many times a muscle had a p-value <0.05 rejecting the null hypothesis (of the two-tailed test) that there was no difference between all repetitions of this participant and all repetitions of the normal group for this given motion and muscle, based on the **correlation measure**. The higher the values, the more statistically significant differences there are across all muscle patterns.*

Permutations on subset	Flexion	Weight Flexion	Abd	Weight abd	Axial rotation	W. axial rotation	Hand head	Total Row
0WL1RZ767E						2 / 6 = 33.3% ['DeltAnt', 'DeltPost']		2 / 6 = 33.3%
7SJS0JZX3A	5 / 6 = 83.3% ['DeltAnt', 'DeltPost', 'InfraSpin', 'MidTrap', 'PecMajor']		5 / 6 = 83.3% ['DeltPost', 'InfraSpin', 'LatDorsi', 'MidTrap', 'PecMajor']	4 / 6 = 66.7% ['DeltAnt', 'InfraSpin', 'LatDorsi', 'PecMajor']	2 / 6 = 33.3% ['DeltAnt', 'InfraSpin']	1 / 6 = 16.7% ['DeltAnt']	4 / 6 = 66.7% ['DeltAnt', 'InfraSpin', 'MidTrap', 'PecMajor']	21 / 36 = 58.3%
26MIB6XDC6		1 / 6 = 16.7% ['LatDorsi']			1 / 6 = 16.7% ['DeltPost']	1 / 6 = 16.7% ['PecMajor']		3 / 18 = 16.7%
905G3EUHWJ					1 / 6 = 16.7% ['DeltAnt']	3 / 6 = 50.0% ['DeltAnt', 'DeltPost', 'InfraSpin']		4 / 12 = 33.3%
CL966HXS0C					2 / 6 = 33.3% ['InfraSpin', 'MidTrap']			2 / 6 = 33.3%
FEH3JSLARJ						2 / 6 = 33.3% ['DeltAnt', 'DeltPost']		2 / 6 = 33.3%
HACIMVVX5A					4 / 6 = 66.7% ['DeltAnt', 'InfraSpin', 'LatDorsi', 'MidTrap']	2 / 6 = 33.3% ['DeltPost', 'LatDorsi']		6 / 12 = 50.0%
TKTEK8R7A0					2 / 6 = 33.3% ['LatDorsi', 'MidTrap']	0		2 / 12 = 16.7%
WWO521323K					3/6 = 50.0% ['DeltAnt', 'InfraSpin', 'MidTrap']	1/6 = 16.7% ['DeltAnt']		4 / 12 = 33.3%
WX3800CYC3	4 / 6 = 66.7% ['DeltPost', 'InfraSpin',	2 / 6 = 33.3% ['MidTrap', 'PecMajor']				1 / 6 = 16.7% ['LatDorsi']		7 / 18 = 38.9%

	'MidTrap', 'PecMajor']							
YRG37Y39YS					2 / 6 = 33.3% ['InfraSpin', 'PecMajor']	4 / 6 = 66.7% ['DeltPost', 'InfraSpin', 'LatDorsi', 'PecMajor']		6 / 12 = 50.0%
Total Column								

Appendix Letter of ethical approval

NHS
Health Research Authority

West Midlands - South Birmingham Research Ethics Committee
The Old Chapel
Royal Standard Place
Nottingham
NG1 6FS

Please note: This is the favourable opinion of the REC only and does not allow you to start your study at NHS sites in England until you receive HRA Approval

02 March 2020

Dr Fraser Philp
Lecturer
Keele University
School of Allied Health Professionals
Mackay Building
Keele
ST5 5BG

Dear Dr Philp

Study title:	**Shoulder instability in children: understanding muscle activity and movement pattern differences**
REC reference:	**20/WM/0021**
Protocol number:	**RG-0303-19 SHAR**
IRAS project ID:	**271729**

Thank you for your letter of 26 February 2020, responding to the Committee's request for further information on the above research and submitting revised documentation.

The further information has been considered on behalf of the Committee by the Chair.

Confirmation of ethical opinion

On behalf of the Committee, I am pleased to confirm a favourable ethical opinion for the above research on the basis described in the application form, protocol and supporting documentation as revised, subject to the conditions specified below.

Conditions of the favourable opinion

The REC favourable opinion is subject to the following conditions being met prior to the start of the study.

Confirmation of Capacity and Capability (in England, Northern Ireland and Wales) or NHS management permission (in Scotland) should be sought from all NHS organisations involved in the study in accordance with NHS research governance arrangements. Each NHS organisation must confirm through the signing of agreements and/or other documents that it has given permission for the research to proceed (except where explicitly specified otherwise).

Guidance on applying for HRA and HCRW Approval (England and Wales)/ NHS permission for research is available in the Integrated Research Application System.

For non-NHS sites, site management permission should be obtained in accordance with the procedures of the relevant host organisation.

Sponsors are not required to notify the Committee of management permissions from host organisations

Registration of Clinical Trials

It is a condition of the REC favourable opinion that **all clinical trials are registered** on a publicly accessible database. For this purpose, 'clinical trials' are defined as the first four project categories in IRAS project filter question 2. Registration is a legal requirement for clinical trials of investigational medicinal products (CTIMPs), except for phase I trials in healthy volunteers (these must still register as a condition of the REC favourable opinion).

Registration should take place as early as possible and within six weeks of recruiting the first research participant at the latest. Failure to register is a breach of these approval conditions, unless a deferral has been agreed by or on behalf of the Research Ethics Committee (see here for more information on requesting a deferral:
https://www.hra.nhs.uk/planning-and-improving-research/research-planning/research-registration-research-project-identifiers/

As set out in the UK Policy Framework, research sponsors are responsible for making information about research publicly available before it starts e.g. by registering the research project on a publicly accessible register. Further guidance on registration is available at:
https://www.hra.nhs.uk/planning-and-improving-research/research-planning/transparency-responsibilities/

You should notify the REC of the registration details. We will audit these as part of the annual progress reporting process.

It is the responsibility of the sponsor to ensure that all the conditions are complied with before the start of the study or its initiation at a particular site (as applicable).

After ethical review: Reporting requirements

The attached document "After ethical review – guidance for researchers" gives detailed guidance on reporting requirements for studies with a favourable opinion, including:

- Notifying substantial amendments
- Adding new sites and investigators
- Notification of serious breaches of the protocol
- Progress and safety reports
- Notifying the end of the study, including early termination of the study
- Final report

The latest guidance on these topics can be found at
https://www.hra.nhs.uk/approvals-amendments/managing-your-approval/.

Ethical review of research sites

NHS/HSC sites

The favourable opinion applies to all NHS/HSC sites listed in the application subject to confirmation of Capacity and Capability (in England, Northern Ireland and Wales) or management permission (in Scotland) being obtained from the NHS/HSC R&D office prior to the start of the study (see "Conditions of the favourable opinion" below).

Non-NHS/HSC sites

I am pleased to confirm that the favourable opinion applies to any non-NHS/HSC sites listed in the application, subject to site management permission being obtained prior to the start of the study at the site.

Approved documents

The final list of documents reviewed and approved by the Committee is as follows:

Document	*Version*	*Date*
Copies of advertisement materials for research participants [Study advertisement]	1.1	01 February 2020
Evidence of Sponsor insurance or indemnity (non NHS Sponsors only) [Sponsor insurance]		
IRAS Application Form [IRAS_Form_17122019]		17 December 2019
Letter from funder [Letter from funder]		
Letter from sponsor [Sponsor letter]		
Letters of invitation to participant [Recruitment e-mail for age matched controls to RJAH staff]	1.0	16 December 2019
Other [CV for PI]		
Other [CV for Co-I]		
Other [CV for Co-I]		
Other [CV for Co-I]		
Other [GCP certificate for CI]		
Other [Informed consent paediatric for CI]		
Other [Response to HRA]	1.0	01 February 2020
Other [Response to HRA - 2nd round]	1.0	21 February 2020

Participant consent form [Assent form - 8 to 10 years - Shoulder instability participant]	1.0	01 February 2020
Participant consent form [Assent form - 11 to 15 years - Shoulder instability participant]	1.0	01 February 2020
Participant consent form [Consent form - 16 years & above - Shoulder instability participants - no track changes]	1.1	01 February 2020
Participant consent form [Consent form - 16 years & above - Shoulder instability participants - track changes]	1.1	01 February 2020
Participant consent form [Assent form - 8 to 10 years - Age matched controls]	1.0	01 February 2020
Participant consent form [Assent form - 11 to 15 years - Age matched controls]	1.0	01 February 2020
Participant consent form [Consent form - 16 years & above - Age matched controls - no track changes]	1.1	01 February 2020
Participant consent form [Consent form - 16 years & above - Age matched controls - track changes]	1.1	01 February 2020
Participant consent form [Consent form - Parents - Shoulder instability participants - no track changes]	1.2	21 February 2020
Participant consent form [Consent form - Parents - Shoulder instability participants - track changes]	1.2	21 February 2020
Participant consent form [Consent form - Parents - Age matched controls - no track changes]	1.2	21 February 2020
Participant consent form [Consent form - Parents - Age matched controls - track changes]	1.2	21 February 2020
Participant information sheet (PIS) [PIS 16 years & above - Shoulder instability participants - no track changes]	1.1	01 February 2020
Participant information sheet (PIS) [PIS 16 years & above - Shoulder instability participants - track changes]	1.1	01 February 2020
Participant information sheet (PIS) [PIS 16 years & above - Age matched controls - no track changes]	1.1	01 February 2020
Participant information sheet (PIS) [PIS 16 years & above - Age matched controls - track changes]	1.1	01 February 2020
Participant information sheet (PIS) [PIS 8 to 10 years - Shoulder instability participants - no track changes]	1.1	21 February 2020
Participant information sheet (PIS) [PIS 8 to 10 years - Shoulder instability participants - track changes]	1.1	21 February 2020
Participant information sheet (PIS) [PIS 11 to 15 years - Shoulder instability participants - no track chnages]	1.1	21 February 2020
Participant information sheet (PIS) [PIS 11 to 15 years - Shoulder instability participants - track changes]	1.1	21 February 2020
Participant information sheet (PIS) [PIS Parents - Shoulder instability participants - no track changes]	1.2	21 February 2020
Participant information sheet (PIS) [PIS Parents - Shoulder instability participants - track changes]	1.2	21 February 2020
Participant information sheet (PIS) [PIS 8 to 10 years - Age matched controls - no track changes]	1.1	21 February 2020
Participant information sheet (PIS) [PIS 8 to 10 years - Age matched controls - track changes]	1.1	21 February 2020
Participant information sheet (PIS) [PIS 11 to 15 years - Age matched controls - no track changes]	1.1	21 February 2020
Participant information sheet (PIS) [PIS 11 to 15 years - Age matched controls - no track changes]	1.1	21 February 2020

Participant information sheet (PIS) [PIS Parents - Age matched controls - no track changes]	1.2	21 February 2020
Participant information sheet (PIS) [PIS Parents - Age matched controls - track changes]	1.2	21 February 2020
Research protocol or project proposal [Protocol]	1.0	16 December 2019
Sample diary card/patient card [Patient instability diary (Shoulder instability participants and age matched controls)]	1.0	16 December 2019
Summary CV for Chief Investigator (CI) [CV for CI]		

Statement of compliance

The Committee is constituted in accordance with the Governance Arrangements for Research Ethics Committees and complies fully with the Standard Operating Procedures for Research Ethics Committees in the UK.

User Feedback

The Health Research Authority is continually striving to provide a high quality service to all applicants and sponsors. You are invited to give your view of the service you have received and the application procedure. If you wish to make your views known please use the feedback form available on the HRA website:
http://www.hra.nhs.uk/about-the-hra/governance/quality-assurance/

HRA Learning

We are pleased to welcome researchers and research staff to our HRA Learning Events and online learning opportunities– see details at:
https://www.hra.nhs.uk/planning-and-improving-research/learning/

20/WM/0021	**Please quote this number on all correspondence**

With the Committee's best wishes for the success of this project.

Yours sincerely

pp

Professor Paula McGee
Chair

Email: southbirmingham.rec@hra.nhs.uk

Copy to: Dr Tracy Nevatte

Appendix Approval letter HRA and Health and Care Research Wales

Ymchwil Iechyd a Gofal Cymru
Health and Care Research Wales

NHS
Health Research Authority

Dr Fraser Philp
Lecturer
Keele University
School of Allied Health Professionals
Mackay Building
Keele
ST5 5BG

Email: hra.approval@nhs.net
HCRW.approvals@wales.nhs.uk

02 March 2020

Dear Dr Philp

HRA and Health and Care Research Wales (HCRW) Approval Letter

Study title:	**Shoulder instability in children: understanding muscle activity and movement pattern differences**
IRAS project ID:	**271729**
Protocol number:	**RG-0303-19 SHAR**
REC reference:	**20/WM/0021**
Sponsor	**Keele University**

I am pleased to confirm that HRA and Health and Care Research Wales (HCRW) Approval has been given for the above referenced study, on the basis described in the application form, protocol, supporting documentation and any clarifications received. You should not expect to receive anything further relating to this application.

Please now work with participating NHS organisations to confirm capacity and capability, in line with the instructions provided in the "Information to support study set up" section towards the end of this letter.

How should I work with participating NHS/HSC organisations in Northern Ireland and Scotland?
HRA and HCRW Approval does not apply to NHS/HSC organisations within Northern Ireland and Scotland.

If you indicated in your IRAS form that you do have participating organisations in either of these devolved administrations, the final document set and the study wide governance report (including this letter) have been sent to the coordinating centre of each participating nation. The relevant national coordinating function/s will contact you as appropriate.

Please see IRAS Help for information on working with NHS/HSC organisations in Northern Ireland and Scotland.

How should I work with participating non-NHS organisations?
HRA and HCRW Approval does not apply to non-NHS organisations. You should work with your non-NHS organisations to obtain local agreement in accordance with their procedures.

What are my notification responsibilities during the study?

The standard conditions document "*After Ethical Review – guidance for sponsors and investigators*", issued with your REC favourable opinion, gives detailed guidance on reporting expectations for studies, including:

- Registration of research
- Notifying amendments
- Notifying the end of the study

The HRA website also provides guidance on these topics, and is updated in the light of changes in reporting expectations or procedures.

Who should I contact for further information?
Please do not hesitate to contact me for assistance with this application. My contact details are below.

Your IRAS project ID is **271729**. Please quote this on all correspondence.

Yours sincerely,

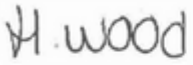

Harriet Wood
Approvals Specialist

Email: hra.approval@nhs.net
Copy to: *Dr Tracy Nevatte*

List of Documents

The final document set assessed and approved by HRA and HCRW Approval is listed below.

Document	*Version*	*Date*
Copies of advertisement materials for research participants [Study advertisement]	1.0	16 December 2019
Copies of advertisement materials for research participants [Study advertisement]	1.1	01 February 2020
Evidence of Sponsor insurance or indemnity (non NHS Sponsors only) [Sponsor insurance]		
IRAS Application Form [IRAS_Form_17122019]		17 December 2019
IRAS Checklist XML [Checklist_17122019]		17 December 2019
IRAS Checklist XML [Checklist_20122019]		20 December 2019
Letter from funder [Letter from funder]		
Letter from sponsor [Sponsor letter]		
Letters of invitation to participant [Recruitment e-mail for age matched controls to RJAH staff]	1.0	16 December 2019
Organisation Information Document [OID]	1.0	
Other [CV for PI]		
Other [CV for Co-I]		
Other [CV for Co-I]		
Other [CV for Co-I]		
Other [GCP certificate for CI]		
Other [Informed consent paediatric for CI]		
Other [Response to HRA]	1.0	01 February 2020
Other [Response to HRA - 2nd round]	1.0	21 February 2020
Participant consent form [Consent form - Parents - Shoulder instability participants - no track changes]	1.2	21 February 2020
Participant consent form [Consent form - Parents - Shoulder instability participants - track changes]	1.2	21 February 2020
Participant consent form [Consent form - Parents - Age matched controls - no track changes]	1.2	21 February 2020
Participant consent form [Consent form - Parents - Age matched controls - track changes]	1.2	21 February 2020
Participant consent form [Assent form - 11 to 15 years - Age matched controls]	1.0	01 February 2020
Participant consent form [Consent form - 16 years & above - Age matched controls - no track changes]	1.1	01 February 2020
Participant consent form [Consent form - 16 years & above - Age matched controls - track changes]	1.1	01 February 2020
Participant consent form [Consent form - Parents - Age matched controls - no track changes]	1.1	01 February 2020
Participant consent form [Consent form - Parents - Age matched controls - track changes]	1.1	01 February 2020
Participant consent form [Assent form - 8 to 10 years - Shoulder instability participant]	1.0	01 February 2020
Participant consent form [Assent form - 11 to 15 years - Shoulder instability participant]	1.0	01 February 2020
Participant consent form [Consent form - 16 years & above - Shoulder instability participants - no track changes]	1.1	01 February 2020

Participant consent form [Consent form - 16 years & above - Shoulder instability participants - track changes]	1.1	01 February 2020
Participant consent form [Assent form - 8 to 10 years - Age matched controls]	1.0	01 February 2020
Participant information sheet (PIS) [PIS 11 to 15 years - Shoulder instability participants - track changes]	1.1	21 February 2020
Participant information sheet (PIS) [PIS Parents - Shoulder instability participants - no track changes]	1.2	21 February 2020
Participant information sheet (PIS) [PIS Parents - Shoulder instability participants - track changes]	1.2	21 February 2020
Participant information sheet (PIS) [PIS 8 to 10 years - Age matched controls - no track changes]	1.1	21 February 2020
Participant information sheet (PIS) [PIS 8 to 10 years - Age matched controls - track changes]	1.1	21 February 2020
Participant information sheet (PIS) [PIS 11 to 15 years - Age matched controls - no track changes]	1.1	21 February 2020
Participant information sheet (PIS) [PIS 11 to 15 years - Age matched controls - no track changes]	1.1	21 February 2020
Participant information sheet (PIS) [PIS Parents - Age matched controls - no track changes]	1.2	21 February 2020
Participant information sheet (PIS) [PIS Parents - Age matched controls - track changes]	1.2	21 February 2020
Participant information sheet (PIS) [PIS 8 to 10 years - Shoulder instability participants]	1.0	01 February 2020
Participant information sheet (PIS) [PIS 16 years & above - Shoulder instability participants - no track changes]	1.1	01 February 2020
Participant information sheet (PIS) [PIS 16 years & above - Shoulder instability participants - track changes]	1.1	01 February 2020
Participant information sheet (PIS) [PIS 16 years & above - Age matched controls - no track changes]	1.1	01 February 2020
Participant information sheet (PIS) [PIS 16 years & above - Age matched controls - track changes]	1.1	01 February 2020
Participant information sheet (PIS) [PIS 8 to 10 years - Shoulder instability participants - no track changes]	1.1	21 February 2020
Participant information sheet (PIS) [PIS 8 to 10 years - Shoulder instability participants - track changes]	1.1	21 February 2020
Participant information sheet (PIS) [PIS 11 to 15 years - Shoulder instability participants - no track chnages]	1.1	21 February 2020
Research protocol or project proposal [Protocol]	1.0	16 December 2019
Sample diary card/patient card [Patient instability diary (Shoulder instability participants and age matched controls)]	1.0	16 December 2019
Schedule of Events or SoECAT [SoECAT]		
Summary CV for Chief Investigator (CI) [CV for CI]		

IRAS project ID	271729

Information to support study set up

The below provides all parties with information to support the arranging and confirming of capacity and capability with participating NHS organisations in England and Wales. This is intended to be an accurate reflection of the study at the time of issue of this letter.

Types of participating NHS organisation	Expectations related to confirmation of capacity and capability	Agreement to be used	Funding arrangements	Oversight expectations	HR Good Practice Resource Pack expectations
There is only one participating NHS organisation therefore there is only one site type.	Research activities should not commence at participating NHS organisations in England or Wales prior to their formal confirmation of capacity and capability to deliver the study.	An Organisation Information Document has been submitted and the sponsor is not requesting and does not expect any other site agreement to be used.	The study is funded by Private Physiotherapy Education Foundation, study funding will be provided to sites as per the organisation information document. A copy of the AcoRD Expert authorised SoECAT has been submitted.	A Principal Investigator should be appointed at the study site.	No Honorary Research Contracts, Letters of Access or pre-engagement checks are expected for local staff employed by the participating NHS organisations. Where arrangements are not already in place, research staff not employed by the NHS host organisation undertaking any of the research activities listed in the research application would be expected to obtain an honorary research contract. This would be on the basis of a Research Passport (if university employed) or an NHS to NHS confirmation of pre-engagement checks letter (if NHS employed). These should confirm enhanced DBS checks, including appropriate barred list checks, and occupational health clearance.

Other information to aid study set-up and delivery

This details any other information that may be helpful to sponsors and participating NHS organisations in England and Wales in study set-up.
The study is intending to apply for inclusion on the NIHR CRN portfolio. The applicant has confirmed that the additional NHS organisations will only be advertising the study and not actively recruiting. Therefore, they are not considered PIC sites.